"Methods and Techniques"

Experimental Techniques for the Study of Magnetism

Prof. Dr. Thomas Brückel

Institute for Scattering Methods

Institute for Solid State Research

History: Loadstone Fe_3O_4 ($\approx$ 800 BC)

100 A.D.
Chinese "south pointer"

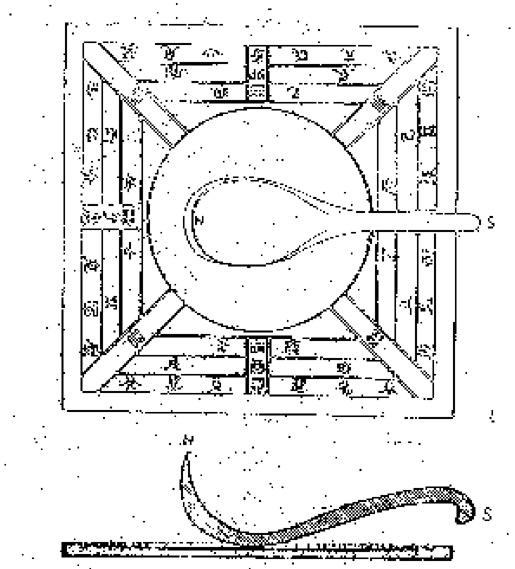

first compass

History: Loadstone Fe_3O_4 (≈ 800 BC)

100 A.D.
Chinese "south pointer"

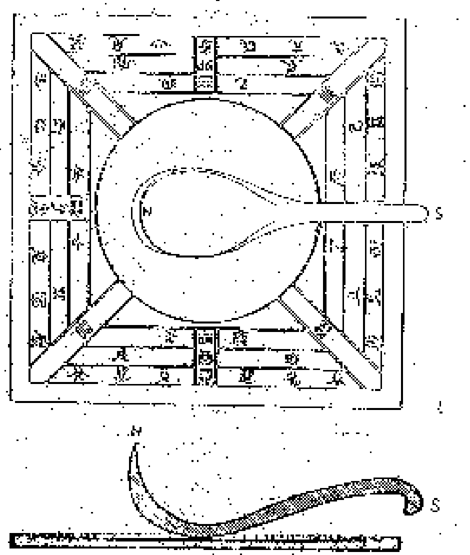

first compass

1269
Europe: Petrus Perigrinus
"Epostolia de Magnete"

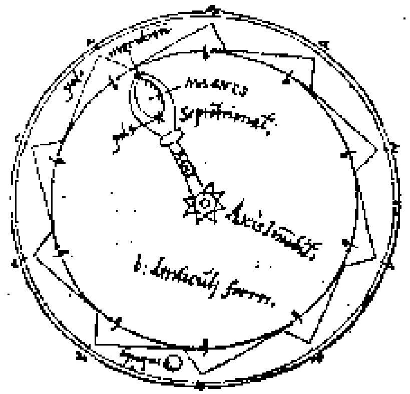

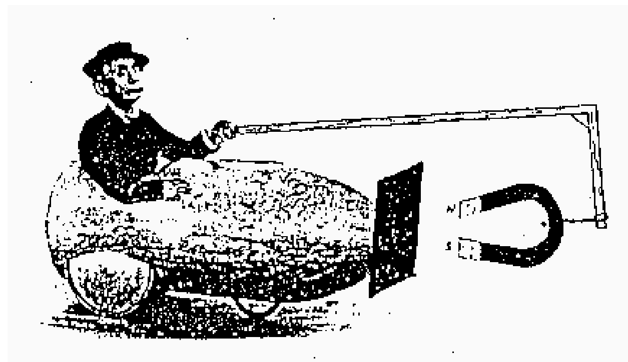

"perpetual motion machine"

History: Loadstone Fe_3O_4 (≈ 800 BC)

100 A.D.
Chinese "south pointer"

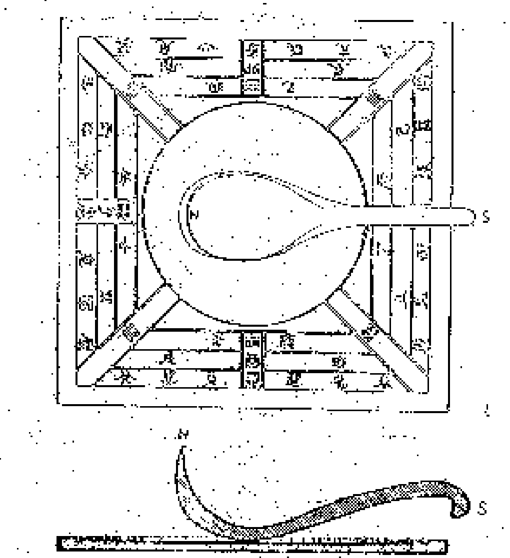

first compass

1269
Europe: Petrus Perigrinus
"Epostolia de Magnete"

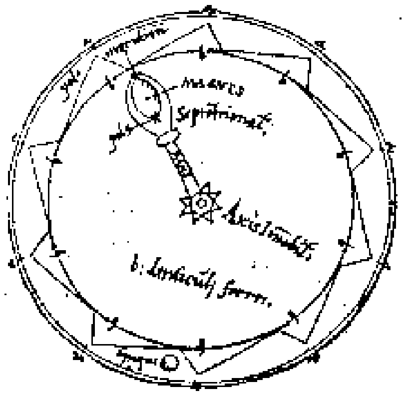

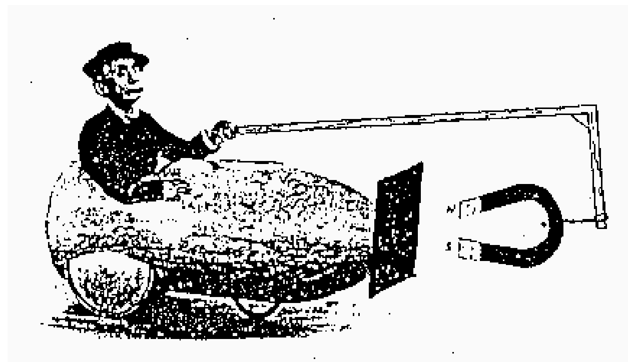

"perpetual motion machine"

what's new ?

magnetic nanostructures

correlated electron systems

...

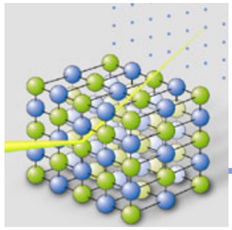

Outline

- What's new in magnetism ?
- Experimental techniques
- Elastic magnetic neutron scattering
- X-ray techniques for magnetism
- Nonresonant magnetic x-ray scattering
- Resonant magnetic x-ray scattering
- Example: Non-resonant scattering from transition metal di-flourides
- Example: Resonance exchange scattering from mixed crystals
- Summary

Magnetic Nanostructures

Thin Film Multilayer:

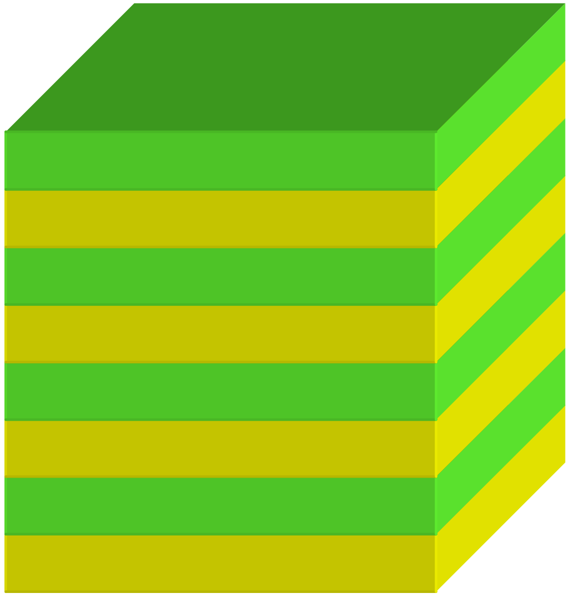

$Fe_{50}Pt_{50}$ Nanoparticle Network by colloidal self organisation

Sun et al; Science 287 (2000), 1989

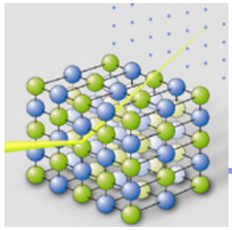

Magnetic Nanostructures

Thin Film Multilayer:

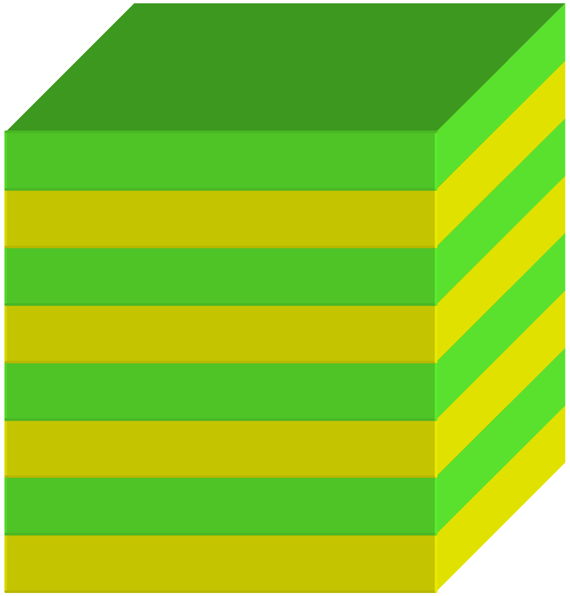

⇒Surfaces,
⇒Interfaces,
⇒Proximity effects

$Fe_{50}Pt_{50}$ Nanoparticle Network by colloidal self organisation

Sun et al; Science 287 (2000), 1989

Magnetic Nanostructures

Thin Film
Multilayer:

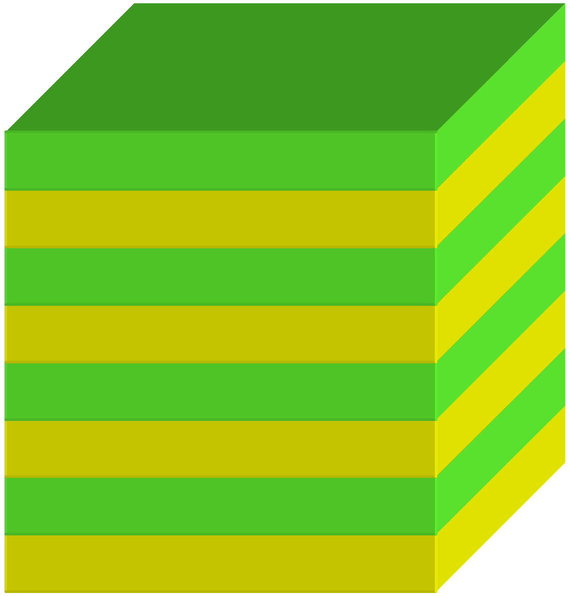

⇒Surfaces,
⇒Interfaces,
⇒Proximity effects

$Fe_{50}Pt_{50}$ Nanoparticle Network
by colloidal self organisation

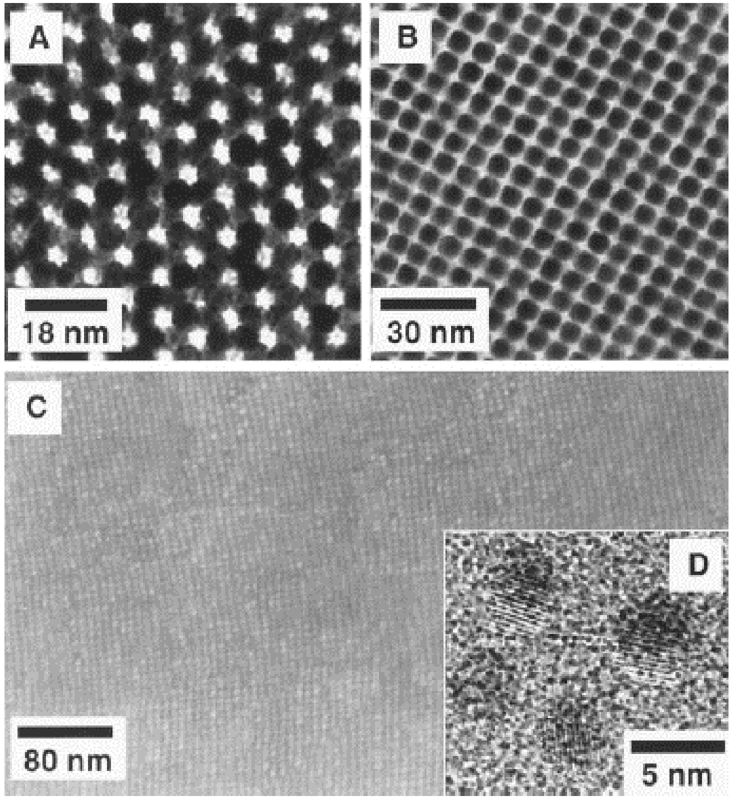

Sun et al; Science 287 (2000), 1989

Interlayer Exchange Coupling

Oscillatory coupling as function of interlayer thickness:

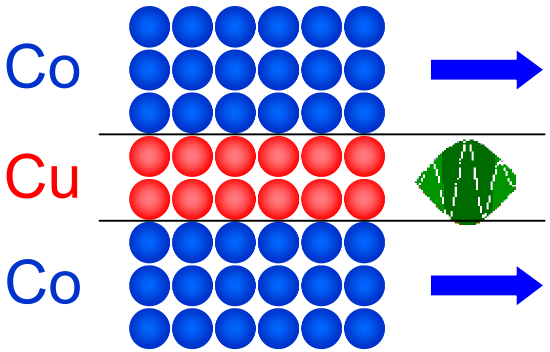

Ferromagnetic

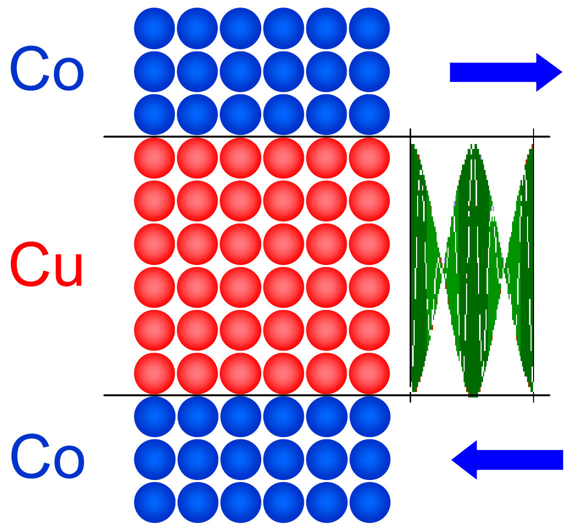

Antiferromagnetic

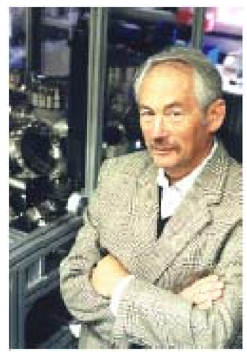

Peter Grünberg:
Interlayer Exchange Coupling in Fe/Cr Multilayers
Phys. Rev. Lett. 57 (1986), 2442

Giant Magnetoresistance (GMR)

GMR-effect

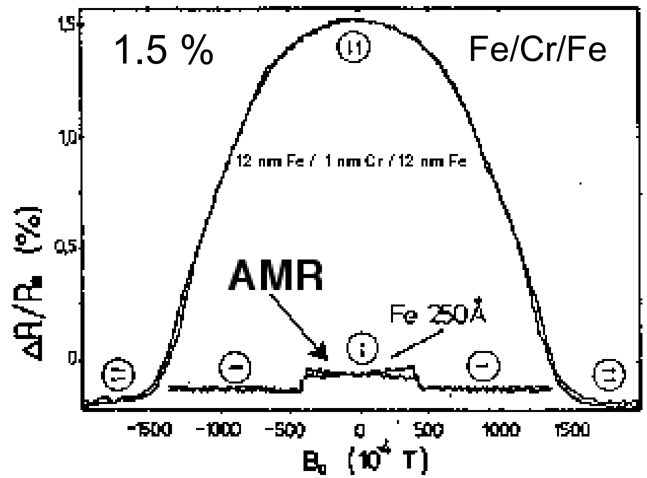

P. Grünberg et al.
Phys. Rev. B 39 (1989), 4828
(and independently: A. Fert, Paris)

Artificial Nano-Structures
→ purpose designed properties

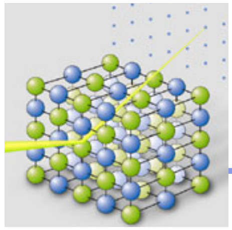

Giant Magnetoresistance (GMR)

GMR-effect

Antiparallel alignment

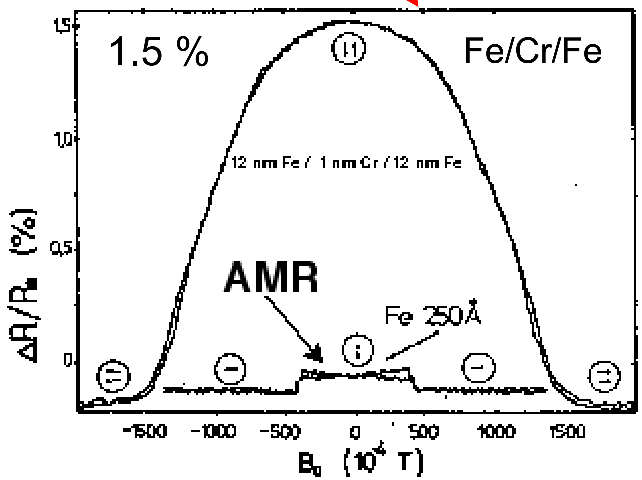

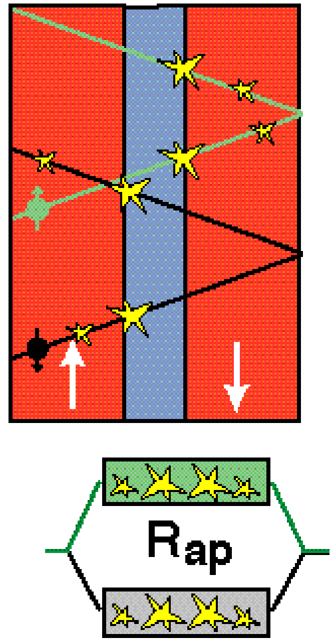

P. Grünberg et al.
Phys. Rev. B 39 (1989), 4828
(and independently: A. Fert, Paris)

Artificial Nano-Structures
→ purpose designed properties

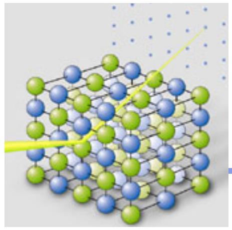

Giant Magnetoresistance (GMR)

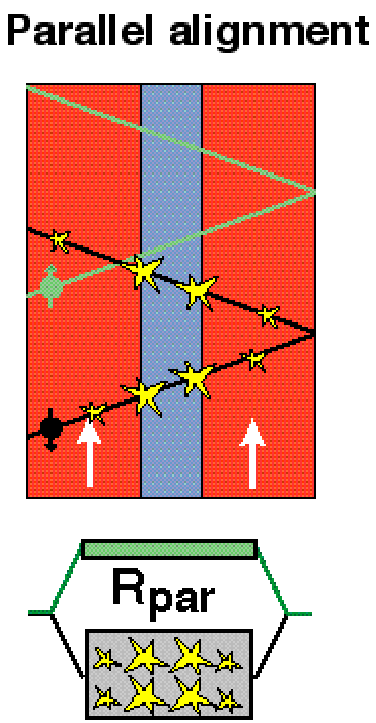

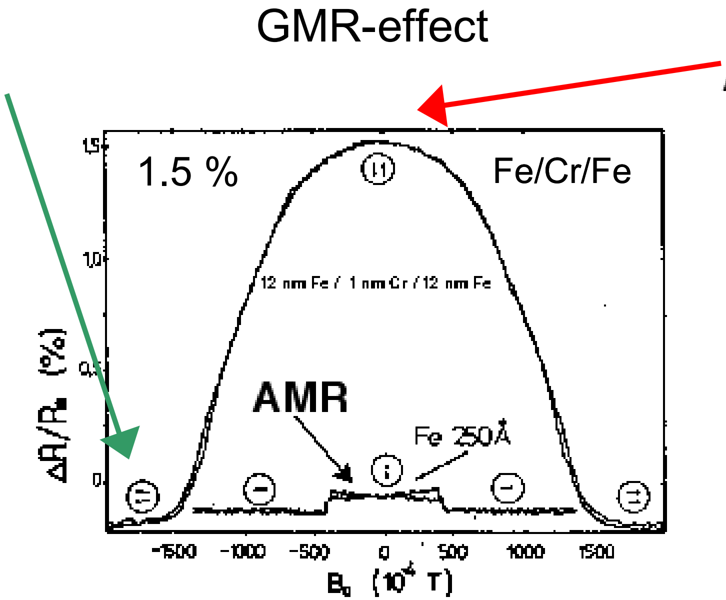

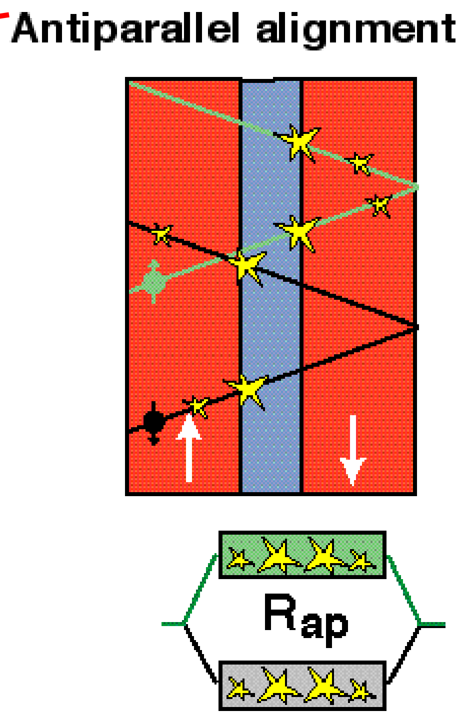

P. Grünberg et al.
Phys. Rev. B 39 (1989), 4828
(and independently: A. Fert, Paris)

Artificial Nano-Structures
→ purpose designed properties

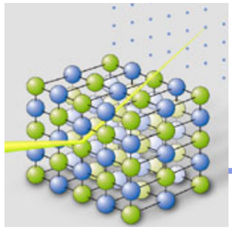

Giant Magnetoresistance (GMR)

GMR-effect

Parallel alignment

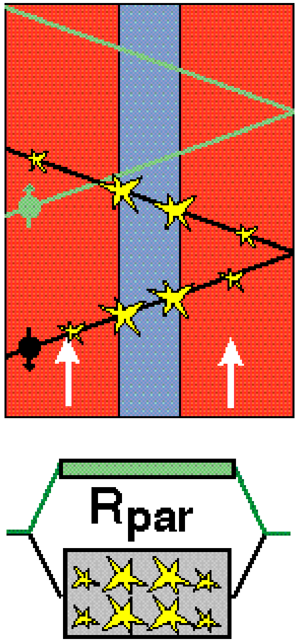

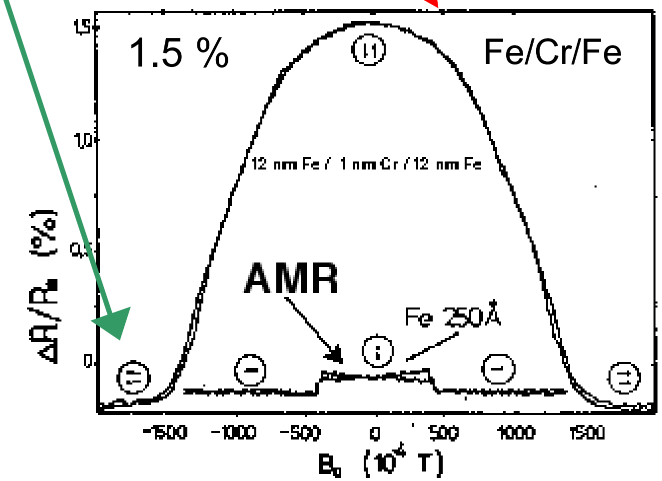

Antiparallel alignment

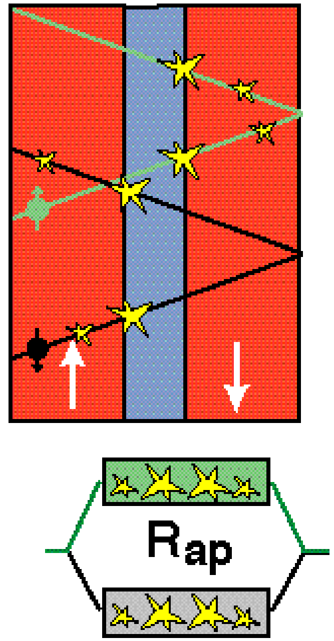

P. Grünberg et al.
Phys. Rev. B 39 (1989), 4828
(and independently: A. Fert, Paris)

Artificial Nano-Structures
→ purpose designed properties

Applications: Hard Disks

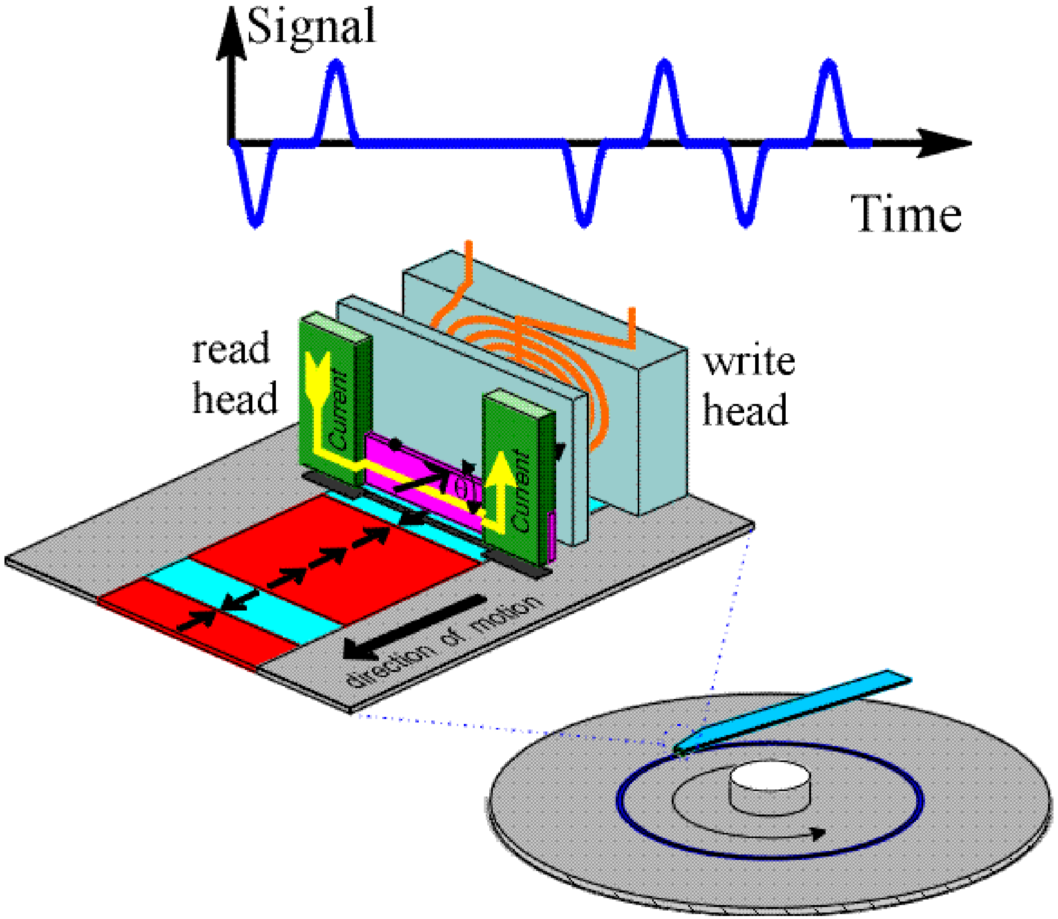

Applications: Hard Disks

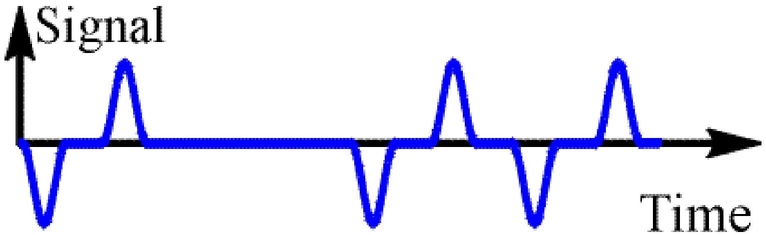

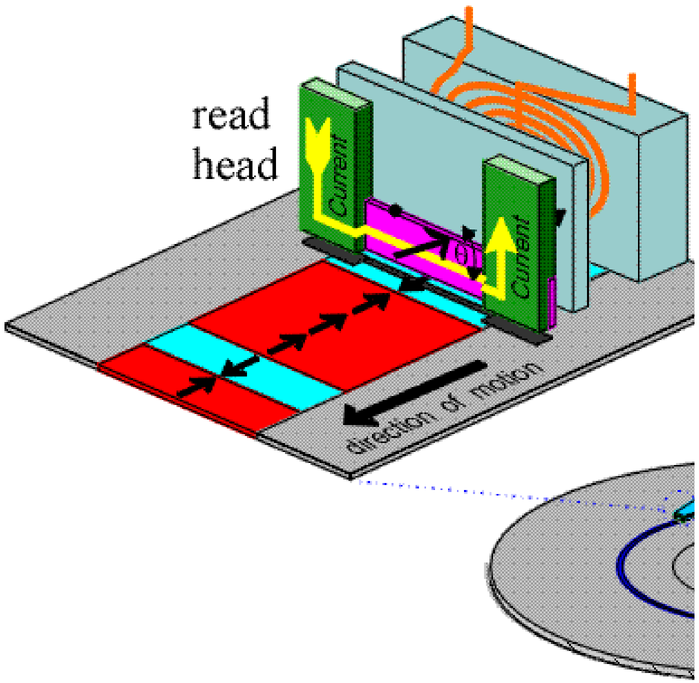

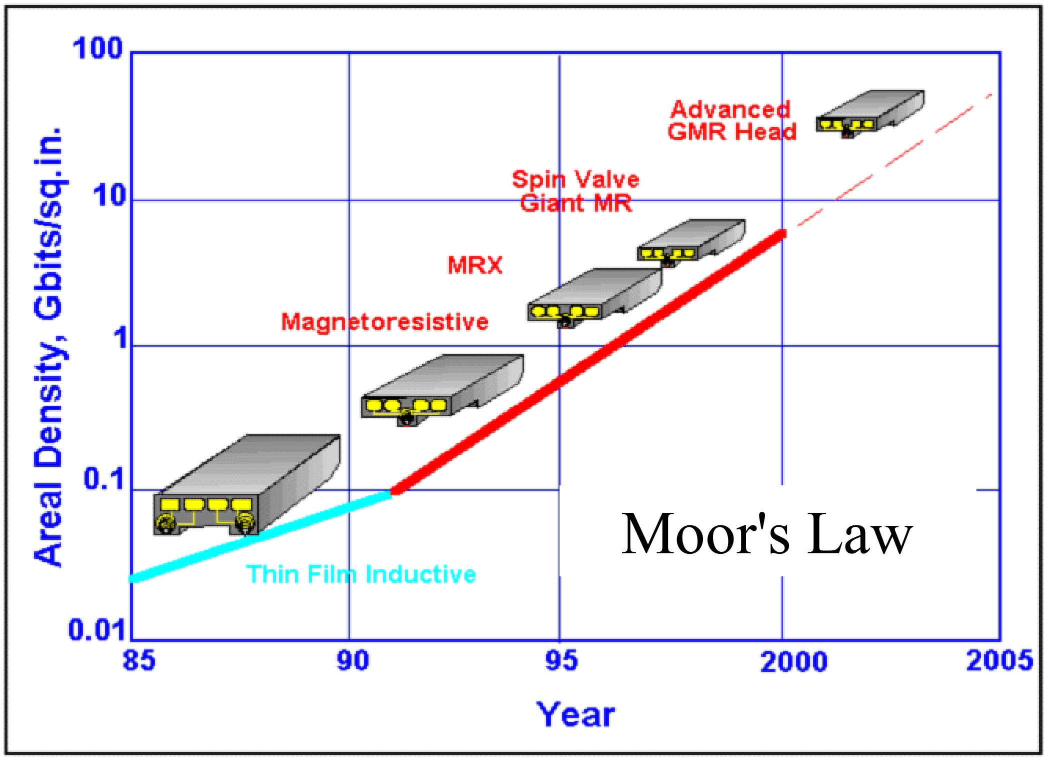

Figure 10. Magnetic head evolution

Applications: MRAM

Magnetic Random Access Memory:

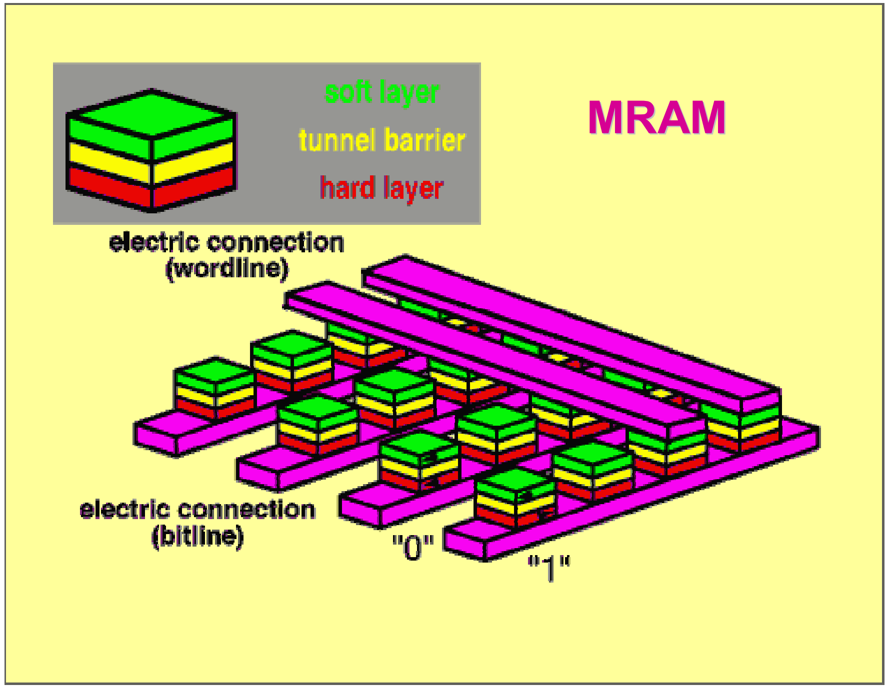

Applications: MRAM

Magnetic Random Access Memory:

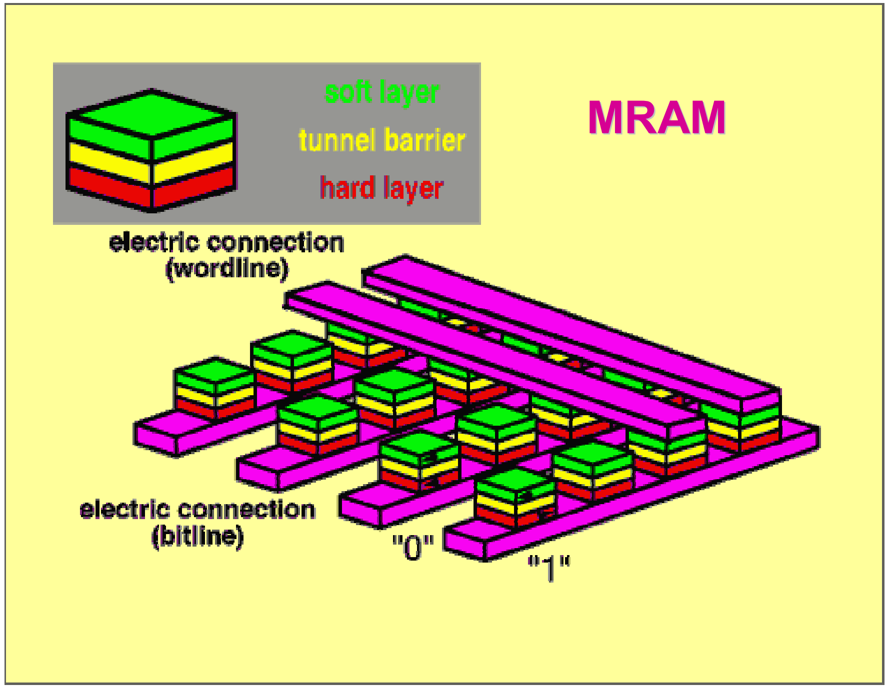

- 100 Million storage elements per mm^2
- 1 /100 Million gram mass per cm^2

Applications: MRAM

Magnetic Random Access Memory:

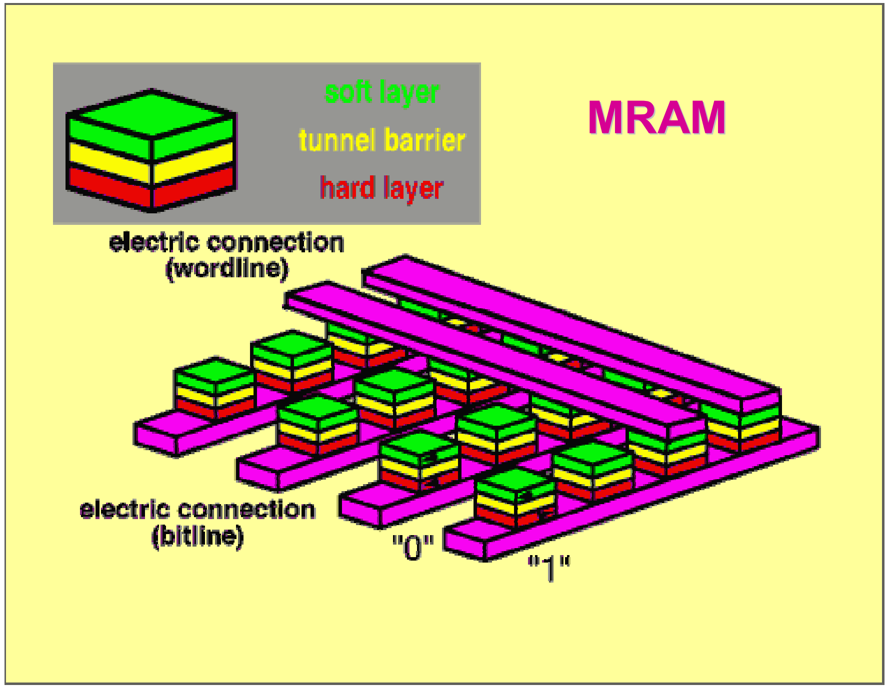

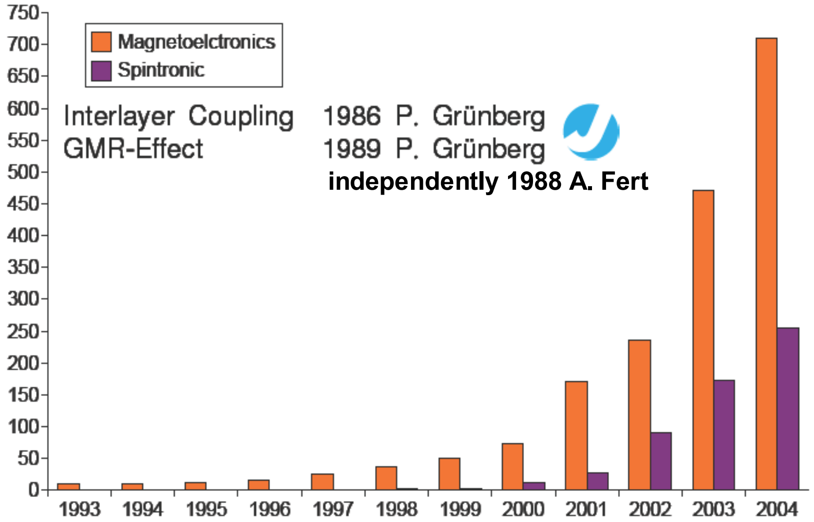

- 100 Million storage elements per mm^2
- 1 /100 Million gram mass per cm^2

Applications: MRAM

Magnetic Random Access Memory:

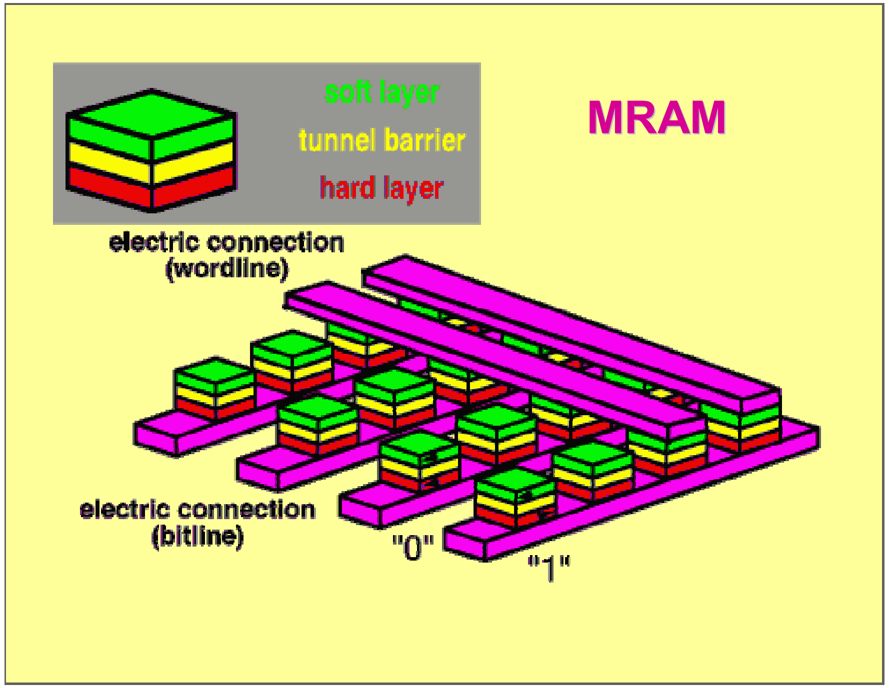

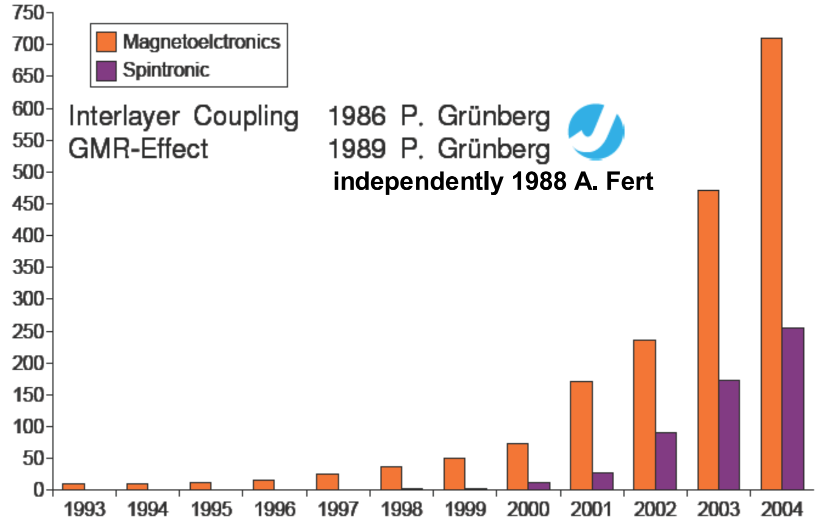

"Spintronics":
Information transport, storage and processing with the spin of the electron (not the charge!)

- 100 Million storage elements per mm^2
- 1 /100 Million gram mass per cm^2

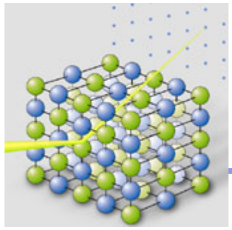

Highly correlated electron systems

Complex transition metal oxides:
High T_C Superconductors; CMR-Manganates; …

New phenomena appear from the bottom of the Fermi sea due to electronic correlations:

- Magnetism
- Superconductivity
- Metal-insulator transition (CMR)
- Charge- & orbital order
- Multiferroica

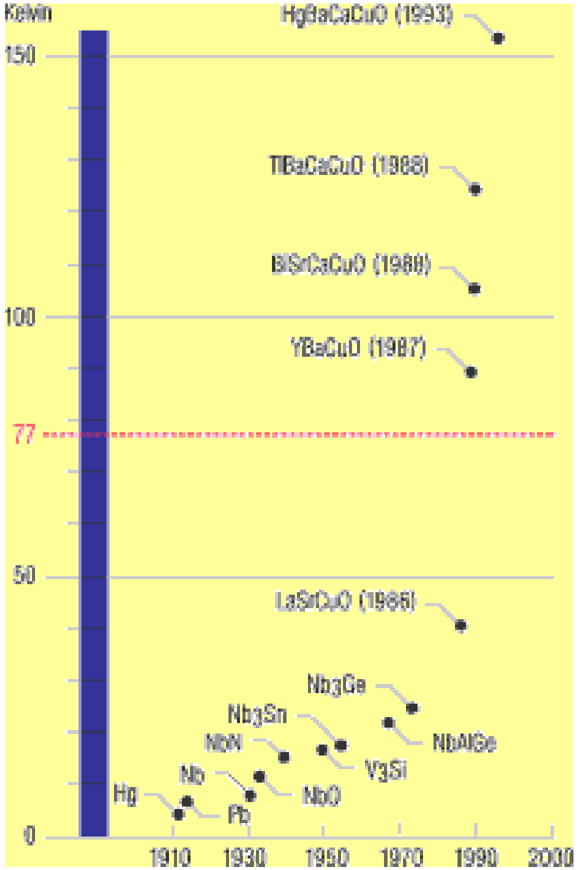

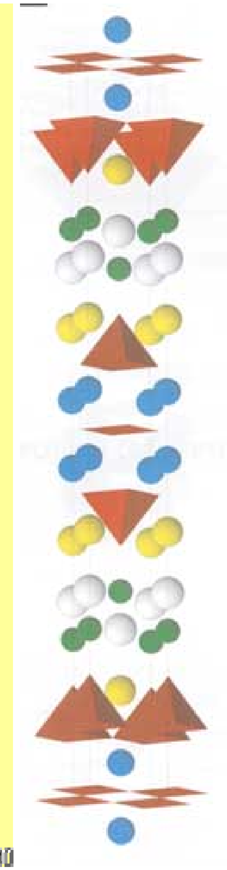

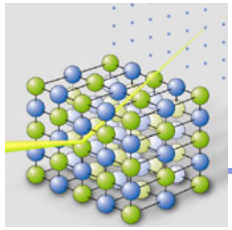

Highly correlated electron systems

No simple Fermi liquids; competing interactions

Oxides

- High T_C Materials ($YBa_2Cu_3O_{6+x}$):
  Magnetism ↔ Superconductivity
- Materials with collosal Magnetoresistance
  Spin ↔ Charge ↔ Lattice ↔ Orbital order

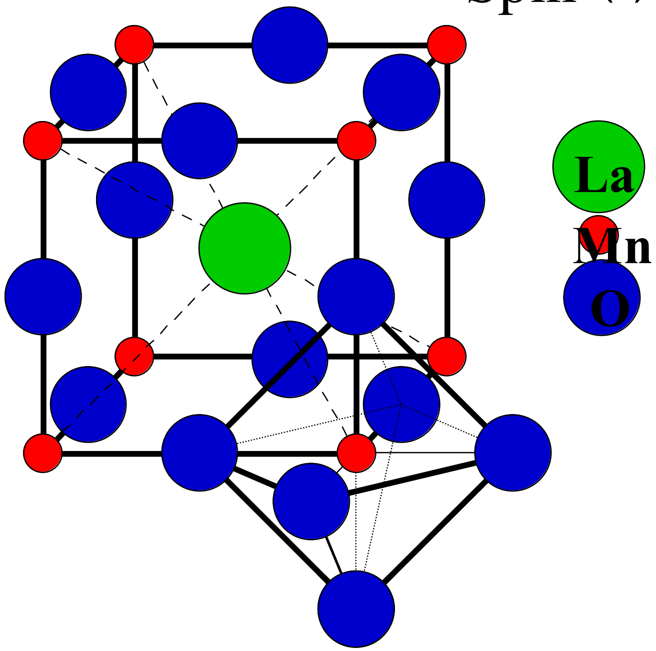

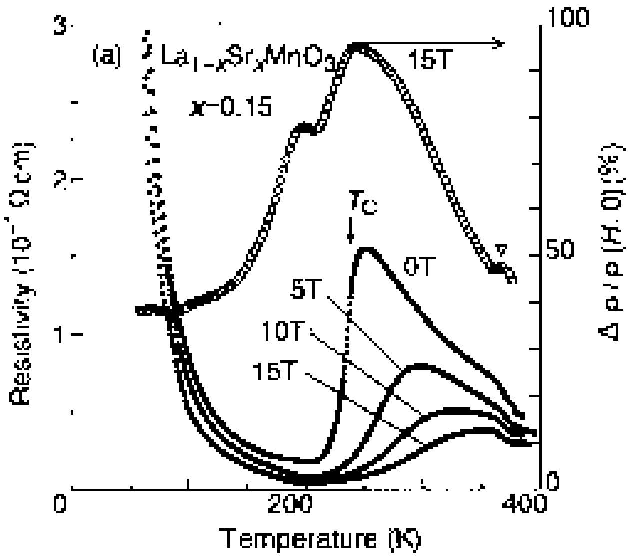

Fundamental microscopic understanding !

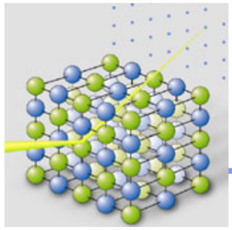

Outline

- What's new in magnetism ?
- Experimental techniques
- Elastic magnetic neutron scattering
- X-ray techniques for magnetism
- Nonresonant magnetic x-ray scattering
- Resonant magnetic x-ray scattering
- Example: Non-resonant scattering from transition metal di-flourides
- Example: Resonance exchange scattering from mixed crystals
- Summary

Susceptibility and Magnetisation

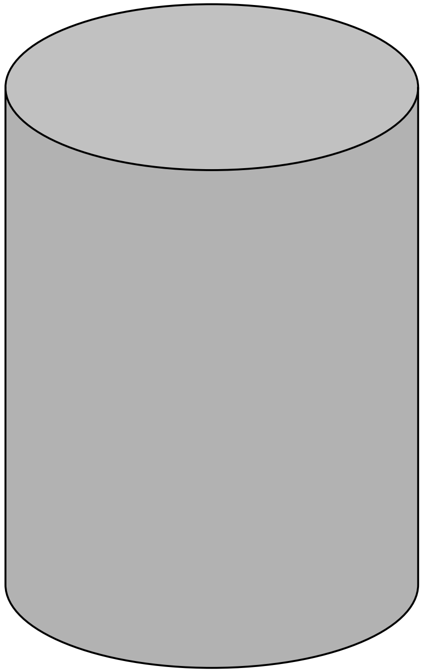

Susceptibility and Magnetisation

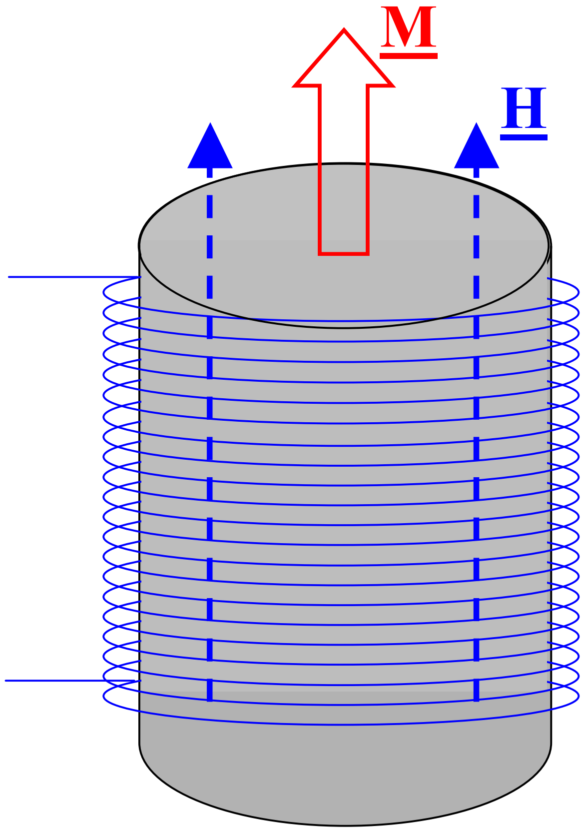

$$\underline{M} = \chi \cdot \underline{H}$$

linear response theory

Susceptibility and Magnetisation

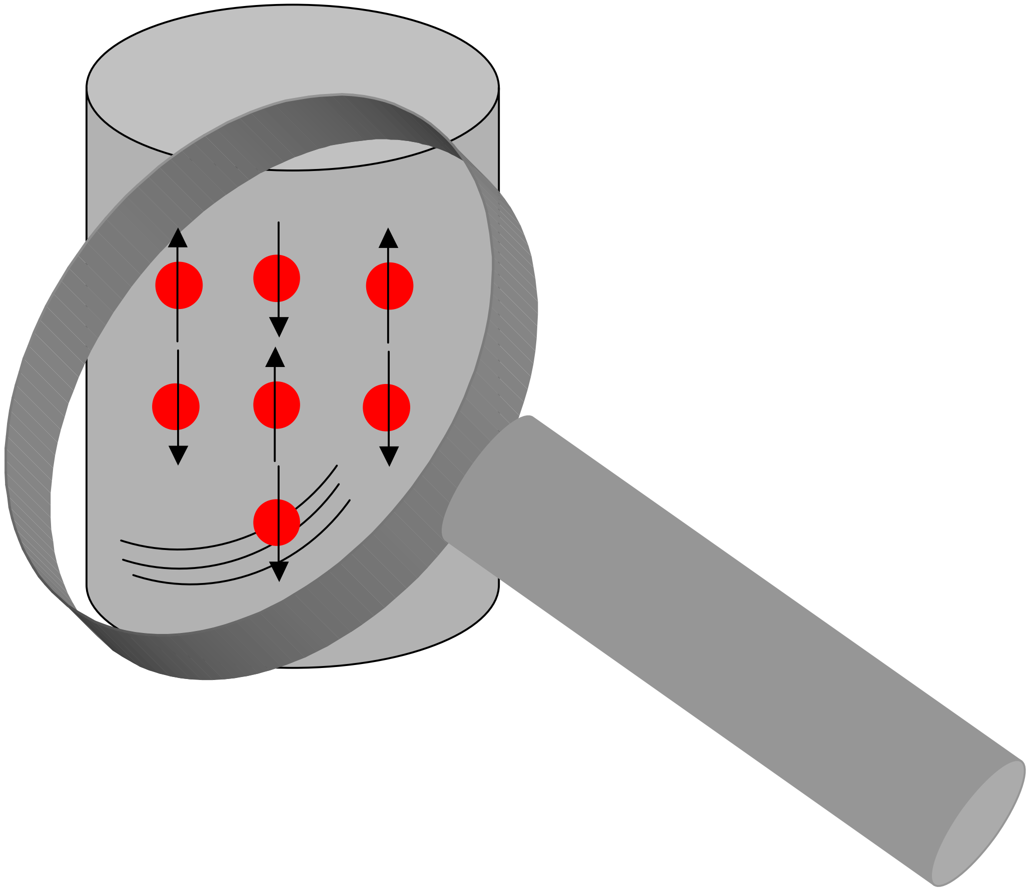

Scattering

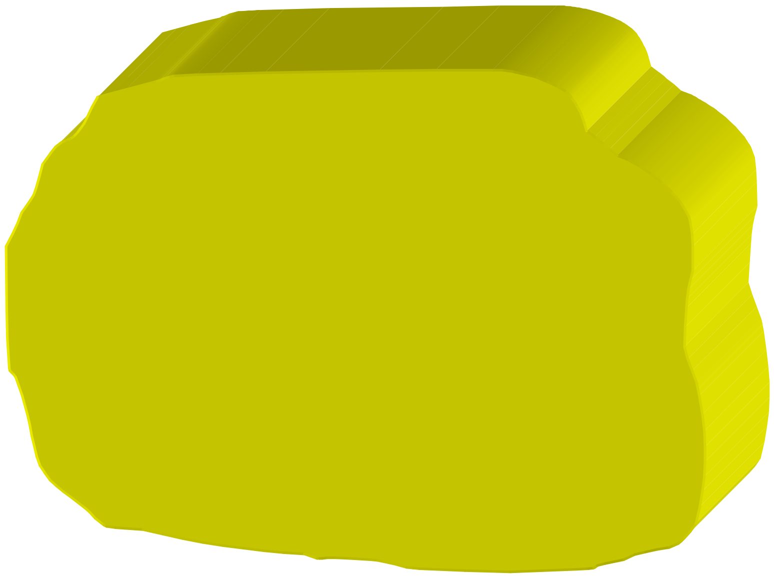

Scattering

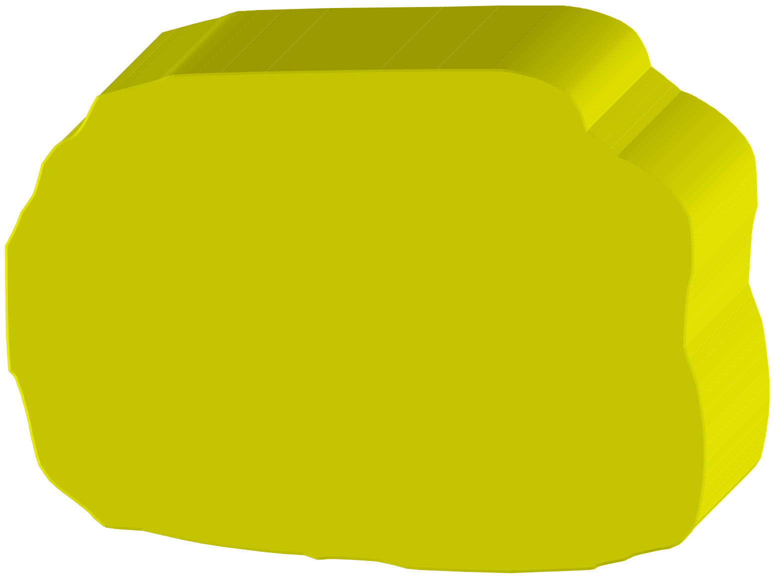

→ Internal structure? (atom positions, moment arrangement)

→ Microscopic dynamics? (atom movements, spin dynamics)

⇒ Macroscopic properties (conductivity, susceptibility, ...)

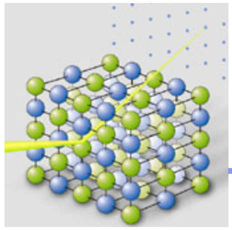

Scattering

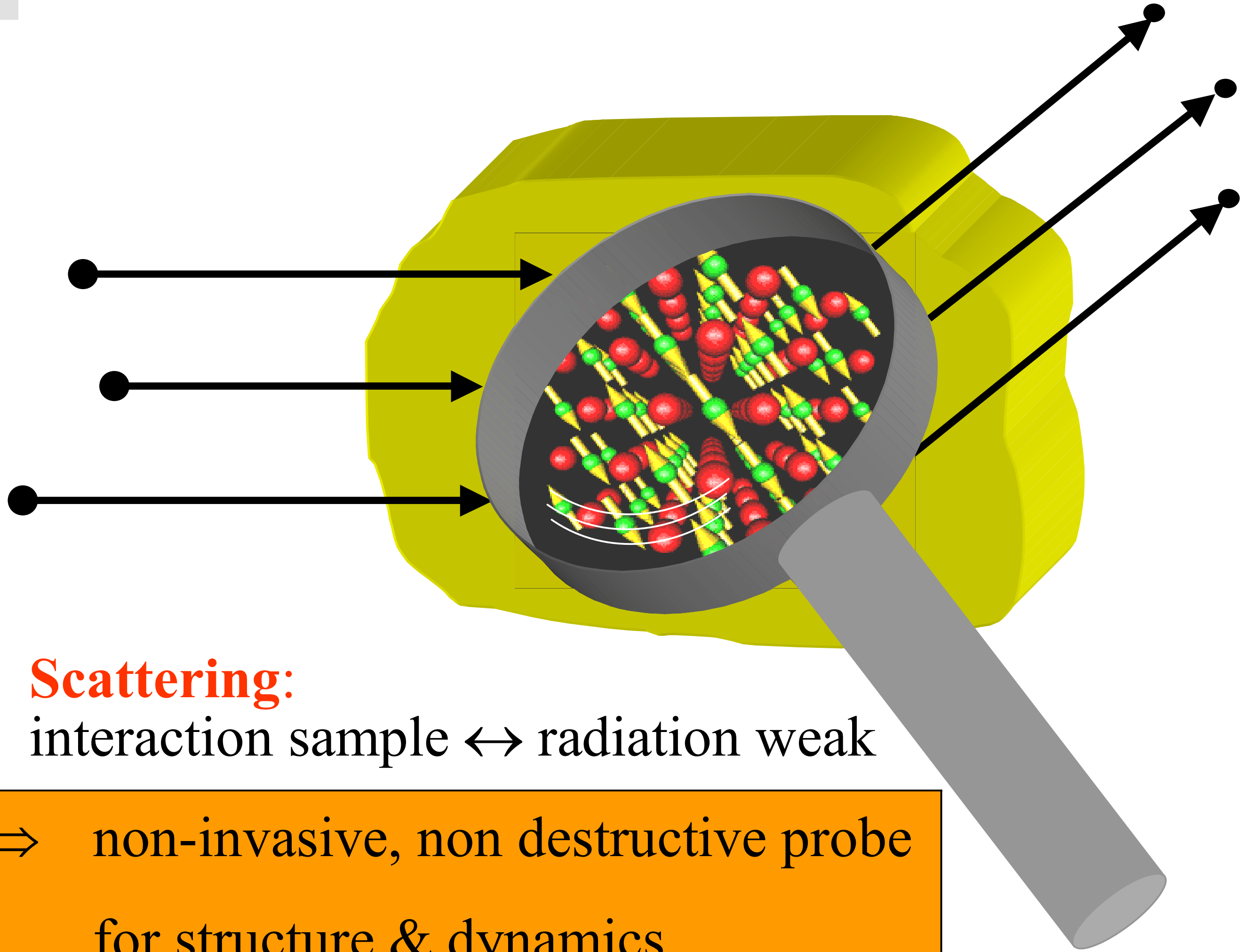

Scattering:
interaction sample ↔ radiation weak

⇒ non-invasive, non destructive probe
for structure & dynamics

Generalised Susceptibility

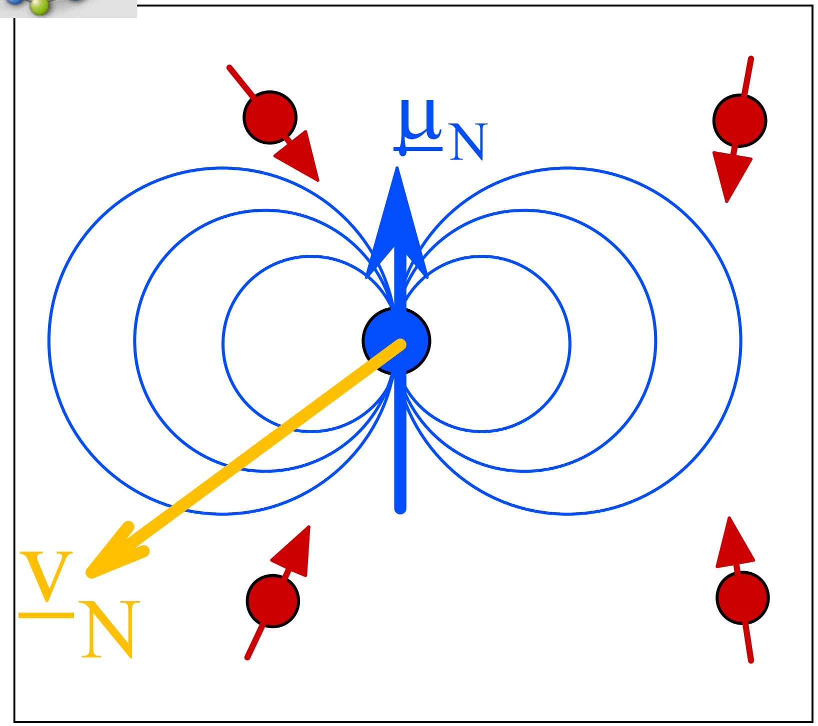

<u>linear response theory:</u>

perturbation of magnetic system described by spacial and temporal varying magnetic field
$\underline{H}(\underline{r}, t)$
system reaction:
local magnetisation
$\underline{M}(\underline{r},t)$
linear response theory → susceptibility
$\underline{\underline{\chi}}(\underline{r},t)$

$$\left\langle M^{\beta}(\underline{R}_{ld},t)\right\rangle = \left\langle M^{\beta}(\underline{R}_{ld},t)\right\rangle_{H=0} + \int_{-\infty}^{t} \sum_{l'd'} \sum_{\alpha} H^{\alpha}(\underline{R}_{l'd'},t')\,\chi^{\alpha\beta}(\underline{R}_{ld}-\underline{R}_{l'd'},t-t')\,dt'$$

$$\chi_{dd'}^{\alpha\beta}(\underline{Q},t-t') = \sum_{l} e^{i\underline{Q}\cdot(\underline{R}_{ld}-\underline{R}_{0d'})}\,\chi^{\alpha\beta}(\underline{R}_{ld}-\underline{R}_{0d'},t-t')$$

$$\chi_{dd'}^{\alpha\beta}(\underline{Q},\omega) = \int_{0}^{\infty} e^{-i\omega t}\,\chi_{dd'}^{\alpha\beta}(\underline{Q},t)\,dt$$

Generalised Susceptibility

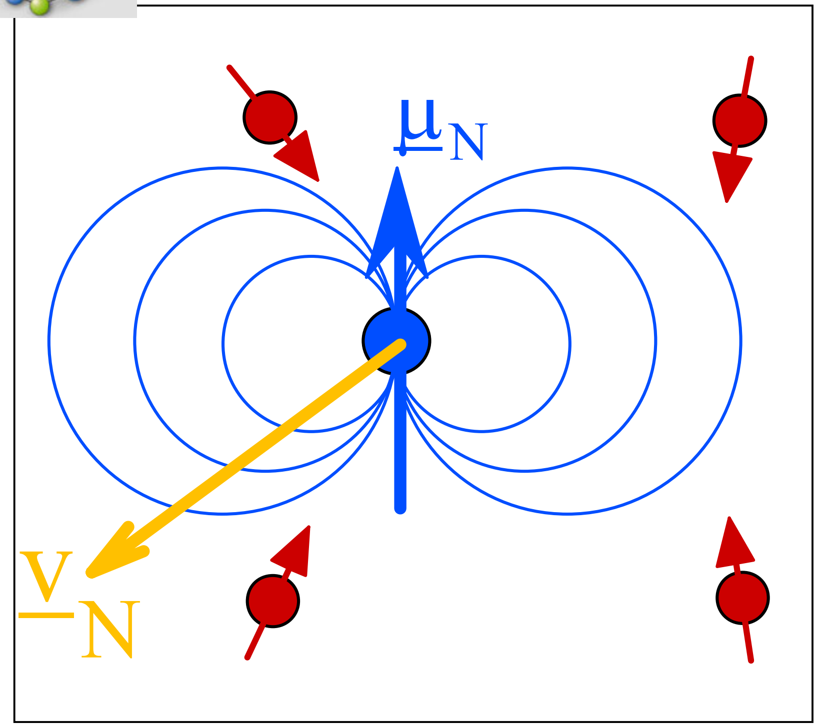

<u>linear response theory:</u>

perturbation of magnetic system described by spacial and temporal varying magnetic field
$\underline{H}\,(\underline{r},\,t)$
system reaction:
local magnetisation
$\underline{M}\,(\underline{r},t)$
linear response theory → susceptibility
$\underline{\underline{\chi}}(\underline{r},t)$

$$\left\langle M^{\beta}(\underline{R}_{ld},t)\right\rangle = \left\langle M^{\beta}(\underline{R}_{ld},t)\right\rangle_{H=0} + \int_{-\infty}^{t}\sum_{l'd'}\sum_{\alpha} H^{\alpha}(\underline{R}_{l'd'},t')\,\chi^{\alpha\beta}(\underline{R}_{ld}-\underline{R}_{l'd'},t-t')\,dt'$$

Fourier transform:
$$\chi_{dd'}^{\alpha\beta}(\underline{Q},t-t') = \sum_{1} e^{i\underline{Q}\cdot(\underline{R}_{ld}-\underline{R}_{0d'})}\,\chi^{\alpha\beta}(\underline{R}_{ld}-\underline{R}_{0d'},t-t')$$
$$\chi_{dd'}^{\alpha\beta}(\underline{Q},\omega) = \int_{0}^{\infty} e^{-i\omega t}\,\chi_{dd'}^{\alpha\beta}(\underline{Q},t)\,dt$$

Neutrons: Length and Time Scales

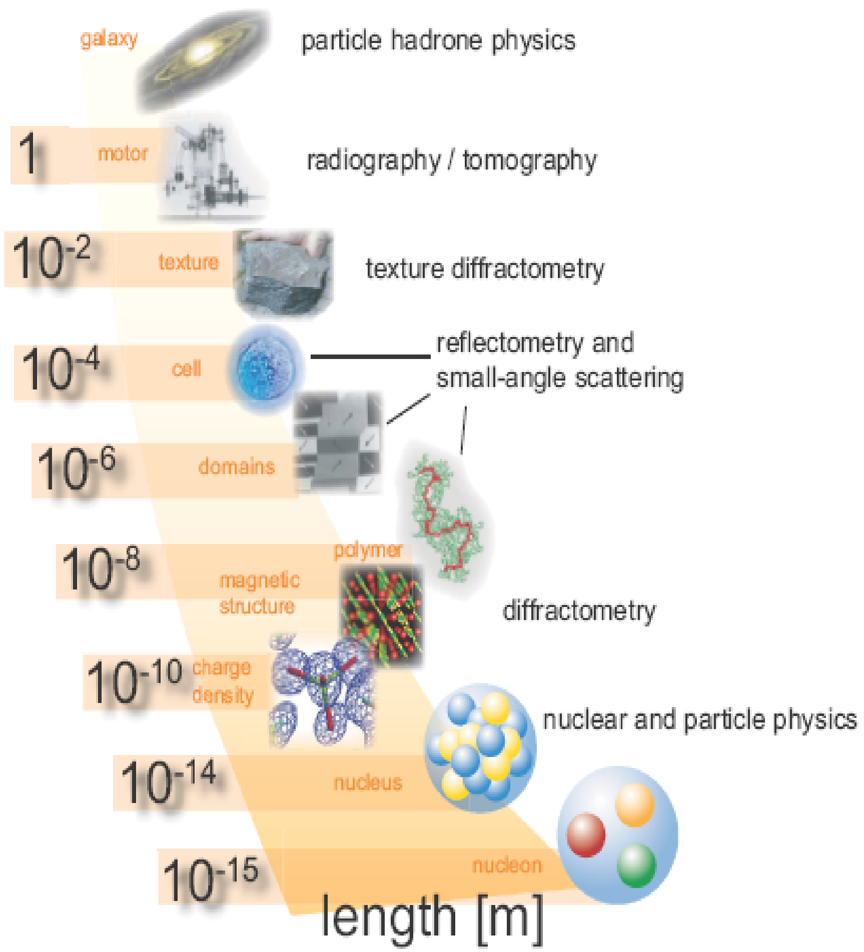

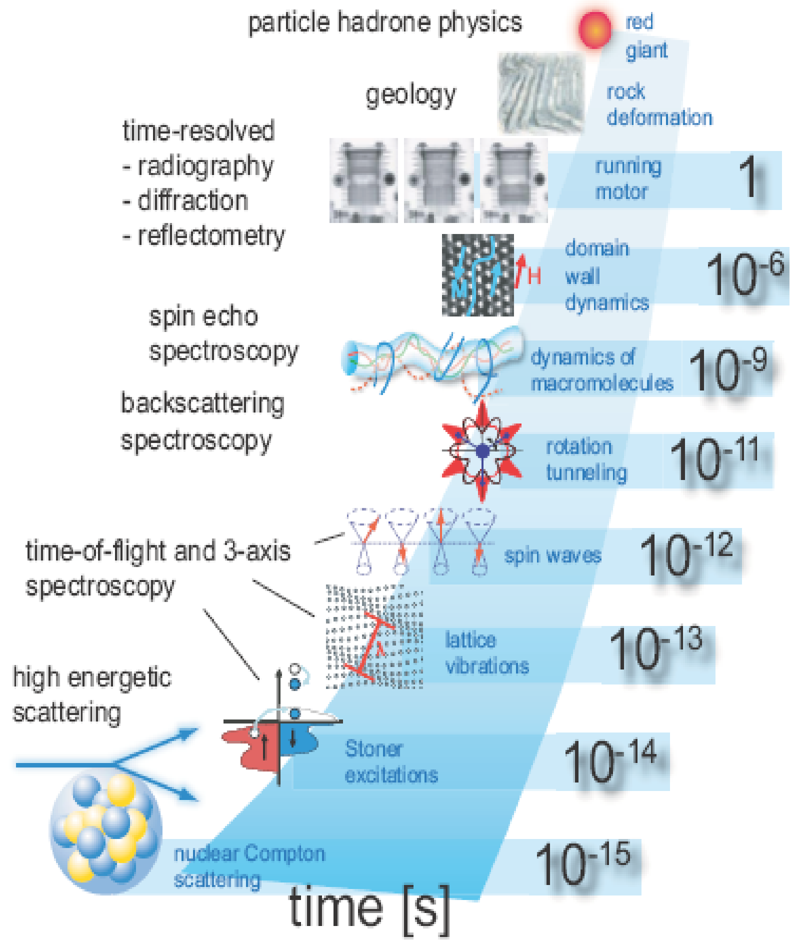

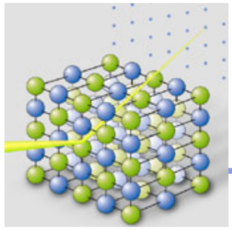

Outline

- What's new in magnetism ?
- Experimental techniques
- Elastic magnetic neutron scattering
- X-ray techniques for magnetism
- Nonresonant magnetic x-ray scattering
- Resonant magnetic x-ray scattering
- Example: Non-resonant scattering from transition metal di-flourides
- Example: Resonance exchange scattering from mixed crystals
- Summary

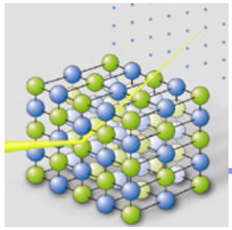

Magnetic Structures

Collinear Antiferromagnets:

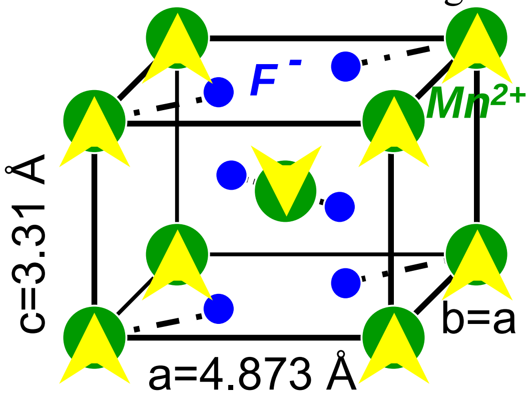

MnF_2:

Modulated Structures:

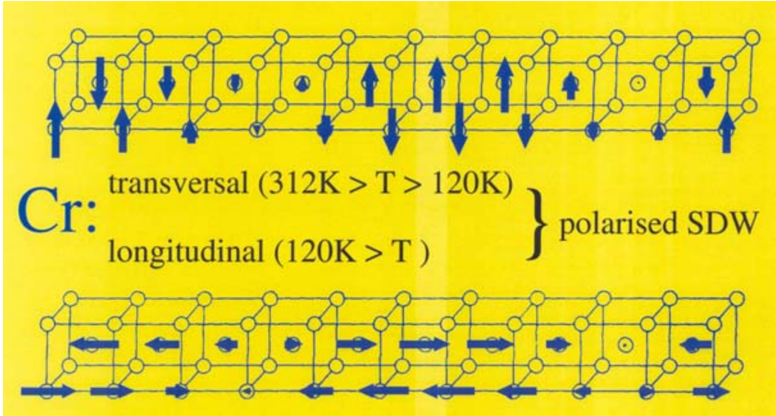

Cr:

Complex Structures:

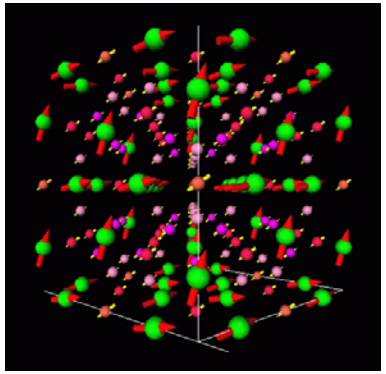

Er_6Mn_{23}:

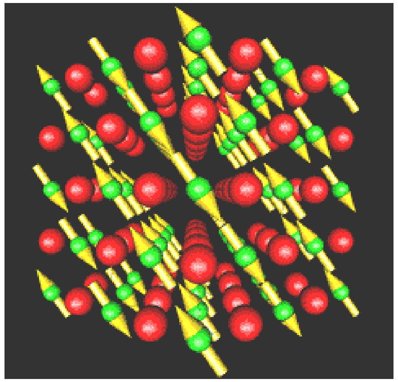

MnO:

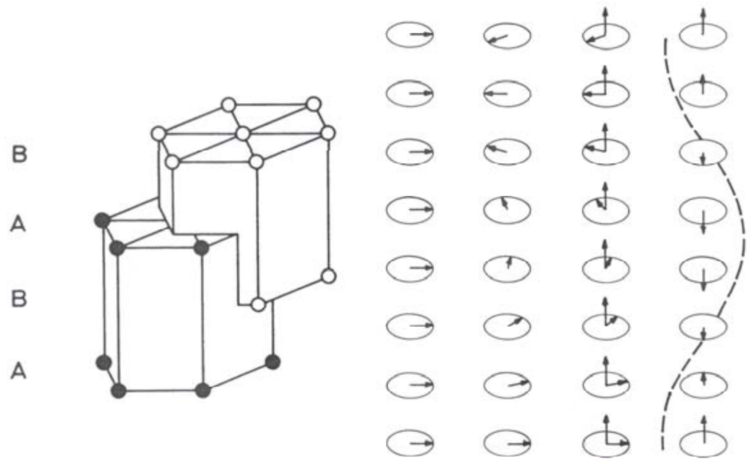

Rare Earth:

General description in Fourier representation:

$$\underline{m}_{\underline{e}_{ij}} = \sum_{\underline{k}} m_{\underline{k}_{ij}} \cdot \exp(-i\underline{k} \cdot \underline{R}_l)$$

Neutron-Matter-Interaction

First Born Approximation: $$\frac{d\sigma}{d\Omega} = \left(\frac{m}{2\pi\hbar}\right)^2 |<\underline{k}'|V|\underline{k}>|^2$$

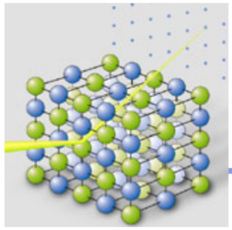

Neutron-Matter-Interaction

First Born Approximation: $$\frac{d\sigma}{d\Omega} = \left(\frac{m}{2\pi\hbar}\right)^2 |<\underline{k}'|V|\underline{k}>|^2$$

$$\int e^{-i\underline{k}'\underline{r}} V(\underline{r}) e^{i\underline{k}\underline{r}} d^3r$$
$$= \int V(\underline{r}) \cdot e^{-i\underline{Q}\cdot\underline{r}} d^3r$$

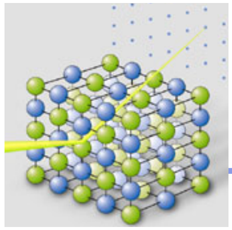

Neutron-Matter-Interaction

First Born Approximation: $\frac{d\sigma}{d\Omega} = \left(\frac{m}{2\pi\hbar}\right)^2 |<\underline{k}'|V|\underline{k}>|^2$

?

$\int e^{-i\underline{k}'\underline{r}} V(\underline{r}) e^{i\underline{k}\underline{r}} d^3r$

$= \int V(\underline{r}) \cdot e^{-i\underline{Q}\cdot\underline{r}} d^3r$

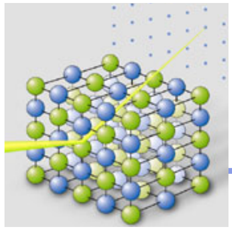

Neutron-Matter-Interaction

First Born Approximation: $$\frac{d\sigma}{d\Omega} = \left(\frac{m}{2\pi\hbar}\right)^2 |\langle \underline{k}' | V | \underline{k} \rangle|^2$$

?

$$\int e^{-i\underline{k}'\underline{r}} V(\underline{r}) e^{i\underline{k}\underline{r}} d^3r$$
$$= \int V(\underline{r}) \cdot e^{-i\underline{Q}\cdot\underline{r}} d^3r$$

- strong interaction n $\leftrightarrow$ nucleus
- magnetic dipole-interaction with B-field of unpaired e^-

} major

Magnetic Interaction Potential

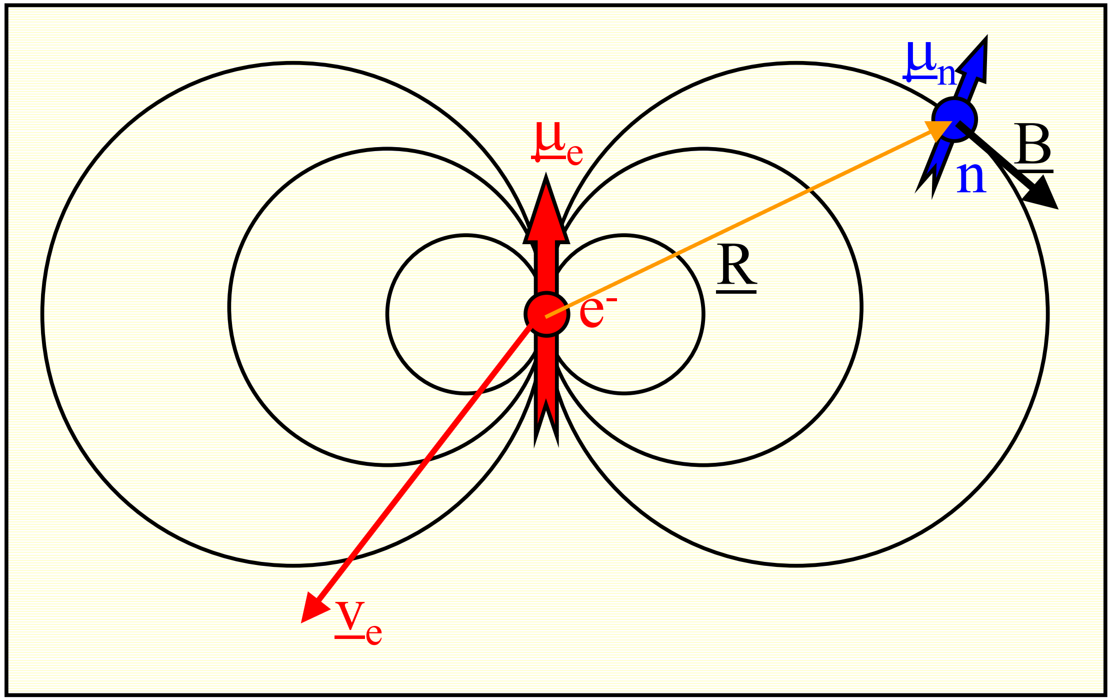

Zeeman energy:

$$\mathbf{V}_m = -\underline{\mu}_n \cdot \underline{B}$$

magnetic moment of the neutron:

$$\underline{\mu}_n = -\gamma \mu_N \cdot \underline{\boldsymbol{\sigma}}$$

magnetic field of the electron:

$$\underline{B} = \underline{B}_S + \underline{B}_L$$

dipolar field of the spin moment: $\underline{B}_S = \underline{\nabla} \times \left(\frac{\underline{\mu}_e x \underline{R}}{R^3} \right)$; $\underline{\mu}_e = -2\mu_B \cdot \underline{S}$

field due to the movement of the electron (Biot-Savart): $\underline{B}_L = \frac{-e}{c} \frac{\underline{v}_e \times \underline{R}}{R^3}$

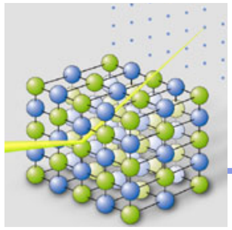

Magnetic Scattering Cross Section

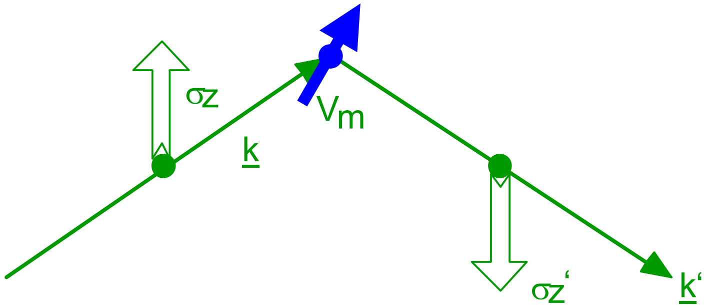

1. Born approximation

$$\frac{d\sigma}{d\Omega} = \left(\frac{m_n}{2\pi\hbar^2}\right)^2 \left|\langle \underline{k}'\sigma_z' | \mathbf{V}_m | \underline{k}\sigma_z \rangle\right|^2$$

$$\boxed{\frac{d\sigma}{d\Omega} = (\gamma r_0)^2 \left| -\frac{1}{2\mu_B} \langle \sigma_z' | \underline{\boldsymbol{\sigma}} \cdot \underline{M}_\perp(\underline{Q}) | \sigma_z \rangle \right|^2}$$

$$\gamma r_0 = 0.539 \cdot 10^{-12}\,\text{cm}$$

$\rightarrow$"equivalent scattering length" for 1 μ_B ($S=\frac{1}{2}$): 2.696 fm $\approx b_{co}$

$$\underline{M}_\perp(\underline{Q}) = \hat{\underline{Q}} \times \underline{M}(\underline{Q}) \times \hat{\underline{Q}}$$

$$\underline{M}(\underline{Q}) = \int \underline{M}(\underline{r}) e^{i\underline{Q}\cdot\underline{r}} d^3r$$

$$\underline{M}(\underline{r}) = \underline{M}_S(\underline{r}) + \underline{M}_L(\underline{r})$$

$$\underline{M}_S(\underline{r}) = -2\mu_B \cdot \underline{S}(\underline{r}) = -2\mu_B \sum_i \delta(\underline{r} - \underline{r}_i)\underline{S}_i$$

Directional Dependence

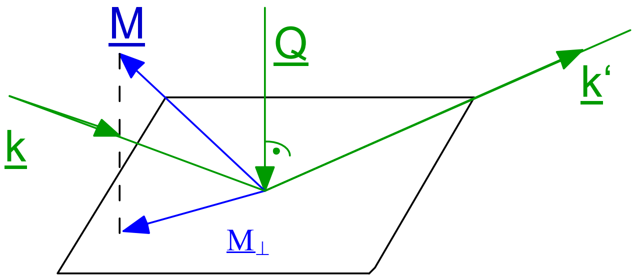

$$\underline{M}_\perp(\underline{Q}) = \underline{\hat{Q}} \times \underline{M} \times \underline{\hat{Q}}$$

Only the component of the magnetisation perpendicular to the scattering vector gives rise to magnetic scattering!

Illustration: scattering from the dipolar field

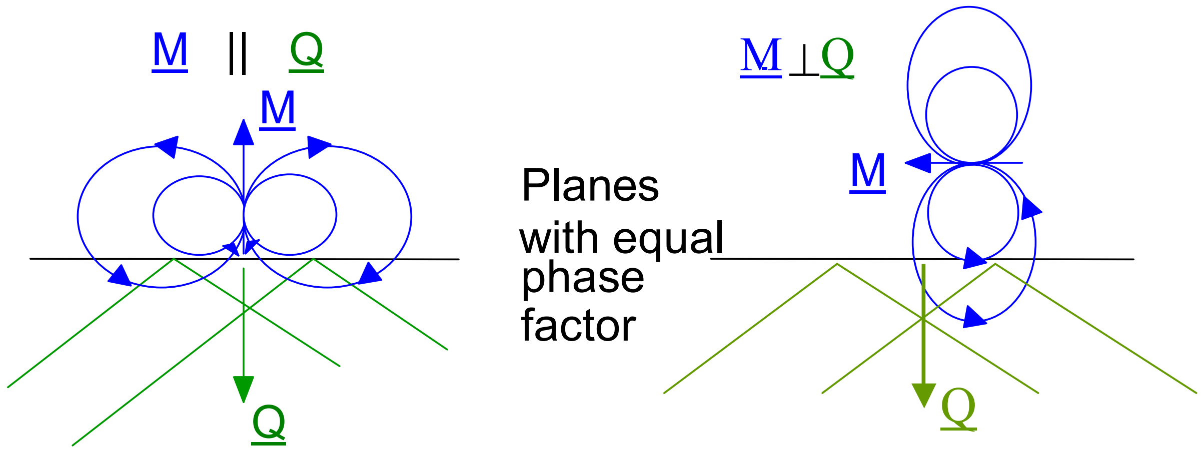

Pure Spin Scattering

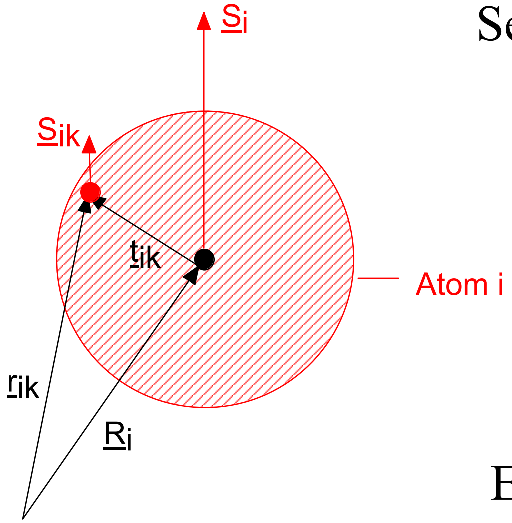

Separation of intra-atomic quantities for localised moments:

$$\underline{r}_{ik} = \underline{R}_i + \underline{t}_{ik} \quad ; \quad \underline{M}_S(\underline{r}) = -2\mu_B \sum_{ik} \delta(\underline{r} - \underline{r}_{ik}) \cdot \underline{s}_{ik}$$

$$\underline{M}(\underline{Q}) = \int \underline{M}_S(\underline{r}) e^{i\underline{Q}\cdot\underline{r}} d^3r$$

$$= \sum_{ik} e^{i\underline{Q}\cdot\underline{r}_i} \underline{s}_{ik} = \sum_i e^{i\underline{Q}\cdot\underline{R}_i} \sum_k e^{i\underline{Q}\cdot\underline{t}_{ik}} \cdot \underline{s}_{ik}$$

Expectation value of the operator for the thermodynamic state of the sample:

$$\underline{M}(\underline{Q}) = -2\mu_B \cdot f_m(\underline{Q}) \cdot \sum e^{i\underline{Q}\cdot\underline{R}_i} \cdot \underline{S}_i$$

$$f_m(\underline{Q}) = \int_{Atom} \rho_s(\underline{r}) e^{i\underline{Q}\cdot\underline{r}} d^3r$$

$$\frac{d\sigma}{d\Omega} = (\gamma r_0)^2 \left| f_m(\underline{Q}) \sum_i S_{i\perp} e^{i\underline{Q}\underline{R}_i} \right|^2$$

Form Factor: Spin, Orbit, Anisotropy

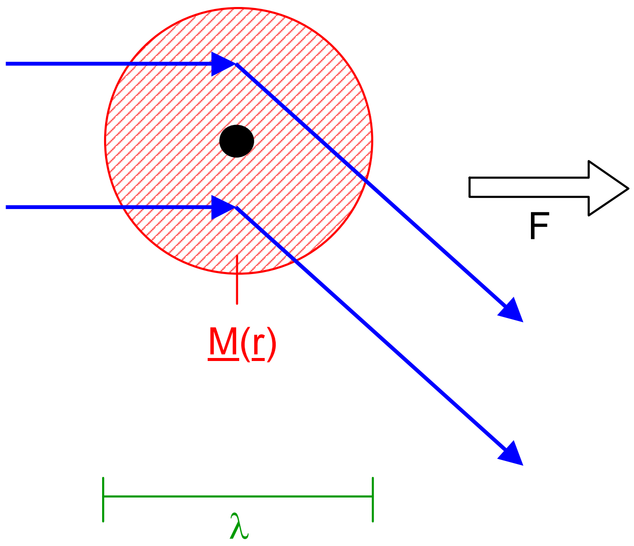

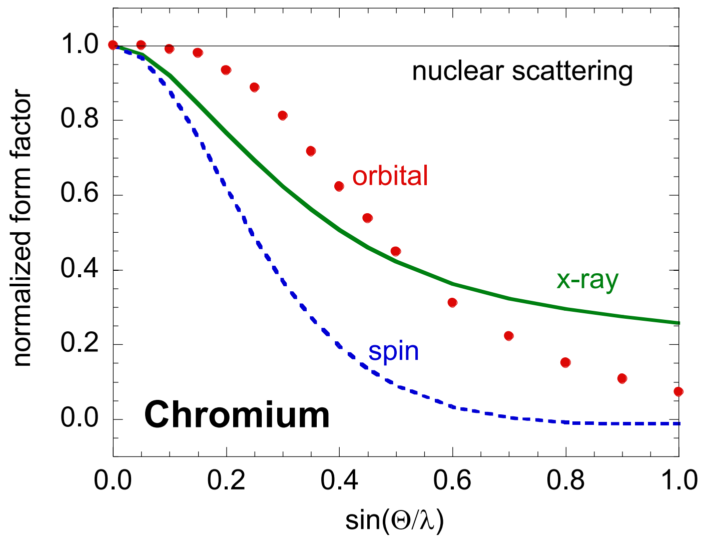

in general anisotropic:

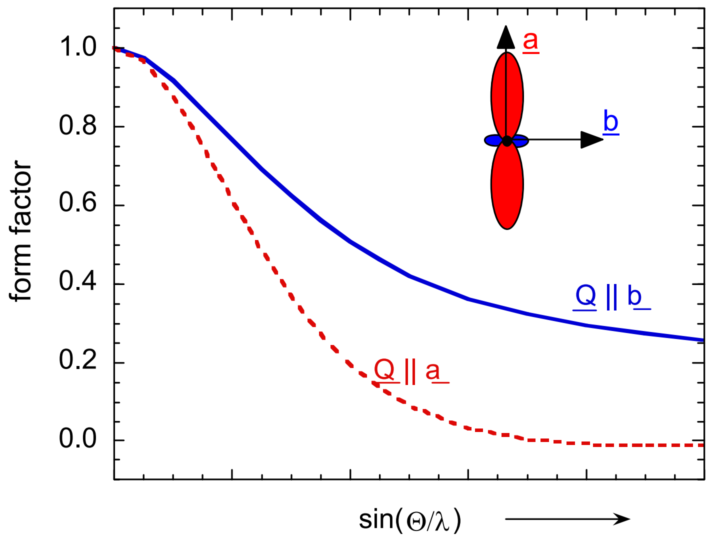

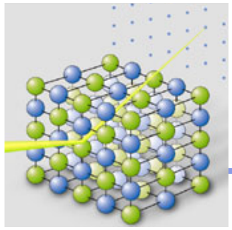

Magnetic Bragg Diffraction from a Type I Antiferromagnet on a tetragonal body-centered lattice

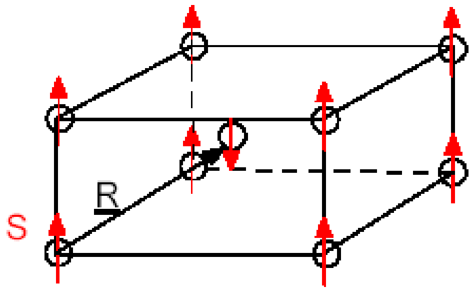

(compare MnF_2)

"scattering potential" $\rho(\underline{r}) =$ 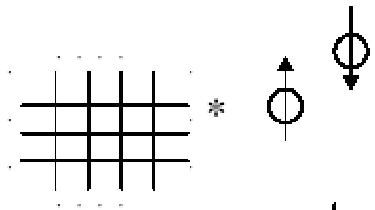

$\xrightarrow{F}$ amplitude $\xrightarrow{\text{squared}}$ intensity

$I(\underline{Q}) = L(Q) \cdot F$ 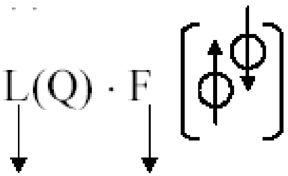

Laue function: Braggrefl. hkl

square of structure factor

nuclear structure factor

$$S_N(h,k,l) = b\left(1 + e^{2\pi i\left(h\cdot\frac{1}{2} + k\cdot\frac{1}{2} + l\cdot\frac{1}{2}\right)}\right)$$

$$= b\left(1 + (-1)^{h+k+l}\right) = \begin{cases} 0 & h+k+l \text{ odd} \\ 2b & h+k+l \text{ even} \end{cases}$$

Magnetic structure factor:

$$S_M(h,k,l) = \gamma r_o f_m S(1 - e^{2\pi i(h\cdot\frac{1}{2}+k\cdot\frac{1}{2}+l\cdot\frac{1}{2})})$$

$$= \gamma r_o f_m S(1-(-1)^{h+k+l}) = \begin{cases} 2\gamma r_o f_m S & h+k+l \text{ odd} \\ 0 & h+k+l \text{ even} \end{cases}$$

directional dependence : only $S \perp Q$

$\Rightarrow$ 00l-peaks are extinct

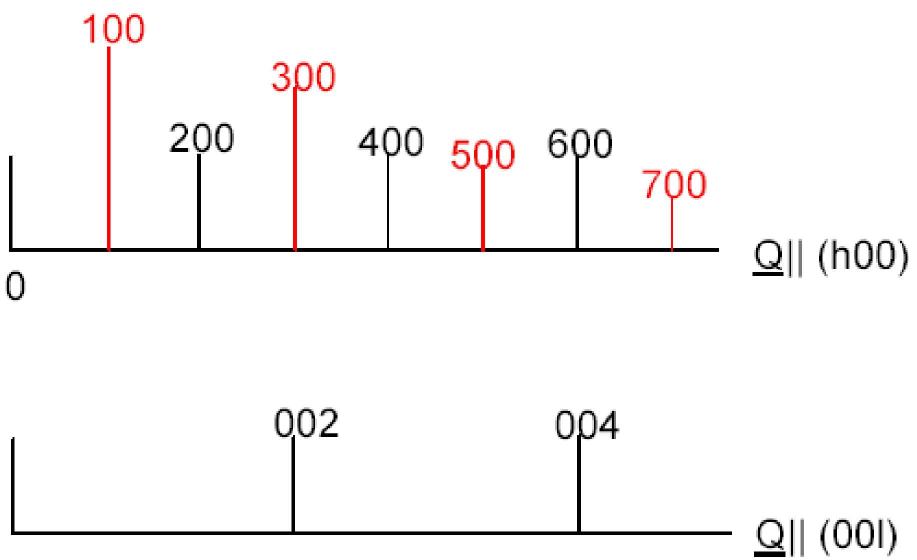

Magnetic Neutron Scattering

Neutron Powder Diffraction

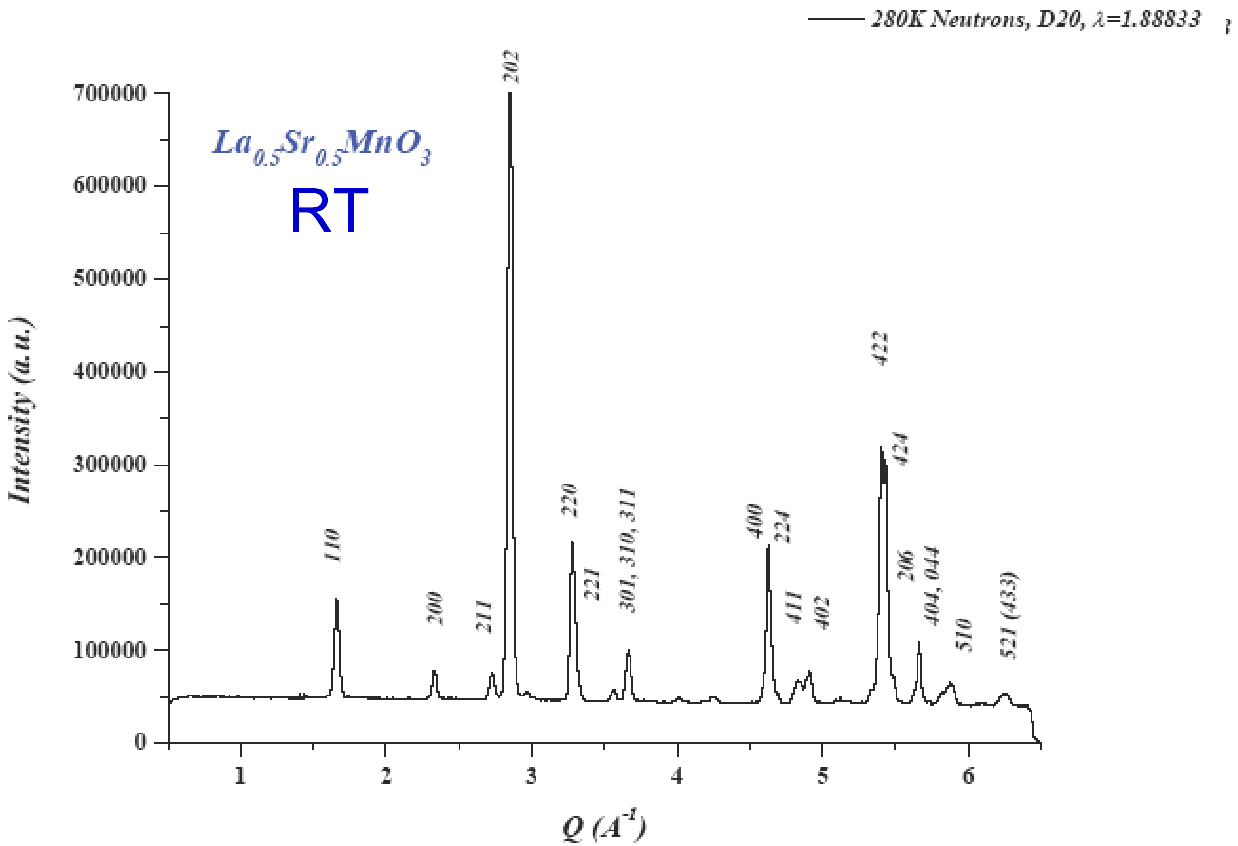

Distorted Perovskite structure

E. Gorelik (2004)

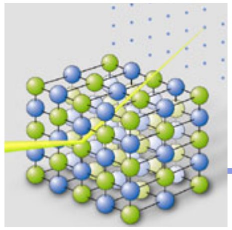

Magnetic Neutron Scattering

Neutron Powder Diffraction

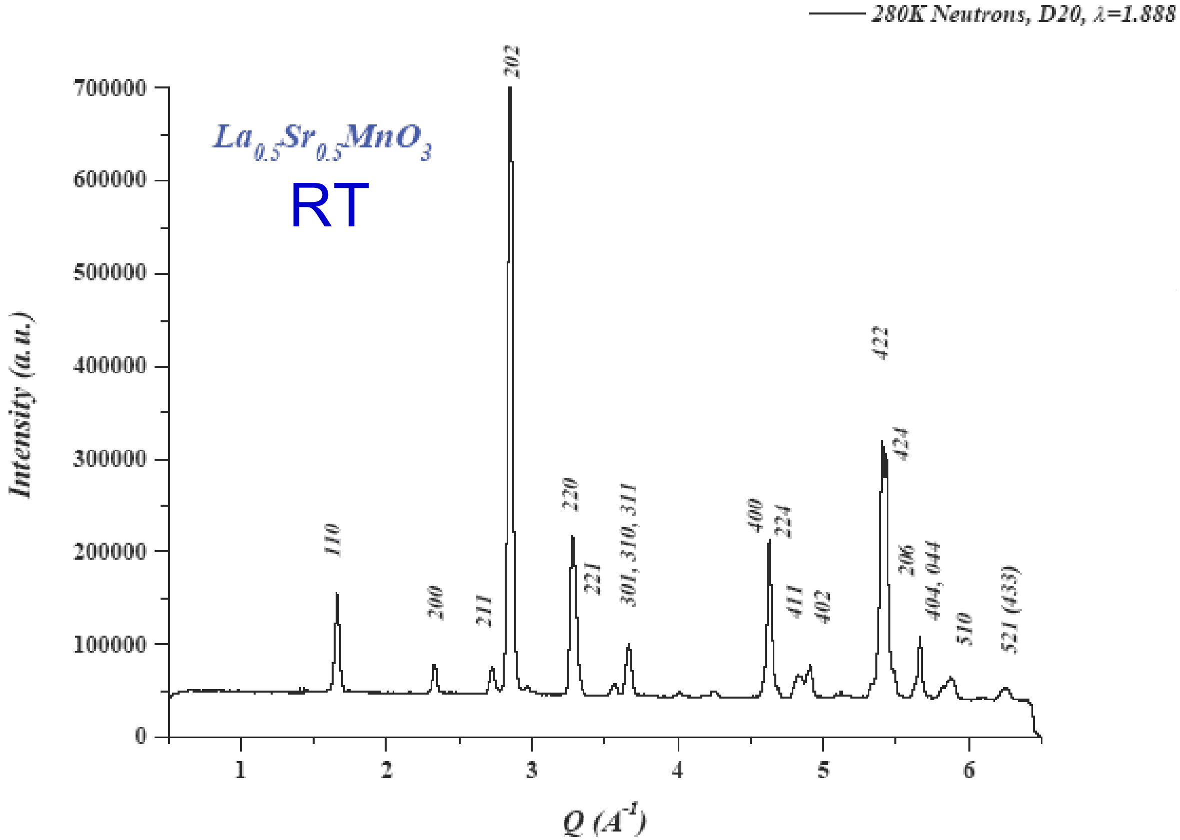

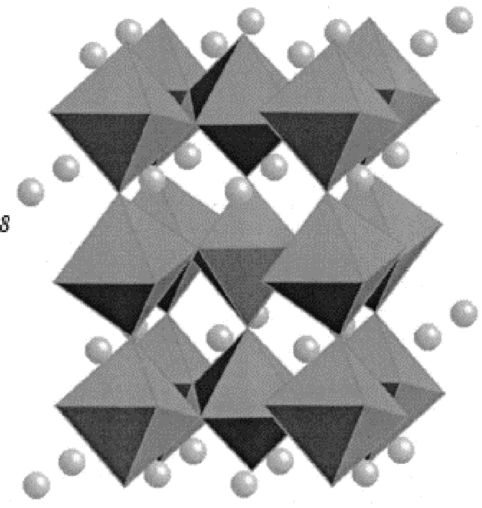

Distorted Perovskite structure

E. Gorelik (2004)

Magnetic Neutron Scattering

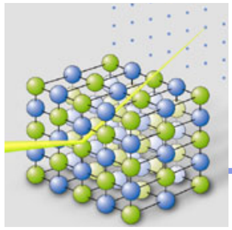

Neutron Powder Diffraction

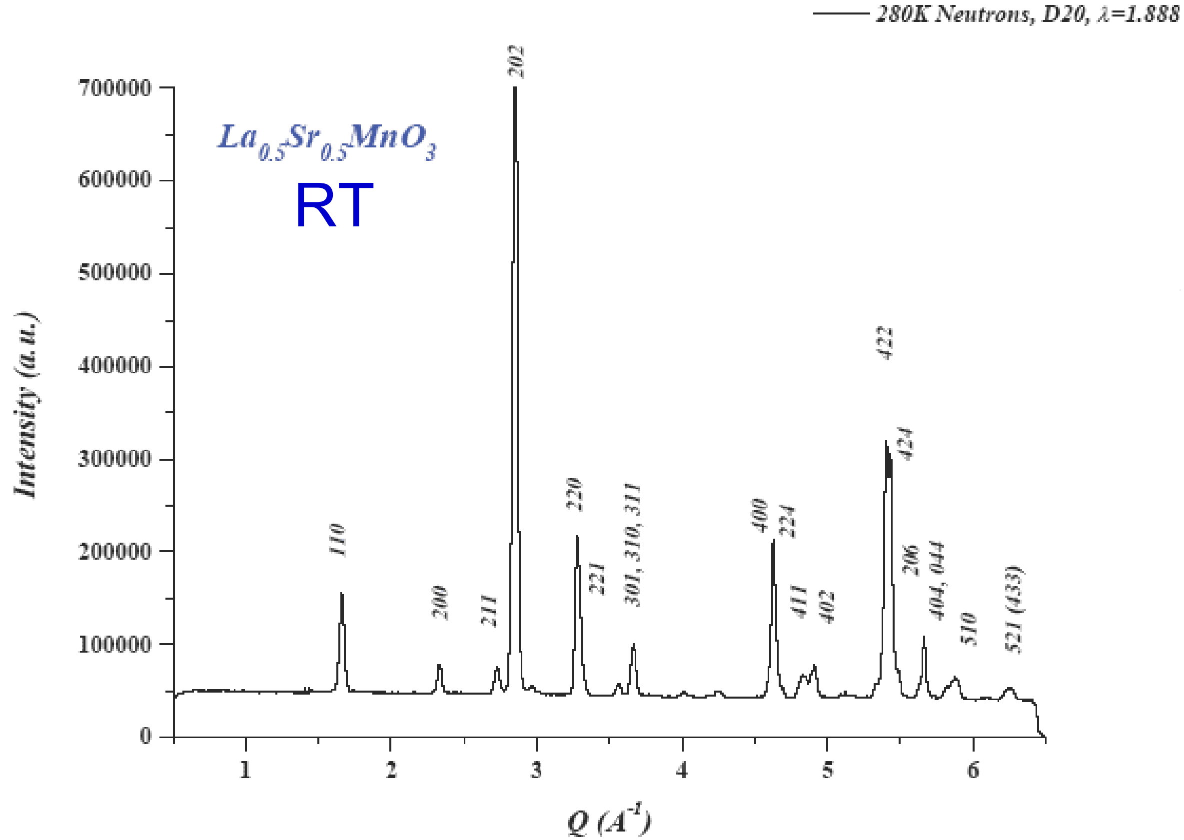

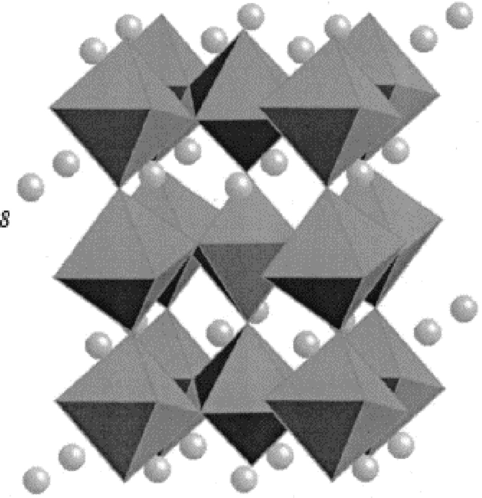

Distorted Perovskite structure

Spin Structure:

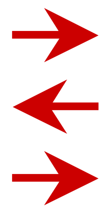

E. Gorelik (2004)

Magnetic Neutron Scattering

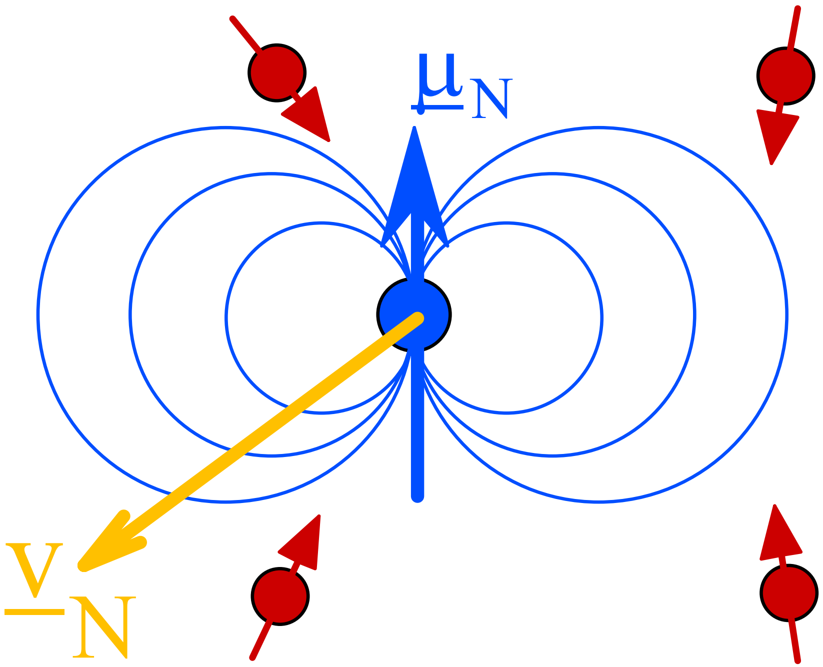

Interaction:

Magnetic Dipole-Dipole

$$\underline{M}(\underline{r},t) = \underline{\underline{\chi}}(\underline{r},\underline{r}',t,t')\cdot\underline{H}(\underline{r}',t')$$

Elastic scattering:

$$\left.\frac{d\sigma}{d\omega}\right|_{mag} = (\gamma_n r_0)^2 \left| -\frac{1}{\mu_B}\langle\sigma_z'|\underline{\sigma}\cdot\underline{M}_\perp(\underline{Q})|\sigma_z\rangle\right|^2$$

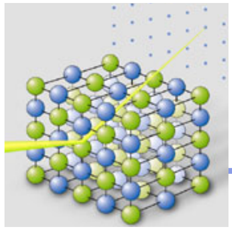

Outline

- What's new in magnetism ?
- Experimental techniques
- Elastic magnetic neutron scattering
- X-ray techniques for magnetism
- Nonresonant magnetic x-ray scattering
- Resonant magnetic x-ray scattering
- Example: Non-resonant scattering from transition metal di-flourides
- Example: Resonance exchange scattering from mixed crystals
- Summary

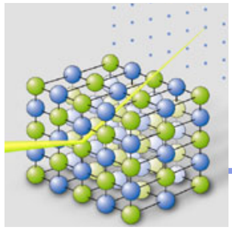

X-Ray Powder Diffraction

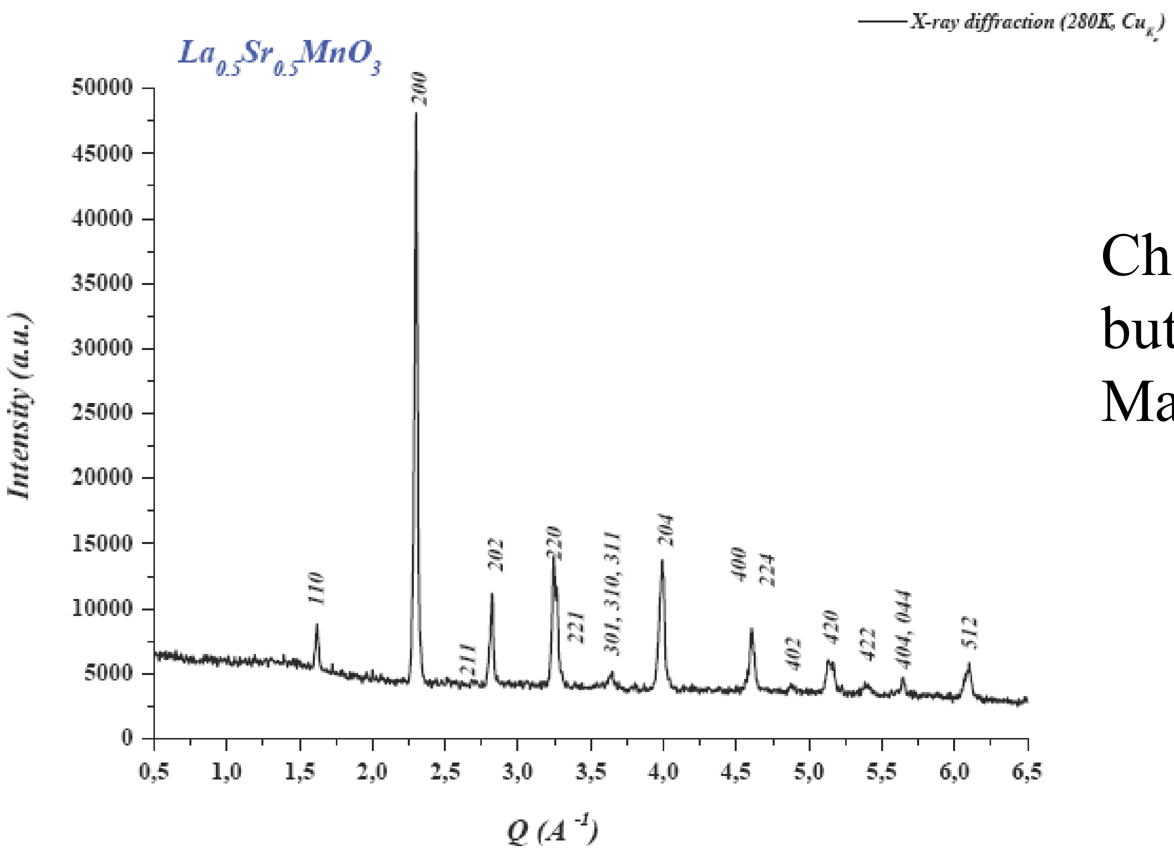

Chemical structure,
but <u>not</u>
Magnetic Structure

510

$La_{7/8}Sr_{1/8}MnO_3$-Kristall

Perßon, Li, Mattauch, Kaiser, Roth, Heger (2004)

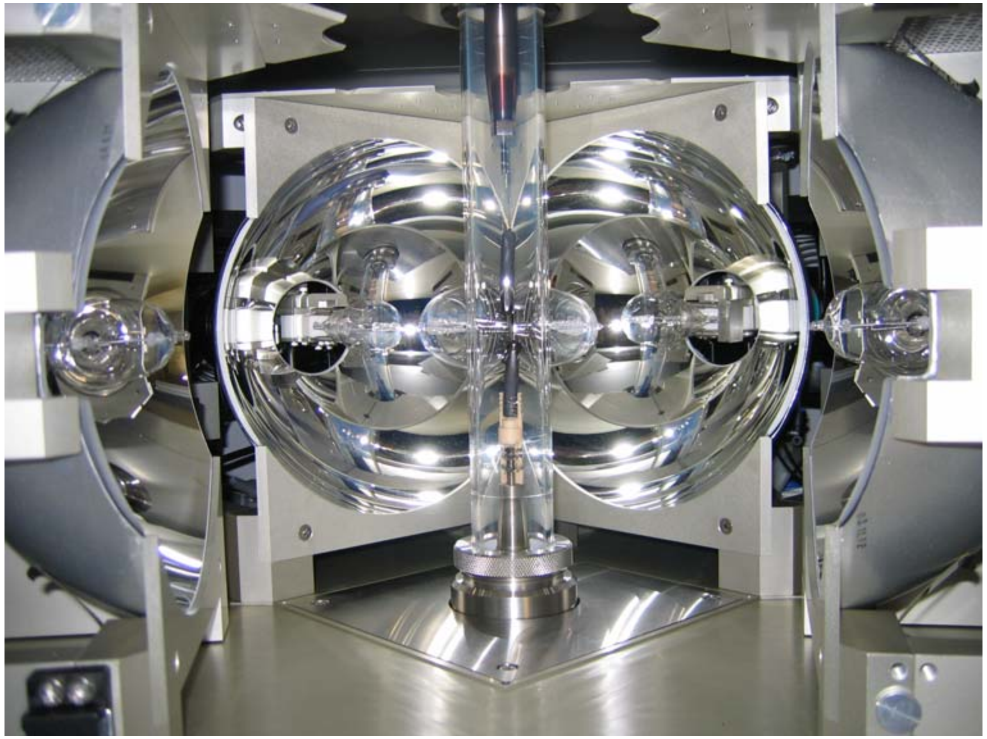

$La_{7/8}Sr_{1/8}MnO_3$-Kristall

Perßon, Li, Mattauch, Kaiser, Roth, Heger (2004)

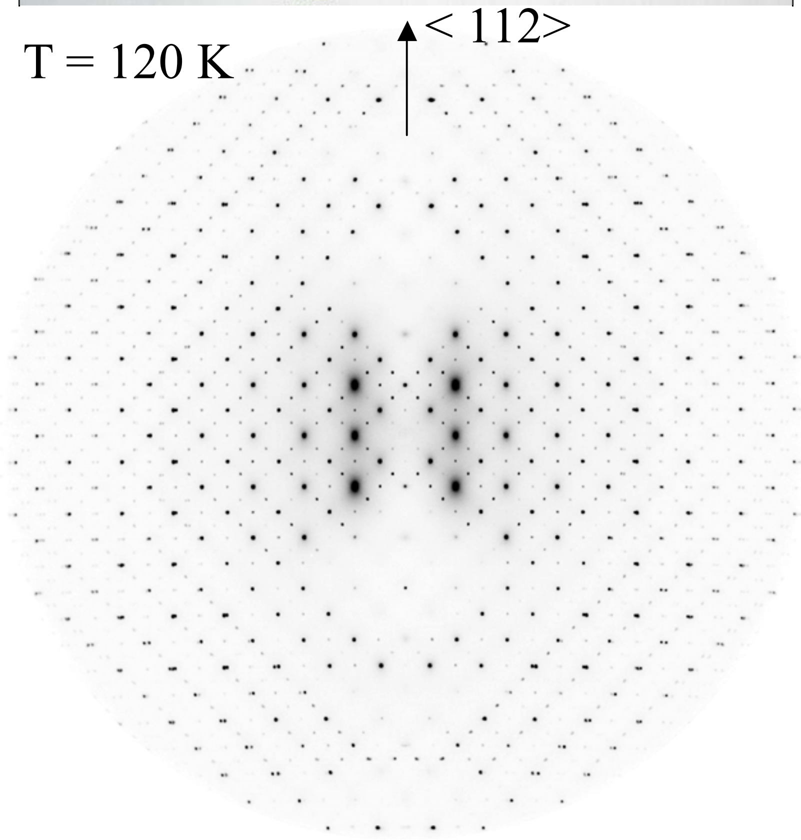

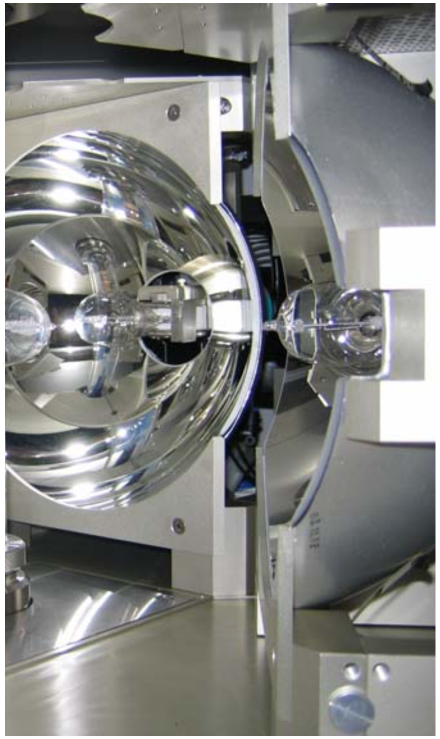

Synchrotron Sources

ESRF @ Grenoble, France
6 GeV

APS @ Argonne/Chicago, USA
7 GeV

SPRING8, Japan, 8 GeV

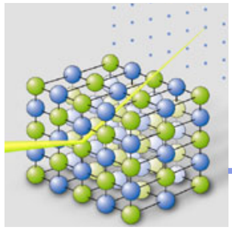

X-Ray Probes of Magnetism

- Kerr-microscopy
- Faraday effect
- Linear x-ray magnetic dichroism
- Circular x-ray magnetic dichroism
- Spin resolved x-ray absorption fine structure SEXAFS
- Magnetic x-ray diffraction (non-resonant scattering)
- Resonant magnetic x-ray scattering (X-ray resonance exchange scattering XRES)
- Nuclear resonant scattering
- Magnetic x-ray reflectivity
- Magnetic Compton scattering
- Angular- and spin resolved photoemission

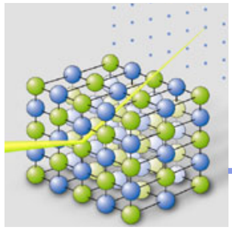

X-Ray Probes of Magnetism

- Kerr-microscopy
- Faraday effect
- Linear x-ray magnetic dichroism
- Circular x-ray magnetic dichroism
- Spin resolved x-ray absorption fine structure SEXAFS
- Magnetic x-ray diffraction (non-resonant scattering)
- Resonant magnetic x-ray scattering (X-ray resonance exchange scattering XRES)
- Nuclear resonant scattering
- Magnetic x-ray reflectivity
- Magnetic Compton scattering
- Angular- and spin resolved photoemission

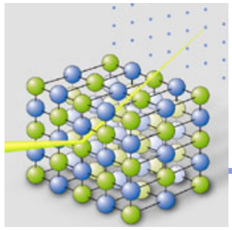

Outline

- What's new in magnetism ?
- Experimental techniques
- Elastic magnetic neutron scattering
- X-ray techniques for magnetism
- Nonresonant magnetic x-ray scattering
- Resonant magnetic x-ray scattering
- Example: Non-resonant scattering from transition metal di-flourides
- Example: Resonance exchange scattering from mixed crystals
- Summary

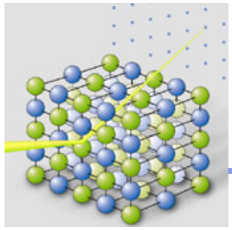

Nonresonant Scattering: Classical

Thomson scattering
from charges
⇒ **Structure**

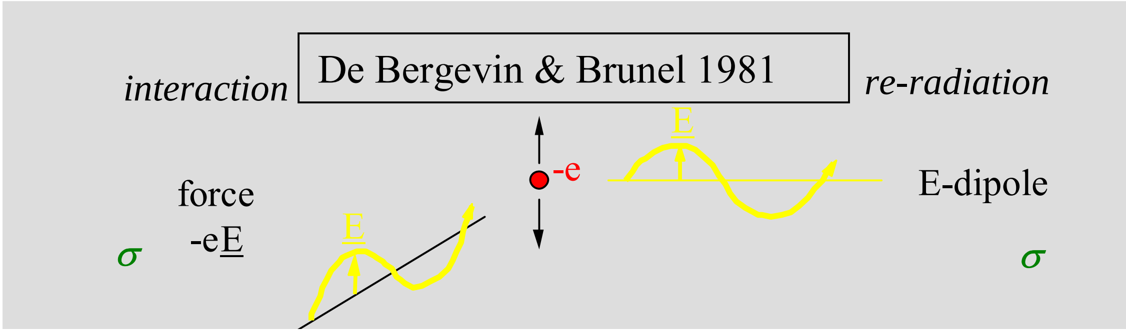

Nonresonant Scattering: Classical

Thomson scattering
from charges
⇒ **Structure**

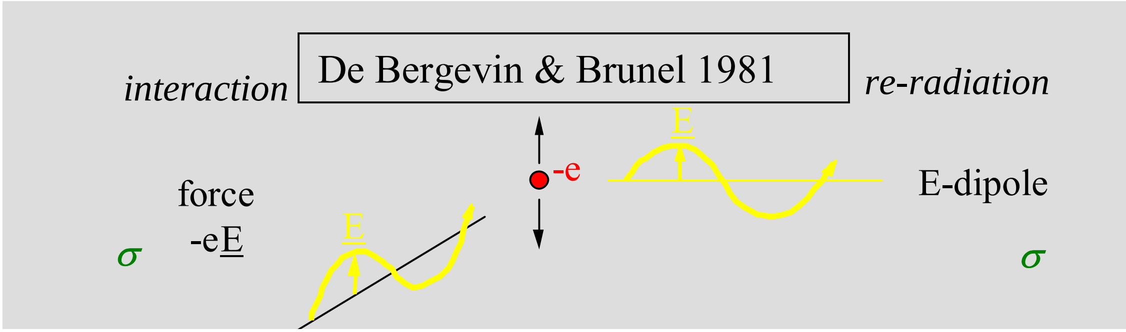

But: X-rays are
electro***magnetic***
radiation ⇒
non resonant
magnetic x-ray
scattering
⇒ **Magnetism**

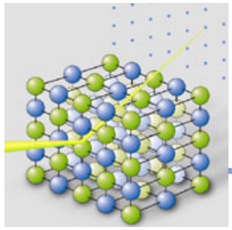

Cross Section for Magnetic X-Ray Scattering

Non-relativistic treatment in second order perturbation theory (Blume 1985, Blume & Gibbs 1988)

- Hamiltonian for e^- in e-m field:

$$H = \sum_j \frac{1}{2m}\left(\underline{P}_j - \frac{e}{c}\underline{A}(\underline{r}_j)\right)^2$$ kinetic energy

$$+ \sum_{ji} V(\underline{r}_{ij})$$ Coulomb interaction

$$- \frac{e\hbar}{mc}\sum_j \underline{s}_j \cdot \underline{\nabla} \times \underline{A}(\underline{r}_j)$$ Zeeman energy $-\underline{\mu} \cdot \underline{H}$

$$- \frac{e\hbar}{2(mc)^2}\sum_j \underline{s}_j \cdot \underline{E}(\underline{r}_j) \times \left(\underline{P}_j - \frac{e}{c}\underline{A}(\underline{r}_j)\right)$$ spin-orbit coupling $-\underline{\mu}\cdot\underline{H} \sim \underline{s}\cdot(\underline{E}\times\underline{v})$

$$+ \sum_{k\lambda} \hbar\omega_k \left(c^+(\underline{k}\lambda)c(\underline{k}\lambda) + \frac{1}{2}\right)$$ self energy of e-m-field

- Vector potential in plane wave expansion:

$$\underline{A}(\underline{r}) = \sum_{\underline{q}\sigma}\left(\frac{2\pi\hbar c^2}{V\omega_q}\right)^{\frac{1}{2}} \times \left[\underline{\varepsilon}(\underline{q}\sigma)c(\underline{q}\sigma)e^{i\underline{q}\cdot\underline{r}} + \underline{\varepsilon}^*(\underline{q}\sigma)c^+(\underline{q}\sigma)e^{-i\underline{q}\cdot\underline{r}}\right]$$

Cross Section for Magnetic X-Ray Scattering

$$H = H_o + H_r + H_{int}$$

e^--system (H_o) e-m-wave (H_r) interaction (H_{int})

→ perturbation theory (Fermi's "golden rule")

$$\frac{d\sigma}{d\Omega} \propto \left| \left\langle \underline{k}', \underline{\varepsilon}', f \middle| H_{\text{int}} \middle| \underline{k}, \underline{\varepsilon}, i \right\rangle \right|^2$$

first order for terms quadratic in $\underline{A}$

second order for terms linear in $\underline{A}$

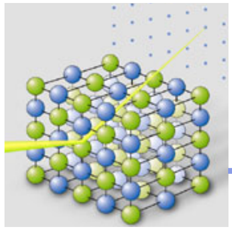

non-resonant elastic scattering cross section:

$$\left.\frac{d\sigma}{d\Omega}\right|_{\varepsilon\to\varepsilon'} = \underbrace{\left[\frac{e^2}{mc^2}\right]}_{r_e = 2.818\ \text{fm}}{}^2 \cdot \left|\left\langle f_C \right\rangle_{\varepsilon\varepsilon'}\right|^2$$

incident and final polarization

Intensity ratio:

non-resonant elastic scattering cross section:

$r_e = 2.818$ fm

$$\left.\frac{d\sigma}{d\Omega}\right|_{\varepsilon\rightarrow\varepsilon'} = \underbrace{\left[\frac{e^2}{mc^2}\right]}_{r_e = 2.818\ \text{fm}}{}^2 \cdot \left| \left\langle f_C \right\rangle_{\varepsilon'\varepsilon} + i\frac{\lambda_C}{d}\left\langle f_M \right\rangle_{\varepsilon'\varepsilon} \right|^2$$

incident and final polarization

Intensity ratio:

non-resonant elastic scattering cross section:

$r_e = 2.818$ fm

$$\left.\frac{d\sigma}{d\Omega}\right|_{\varepsilon\to\varepsilon'} = \underbrace{\left[\frac{e^2}{mc^2}\right]}_{r_e}{}^2 \cdot \left| \left\langle f_C \right\rangle_{\varepsilon'\varepsilon} + i\frac{\lambda_C}{d}\left\langle f_M \right\rangle_{\varepsilon'\varepsilon} \right|^2$$

incident and final polarization

charge ~ $|f_C|^2$

Intensity ratio:

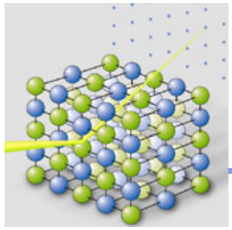

non-resonant elastic scattering cross section:

$$\left.\frac{d\sigma}{d\Omega}\right|_{\varepsilon\to\varepsilon'} = \Big[\underbrace{\frac{e^2}{mc^2}}_{r_e\,=\,2.818\ \mathrm{fm}}\Big]^2 \cdot \left| \langle f_C \rangle_{\varepsilon'\varepsilon} + i\frac{\lambda_C}{d}\langle f_M \rangle_{\varepsilon'\varepsilon} \right|^2$$

incident and final polarization

charge ~ $|f_C|^2$

magnetic~ $|f_M|^2$

Intensity ratio:

non-resonant elastic scattering cross section:

$r_e = 2.818$ fm

$$\left.\frac{d\sigma}{d\Omega}\right|_{\varepsilon\to\varepsilon'} = \left[\frac{e^2}{mc^2}\right]^2 \cdot \left| \langle f_C \rangle_{\varepsilon'\varepsilon} + i\frac{\lambda_C}{d}\langle f_M \rangle_{\varepsilon'\varepsilon} \right|^2$$

incident and final polarization

charge ~ $|f_C|^2$ magnetic~ $|f_M|^2$

interference~ $f_C \cdot f_M$

Intensity ratio:

non-resonant elastic scattering cross section:

$r_e = 2.818$ fm $\pi/2$ phase shift

$$\left.\frac{d\sigma}{d\Omega}\right|_{\varepsilon\to\varepsilon'} = \left[\frac{e^2}{mc^2}\right]^2 \cdot \left| \langle f_C \rangle_{\varepsilon'\varepsilon} + i\frac{\lambda_C}{d}\langle f_M \rangle_{\varepsilon'\varepsilon} \right|^2$$

incident and final polarization

charge ~ $|f_C|^2$ magnetic~ $|f_M|^2$

interference~ $f_C \cdot f_M$

Intensity ratio:

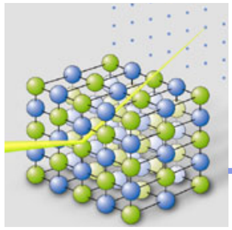

non-resonant elastic scattering cross section:

$r_e = 2.818$ fm π/2 phase shift h/mc = 2.426 pm

$$\left.\frac{d\sigma}{d\Omega}\right|_{\varepsilon\rightarrow\varepsilon'} = \left[\frac{e^2}{mc^2}\right]^2 \cdot \left| \langle f_C \rangle_{\varepsilon'\varepsilon} + i\frac{\lambda_C}{d}\langle f_M \rangle_{\varepsilon'\varepsilon} \right|^2$$

incident and final polarization

charge ~ $|f_C|^2$ magnetic~ $|f_M|^2$

interference~ $f_C \cdot f_M$

Intensity ratio:

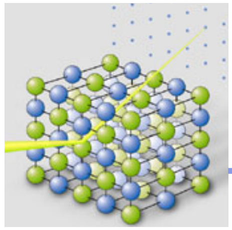

non-resonant elastic scattering cross section:

$r_e = 2.818$ fm $\qquad$ $\pi/2$ phase shift $\qquad$ $h/mc = 2.426$ pm

$$\left.\frac{d\sigma}{d\Omega}\right|_{\varepsilon\to\varepsilon'} = \left[\frac{e^2}{mc^2}\right]^2 \cdot \left| \langle f_C \rangle_{\varepsilon'\varepsilon} + i\,\frac{\lambda_C}{d} \langle f_M \rangle_{\varepsilon'\varepsilon} \right|^2$$

incident and final polarization

charge ~ $|f_C|^2$ $\qquad$ magnetic~ $|f_M|^2$

interference~ $f_C \cdot f_M$

Intensity ratio: $\frac{I_M}{I_C} \sim \left| \frac{\lambda_c}{d} \cdot \frac{N_M \cdot f_M}{N \cdot f} \langle S \rangle \right|^2 \sim 10^{-6}$

Cross Section: Nonresonant

scattering geometry:

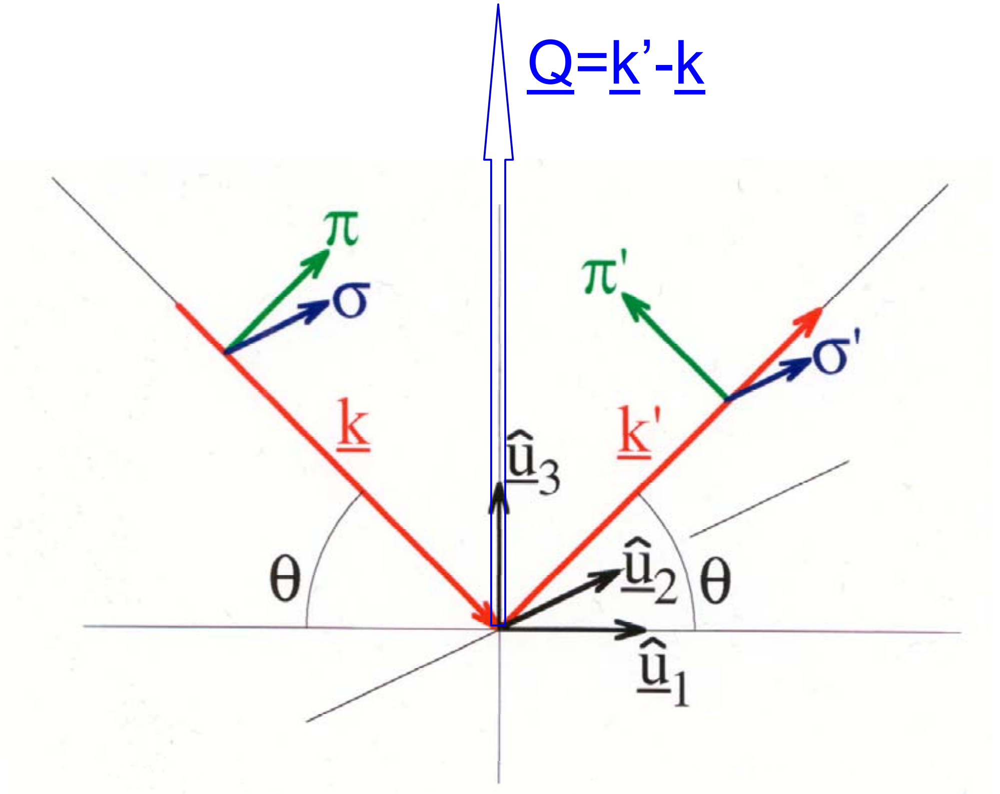

cross section:

$$\left.\frac{d\sigma}{d\Omega}\right|_{\varepsilon\to\varepsilon'} = \left[\frac{e^2}{mc^2}\right]^2 \cdot \left| \langle f_C \rangle_{\varepsilon'\varepsilon} + i\frac{\lambda_C}{d}\langle f_M \rangle_{\varepsilon'\varepsilon} \right|^2$$

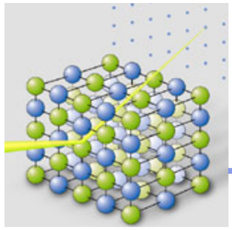

Amplitude-matrices:

$\langle f_C \rangle$ for charge scattering:

to \ from	σ	π
σ'	$\rho(\underline{Q})$	0
π'	0	$\rho(\underline{Q})(\cos 2\theta)$

$\Rightarrow$ **charge density $\boldsymbol{\rho}(\underline{\mathbf{Q}})$**

Amplitude-matrices:

$\langle f_C \rangle$ for charge scattering:

to \ from	σ	π
σ'	$\rho(\underline{Q})$	0
π'	0	$\rho(\underline{Q})(\cos 2\theta)$

⇒ charge density $\rho(\underline{Q})$

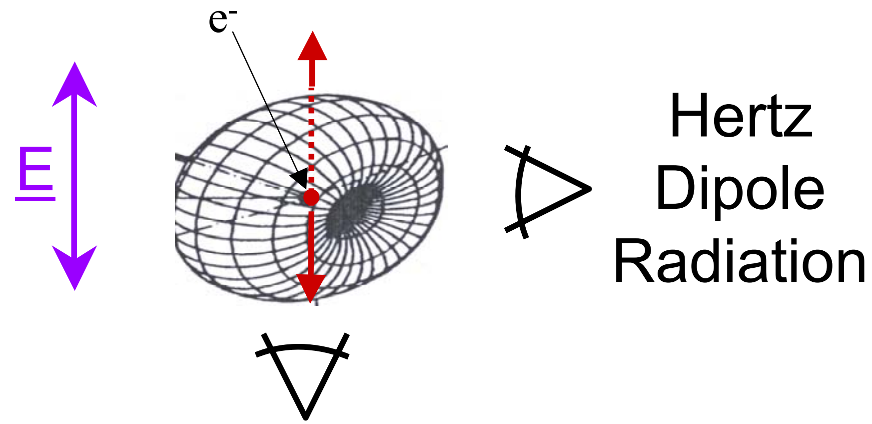

Amplitude-matrices:

$\langle f_C \rangle$ for charge scattering:

to \ from	σ	π
σ'	$\rho(\underline{Q})$	0
π'	0	$\rho(\underline{Q})(\cos 2\theta)$

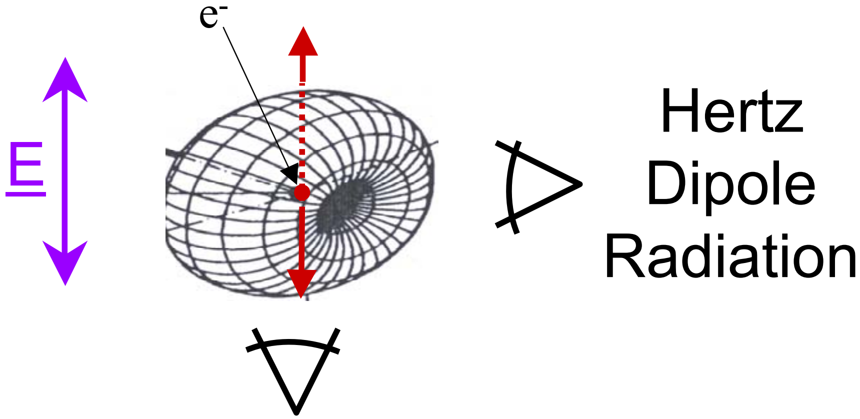

⇒ charge density ρ(Q)

$\langle f_M \rangle$ for the magnetic part:

to \ from	σ	π
σ'	$S_2 \cdot \cos\theta$	$[(L_1 + S_1) \cdot \cos\theta + S_3 \cdot \sin\theta] \cdot \sin\theta$
π'	$[-(L_1 + S_1) \cdot \cos\theta + S_3 \cdot \sin\theta] \cdot \sin\theta$	$[2 L_2 \cdot \sin^2\theta + S_2] \cdot \cos\theta$

⇒ spin density S(Q) and orbital angular momentum density L(Q)

Amplitude-matrices:

<f_C> for charge scattering:

to \ from	σ	π
σ'	$\rho(\underline{Q})$	0
π'	0	$\rho(\underline{Q})(\cos 2\theta)$

⇒ charge density $\rho(\underline{Q})$

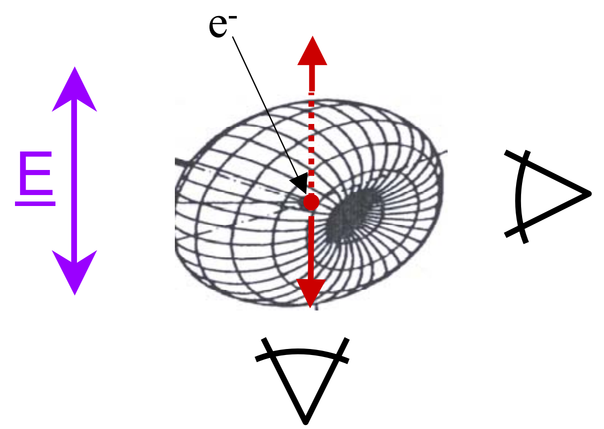

Hertz Dipole Radiation

<f_M> for the magnetic part:

to \ from	σ	π
σ'	$S_2 \cdot \cos\theta$	$[(L_1 + S_1)\cdot\cos\theta + S_3\cdot\sin\theta]\cdot\sin\theta$
π'	$[-(L_1 + S_1)\cdot\cos\theta + S_3\cdot\sin\theta]\cdot\sin\theta$	$\left[2L_2\cdot\sin^2\theta + S_2\right]\cdot\cos\theta$

⇒ spin density $\underline{S}(\underline{Q})$ and orbital angular momentum density $\underline{L}(\underline{Q})$

➡ Charge scattering: "NSF"

➡ Magnetic scattering: "NSF" (S_2, L_2) – ⊥ scattering plane
+ "SF" (S_1, S_3, L_1) – in scattering plane

⇒ **Separation $\underline{S} \leftrightarrow \underline{L}$**

Synchrotron X-Ray Source

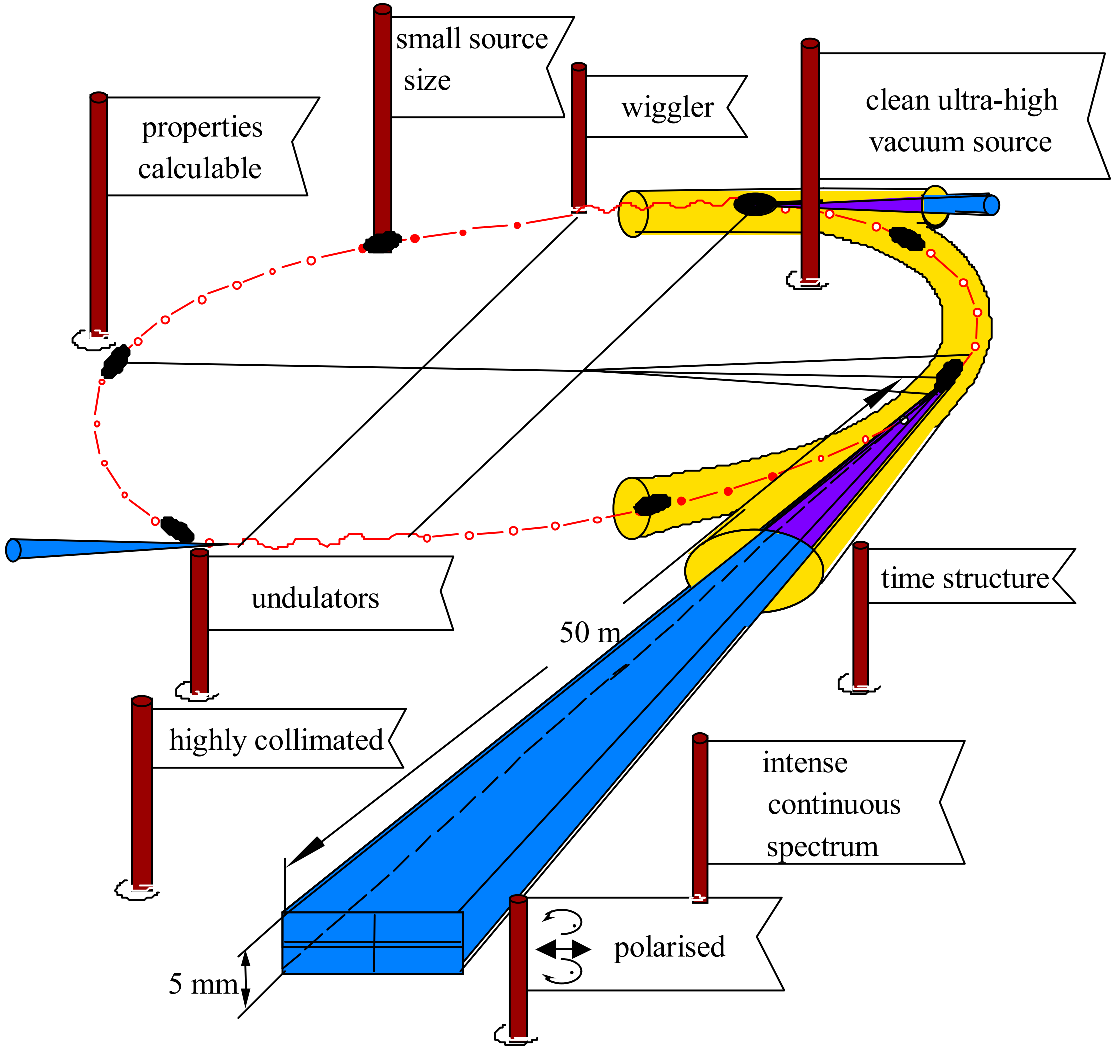

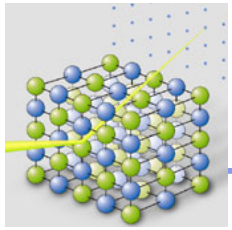

Outline

- What's new in magnetism ?
- Experimental techniques
- Elastic magnetic neutron scattering
- X-ray techniques for magnetism
- Nonresonant magnetic x-ray scattering
- Resonant magnetic x-ray scattering
- Example: Non-resonant scattering from transition metal di-flourides
- Example: Resonance exchange scattering from mixed crystals
- Summary

Resonant Magnetic X-Ray Scattering

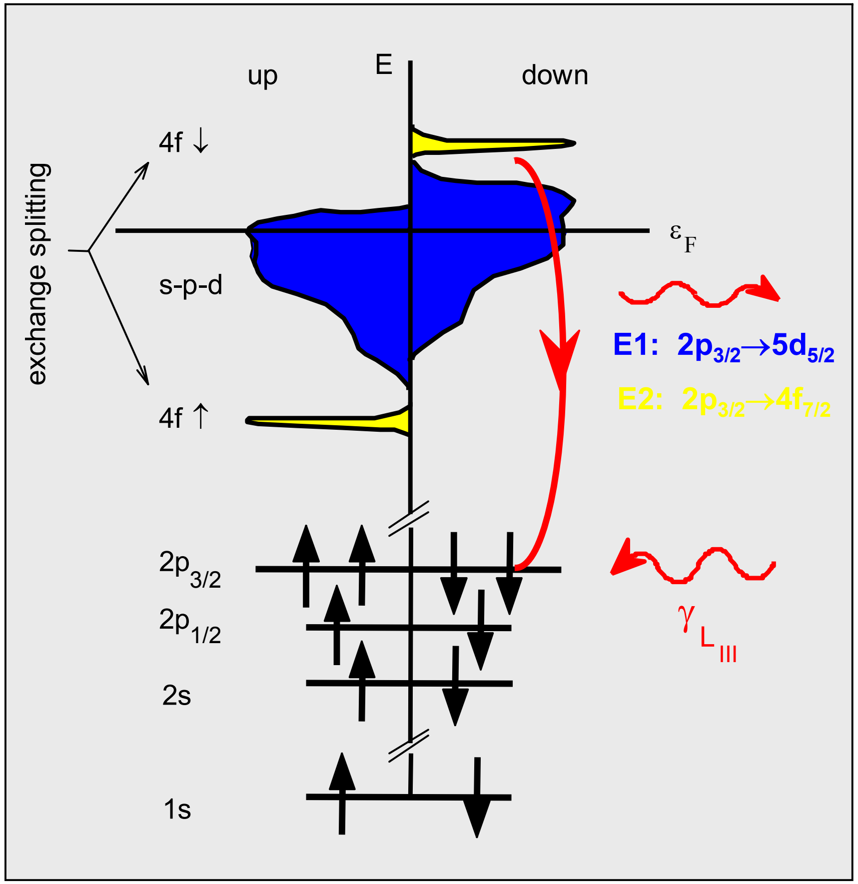

Hannon, Trammell, Blume & Gibbs
PRL 61 (1988), 1245

Resonant Magnetic X-Ray Scattering

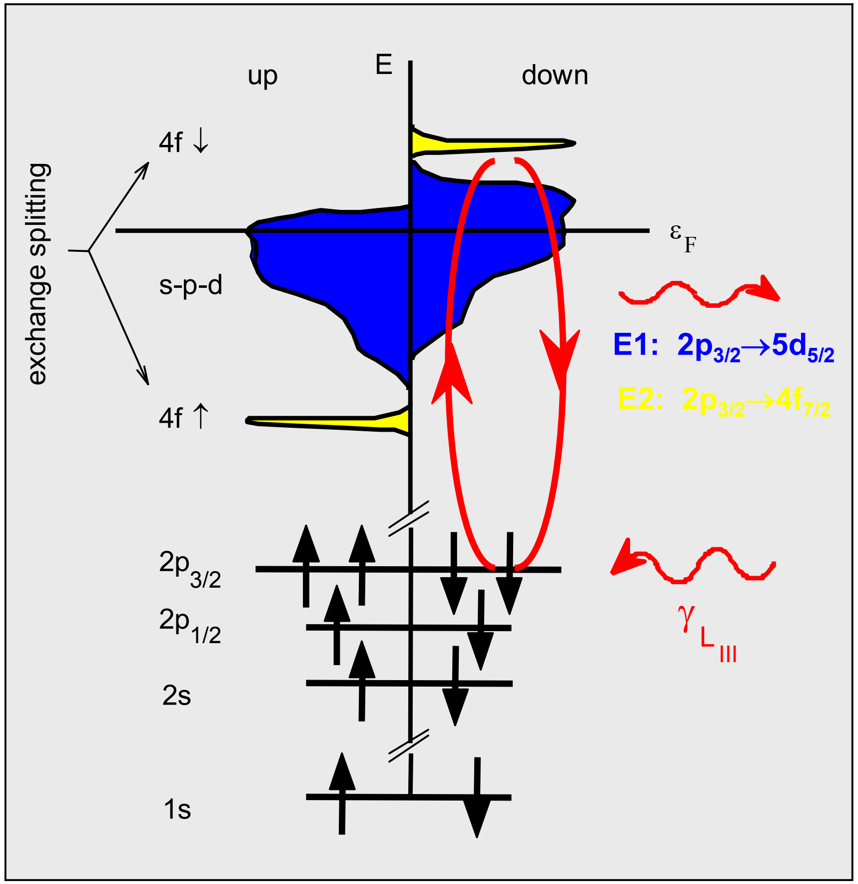

Hannon, Trammell, Blume & Gibbs
PRL 61 (1988), 1245

Resonant Magnetic X-Ray Scattering

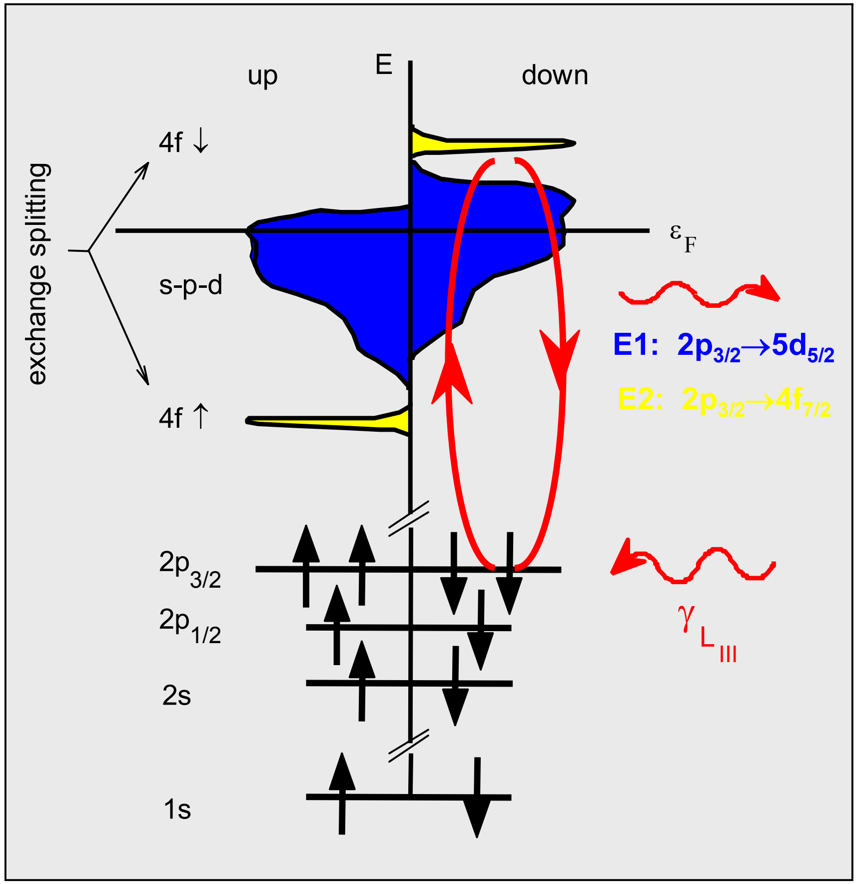

resonance exchange scattering

Hannon, Trammell, Blume & Gibbs
PRL 61 (1988), 1245

Resonant Magnetic X-Ray Scattering

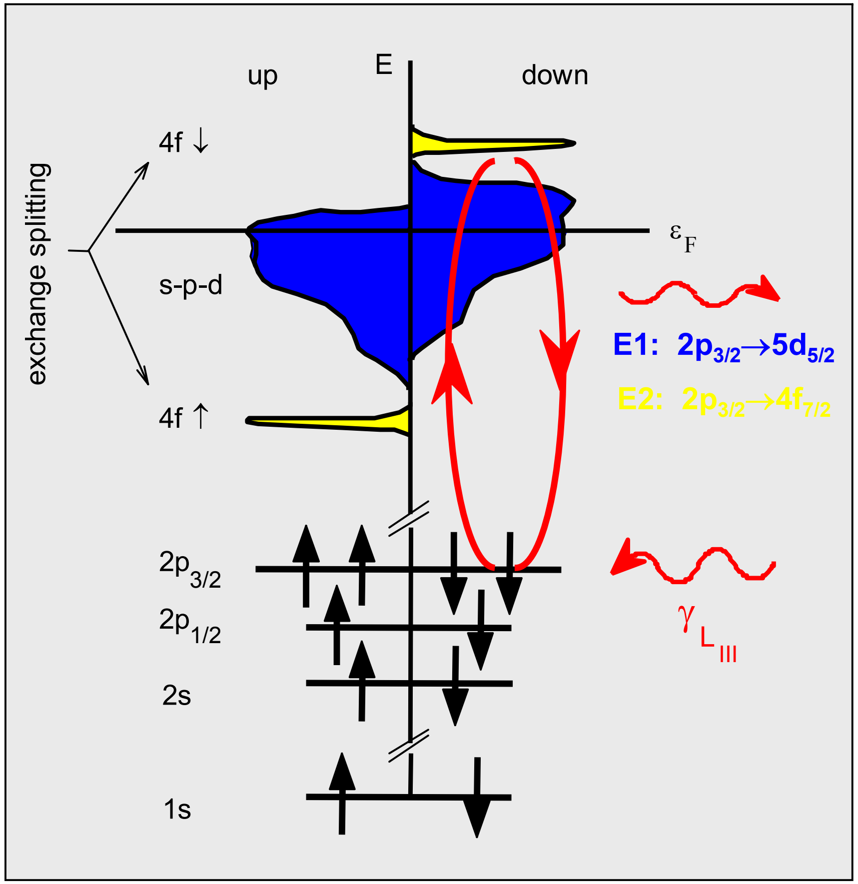

resonance exchange scattering

$$\left.\frac{d\sigma}{d\Omega}\right|_{mag} \propto \left|\frac{\alpha_M / E}{(E - E_0) - i\Gamma / 2}\right|^2$$

Hannon, Trammell, Blume & Gibbs
PRL 61 (1988), 1245

Resonant Magnetic X-Ray Scattering

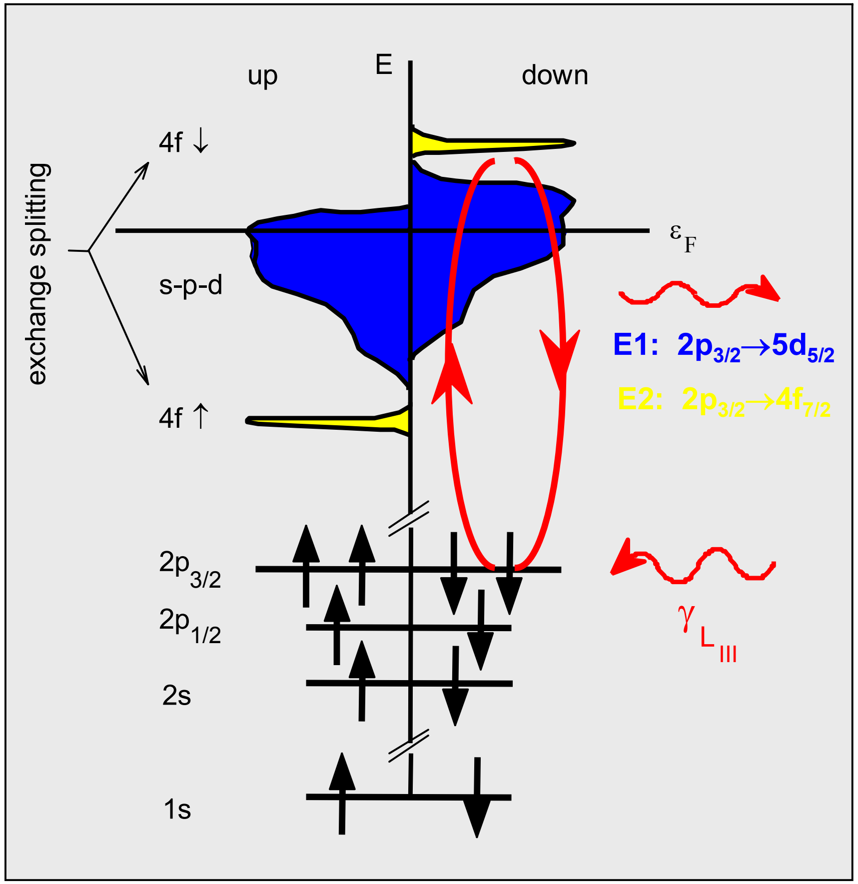

resonance exchange scattering

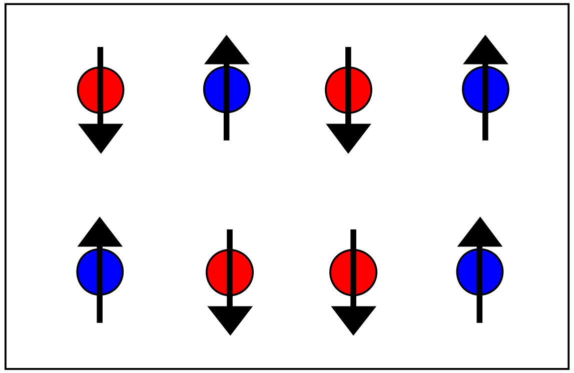

neutron scattering

$$\left.\frac{d\sigma}{d\Omega}\right|_{mag} \propto \left| \frac{\alpha_M / E}{(E - E_0) - i\Gamma/2} \right|^2$$

Hannon, Trammell, Blume & Gibbs
PRL 61 (1988), 1245

Resonant Magnetic X-Ray Scattering

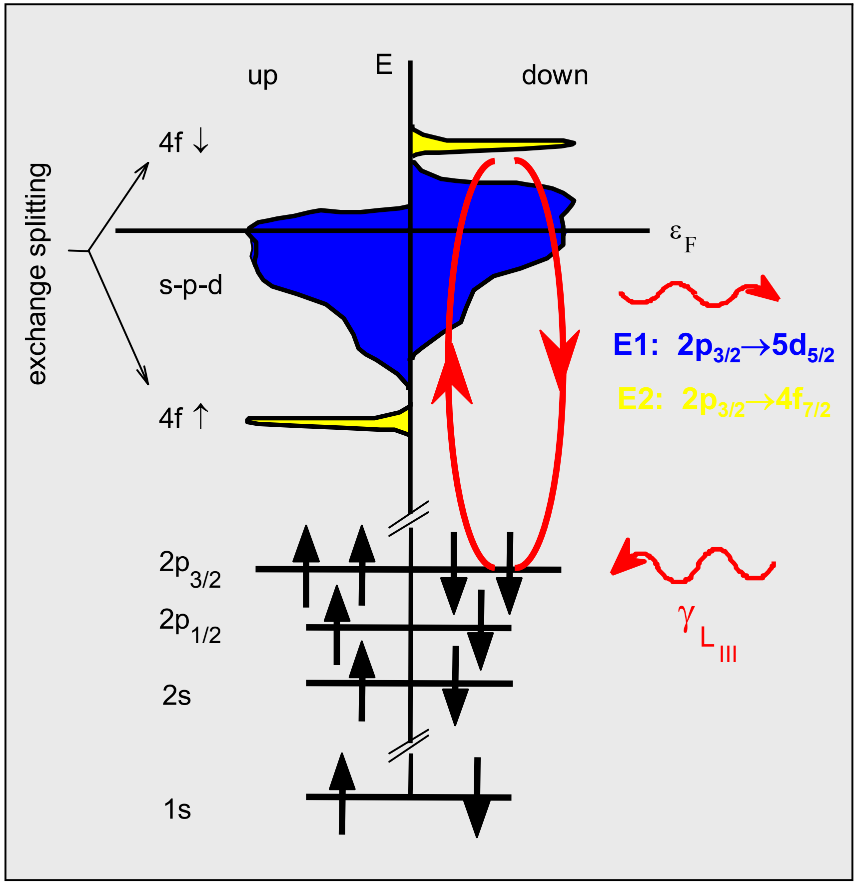

resonance exchange scattering

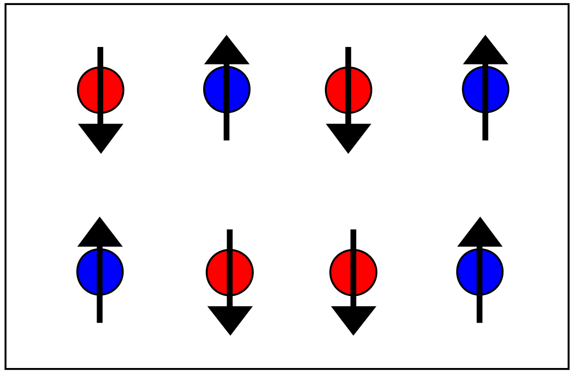

neutron scattering

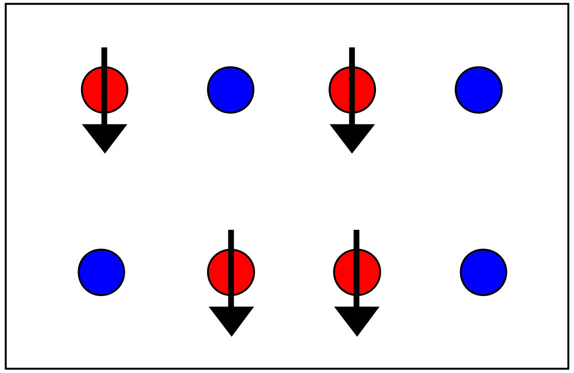

resonant x-ray scattering

$$\left.\frac{d\sigma}{d\Omega}\right|_{mag} \propto \left|\frac{\alpha_M / E}{(E - E_0) - i\Gamma/2}\right|^2$$

Hannon, Trammell, Blume & Gibbs
PRL <u>61</u> (1988), 1245

GdS: L_{II} Edge Resonance

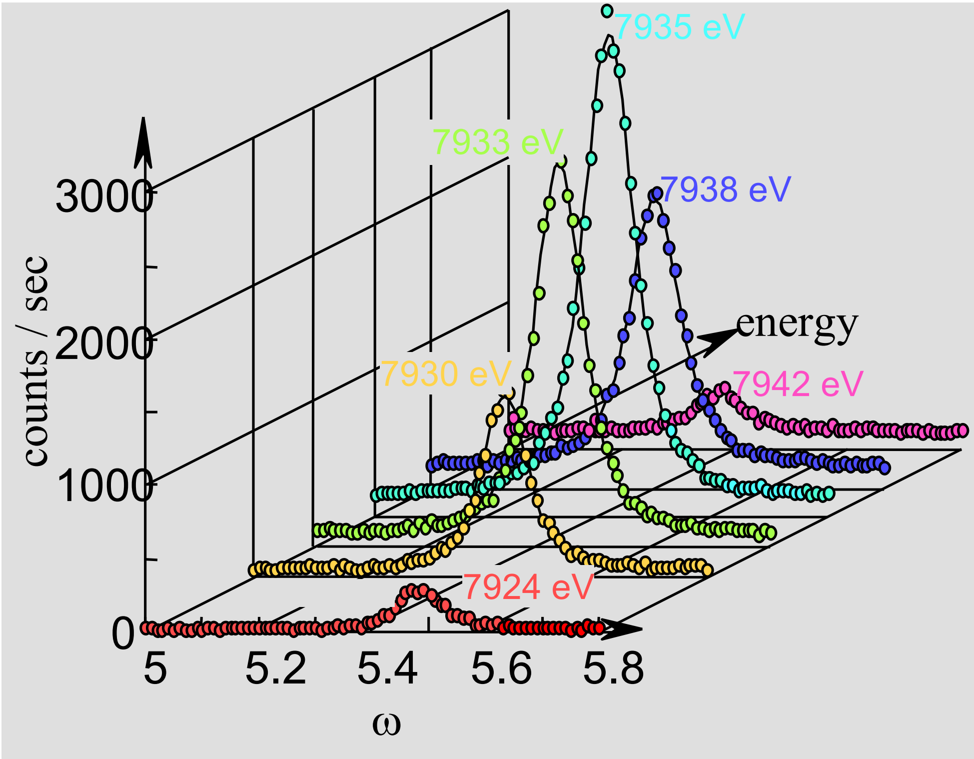

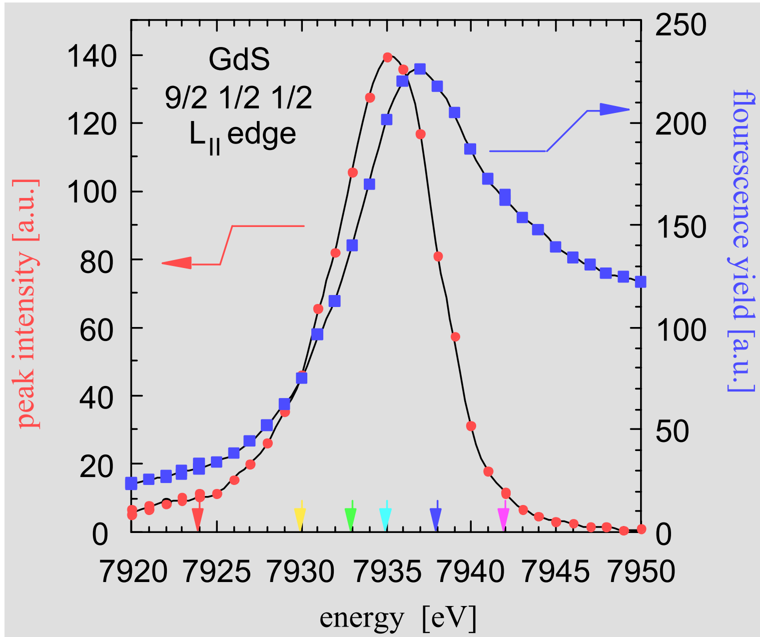

Brückel, Hupfeld, Strempfer, Caliebe, Mattenberger, Stunault, Bernhoeft, McIntyre; Eur. Phys. J B19 (2001); 475

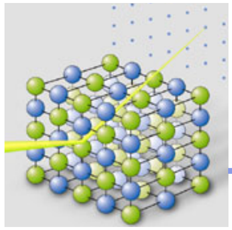

Anomalous Scattering: Cross Section

$$\left.\frac{d\sigma}{d\Omega}\right|_{\varepsilon\to\varepsilon'} = \left(\frac{e^2}{mc^2}\right)^2 \cdot \left| \left\langle f_c \right\rangle_{\varepsilon'\varepsilon} + i\frac{\lambda c}{d}\left\langle f_M \right\rangle_{\varepsilon'\varepsilon} + \left\langle f_{res}^{E1}(E) \right\rangle_{\varepsilon'\varepsilon} + \ldots \right|^2$$

Dipole Approximation:

$$f_{res}^{E1}(E) = f_o(E) + f_{circ}(E) + f_{lin}(E)$$

Amplitudes:

$$f_0(E) = (\underline{\varepsilon}' \cdot \underline{\varepsilon})\left[F_{+1}^1 + F_{-1}^1\right]$$

$$f_{circ}(E) = i(\underline{\varepsilon}' \times \underline{\varepsilon}) \cdot \underline{m}\left[F_{-1}^1 - F_{+1}^1\right]$$

$$f_{lin}(E) = (\underline{\varepsilon}' \cdot \underline{m})(\underline{\varepsilon} \cdot \underline{m})\left[2F_0^1 - F_{+1}^1 - F_{-1}^1\right]$$

Oscillator Strengths:

$$F_M^1 = \frac{\alpha_M}{(\omega - \omega_{res}) - i\Gamma/2\hbar}$$

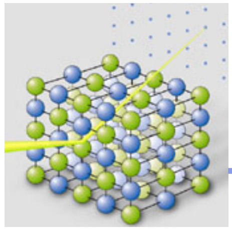

XRES: Resonance Enhancements

elements	edge	transition	energy range [keV]	resonance strength	comment
3d	K	1s → 4p	5 - 9	weak	small overlap
3d	L_I	2s → 3d	0.5 - 1.2	weak	small overlap
3d	L_{II}, L_{III}	2p → 3d	0.4 - 1.0	strong	dipolar, large overlap, high spin polarisation of 3d
4f	K	1s → 5p	40 - 63	weak	small overlap
4f	L_I	2s → 5d	6.5 - 11	weak	small overlap
4f	L_{II}, L_{III}	2p → 5d 2p → 4f	6 - 10	medium	dipolar quadrupolar
4f	M_I	3s → 5p	1.4 - 2.5	weak	small overlap
4f	M_{II}, M_{III}	3p → 5d 3p → 4f	1.3 - 2.2	medium to strong	dipolar quadrupolar
4f	M_{IV}, M_V	3d → 4f	0.9 - 1.6	strong	dipolar, large overlap, high spin polarisation of 4f
5f	M_{IV}, M_{II}	3d → 5f	3.3 - 3.9	strong	dipolar, large overlap, high spin polarisation of 5f

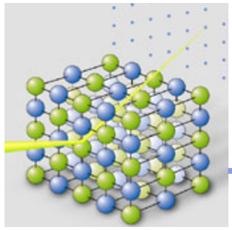

XRES: Resonance Enhancements

thin films

elements	edge	transition	energy range [keV]	resonance strength	comment
3d	K	1s $\rightarrow$ 4p	5 - 9	weak	small overlap
3d	L_I	2s $\rightarrow$ 3d	0.5 - 1.2	weak	small overlap
3d	L_{II}, L_{III}	2p $\rightarrow$ 3d	0.4 - 1.0	strong	dipolar, large overlap, high spin polarisation of 3d
4f	K	1s $\rightarrow$ 5p	40 - 63	weak	small overlap
4f	L_I	2s $\rightarrow$ 5d	6.5 - 11	weak	small overlap
4f	L_{II}, L_{III}	2p $\rightarrow$ 5d 2p $\rightarrow$ 4f	6 - 10	medium	dipolar quadrupolar
4f	M_I	3s $\rightarrow$ 5p	1.4 - 2.5	weak	small overlap
4f	M_{II}, M_{III}	3p $\rightarrow$ 5d 3p $\rightarrow$ 4f	1.3 - 2.2	medium to strong	dipolar quadrupolar
4f	M_{IV}, M_V	3d $\rightarrow$ 4f	0.9 - 1.6	strong	dipolar, large overlap, high spin polarisation of 4f
5f	M_{IV}, M_{II}	3d $\rightarrow$ 5f	3.3 - 3.9	strong	dipolar, large overlap, high spin polarisation of 5f

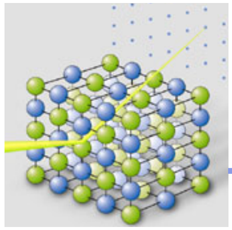

XRES: Resonance Enhancements

thin films

elements	edge	transition	energy range [keV]	resonance strength	comment
3d	K	1s $\rightarrow$ 4p	5 - 9	weak	small overlap
3d	L_I	2s $\rightarrow$ 3d	0.5 - 1.2	weak	small overlap
3d	L_{II}, L_{III}	2p $\rightarrow$ 3d	0.4 - 1.0	strong	dipolar, large overlap, high spin polarisation of 3d
4f	K	1s $\rightarrow$ 5p	40 - 63	weak	small overlap
4f	L_I	2s $\rightarrow$ 5d	6.5 - 11	weak	small overlap
4f	L_{II}, L_{III}	2p $\rightarrow$ 5d 2p $\rightarrow$ 4f	6 - 10	medium	dipolar quadrupolar
4f	M_I	3s $\rightarrow$ 5p	1.4 - 2.5	weak	small overlap
4f	M_{II}, M_{III}	3p $\rightarrow$ 5d 3p $\rightarrow$ 4f	1.3 - 2.2	medium to strong	dipolar quadrupolar
4f	M_{IV}, M_V	3d $\rightarrow$ 4f	0.9 - 1.6	strong	dipolar, large overlap, high spin polarisation of 4f
5f	M_{IV}, M_{II}	3d $\rightarrow$ 5f	3.3 - 3.9	strong	dipolar, large overlap, high spin polarisation of 5f

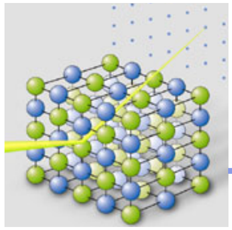

XRES: Resonance Enhancements

	elements	edge	transition	energy range [keV]	resonance strength	comment
	3d	K	$1s \rightarrow 4p$	5 - 9	weak	small overlap
	3d	L_I	$2s \rightarrow 3d$	0.5 - 1.2	weak	small overlap
thin films	**3d**	L_{II}, L_{III}	$2p \rightarrow 3d$	0.4 - 1.0	strong	dipolar, large overlap, high spin polarisation of 3d
	4f	K	$1s \rightarrow 5p$	40 - 63	weak	small overlap
	4f	L_I	$2s \rightarrow 5d$	6.5 - 11	weak	small overlap
	4f	L_{II}, L_{III}	$2p \rightarrow 5d$ $2p \rightarrow 4f$	6 - 10	medium	dipolar quadrupolar
	4f	M_I	$3s \rightarrow 5p$	1.4 - 2.5	weak	small overlap
	4f	M_{II}, M_{III}	$3p \rightarrow 5d$ $3p \rightarrow 4f$	1.3 - 2.2	medium to strong	dipolar quadrupolar
thin films	**4f**	M_{IV}, M_V	$3d \rightarrow 4f$	0.9 - 1.6	strong	dipolar, large overlap, high spin polarisation of 4f
	5f	M_{IV}, M_{II}	$3d \rightarrow 5f$	3.3 - 3.9	strong	dipolar, large overlap, high spin polarisation of 5f

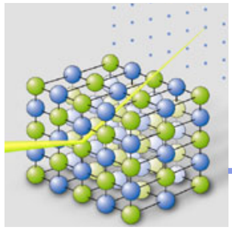

XRES: Resonance Enhancements

	elements	edge	transition	energy range [keV]	resonance strength	comment
	3d	K	1s → 4p	5 - 9	weak	small overlap
	3d	L_I	2s → 3d	0.5 - 1.2	weak	small overlap
thin films	**3d**	L_{II}, L_{III}	2p → 3d	0.4 - 1.0	strong	dipolar, large overlap, high spin polarisation of 3d
	4f	K	1s → 5p	40 - 63	weak	small overlap
	4f	L_I	2s → 5d	6.5 - 11	weak	small overlap
	4f	L_{II}, L_{III}	2p → 5d 2p → 4f	6 - 10	medium	dipolar quadrupolar
	4f	M_I	3s → 5p	1.4 - 2.5	weak	small overlap
	4f	M_{II}, M_{III}	3p → 5d 3p → 4f	1.3 - 2.2	medium to strong	dipolar quadrupolar
<u>thin films</u>	**4f**	M_{IV}, M_V	3d → 4f	0.9 - 1.6	strong	dipolar, large overlap, high spin polarisation of 4f
	5f	M_{IV}, M_{II}	3d → 5f	3.3 - 3.9	strong	dipolar, large overlap, high spin polarisation of 5f

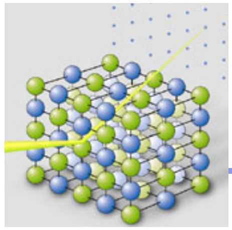

Outline

- What's new in magnetism ?
- Experimental techniques
- Elastic magnetic neutron scattering
- X-ray techniques for magnetism
- Nonresonant magnetic x-ray scattering
- Resonant magnetic x-ray scattering
- Example: Non-resonant scattering from transition metal di-flourides
- Example: Resonance exchange scattering from mixed crystals
- Summary

High Energy X-Ray Scattering

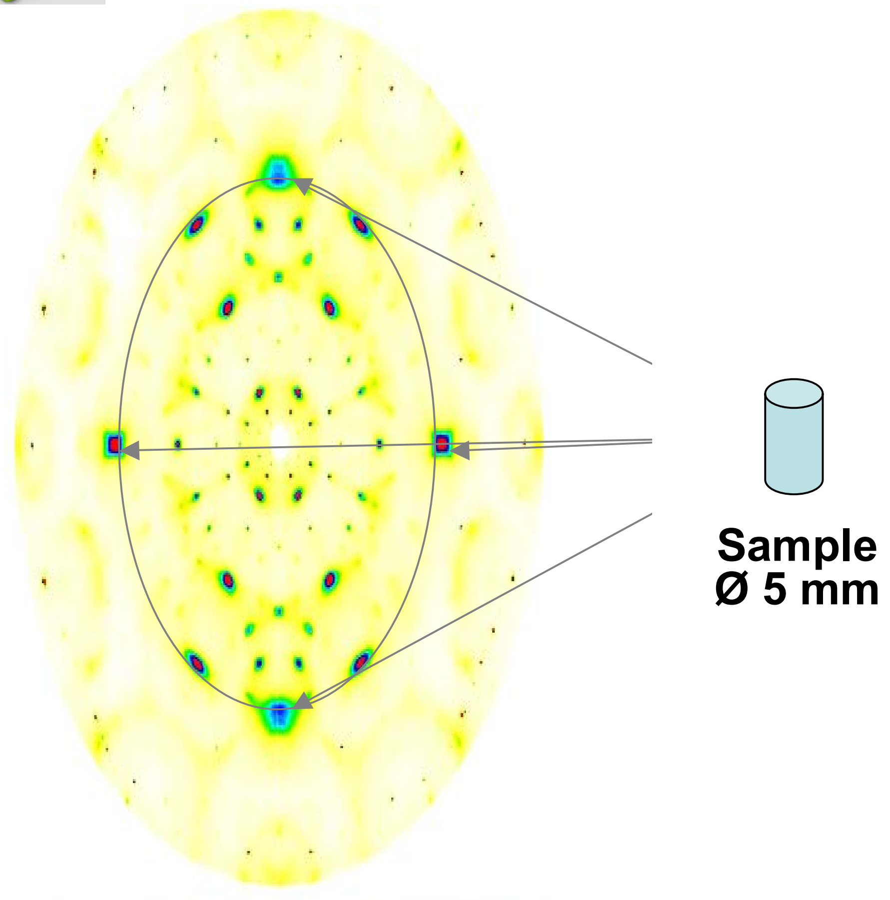

W. Schweika:
ico-AlPdMn: phason modes

High Energy X-Ray Scattering

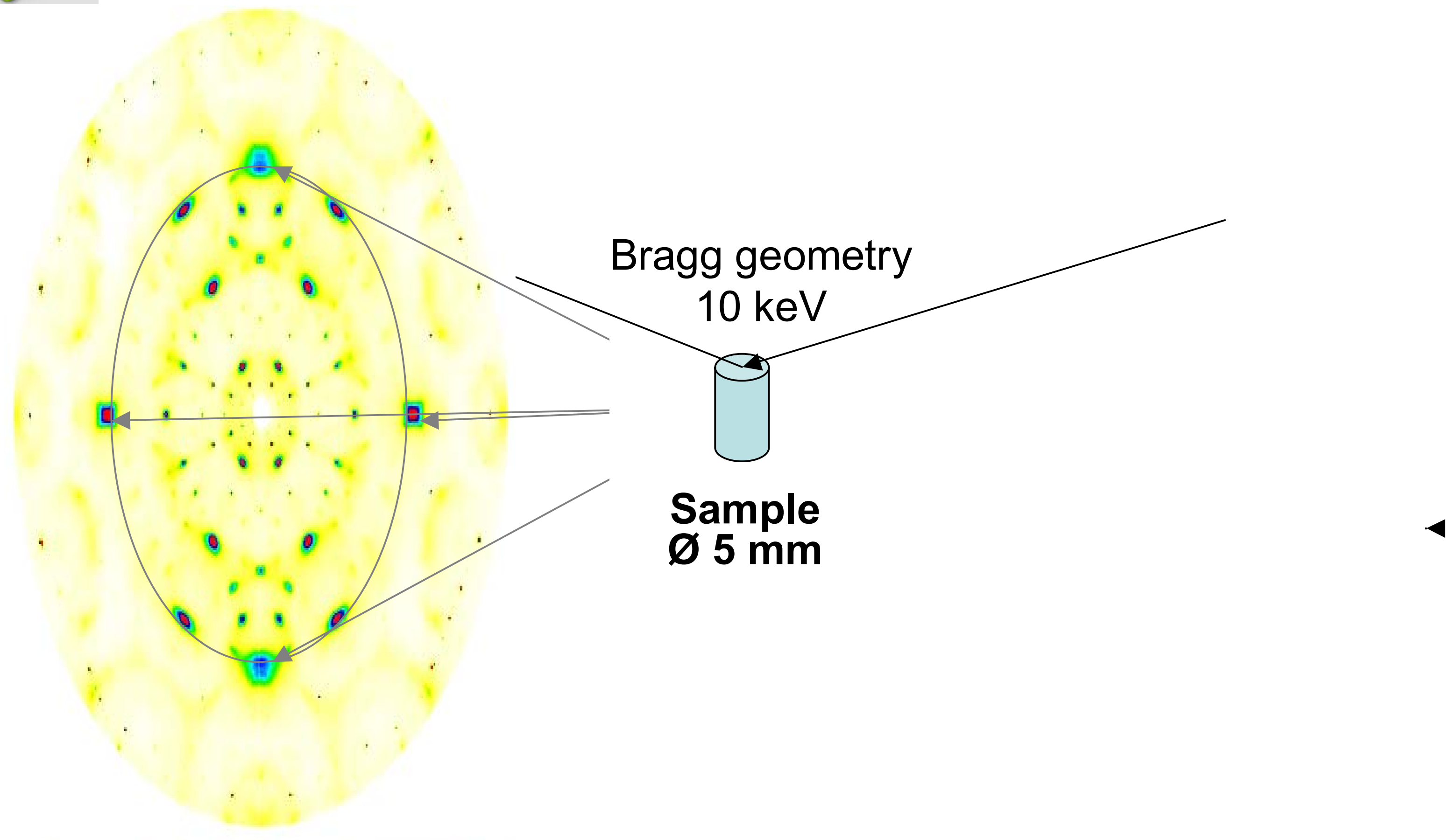

W. Schweika:
ico-AlPdMn: phason modes

High Energy X-Ray Scattering

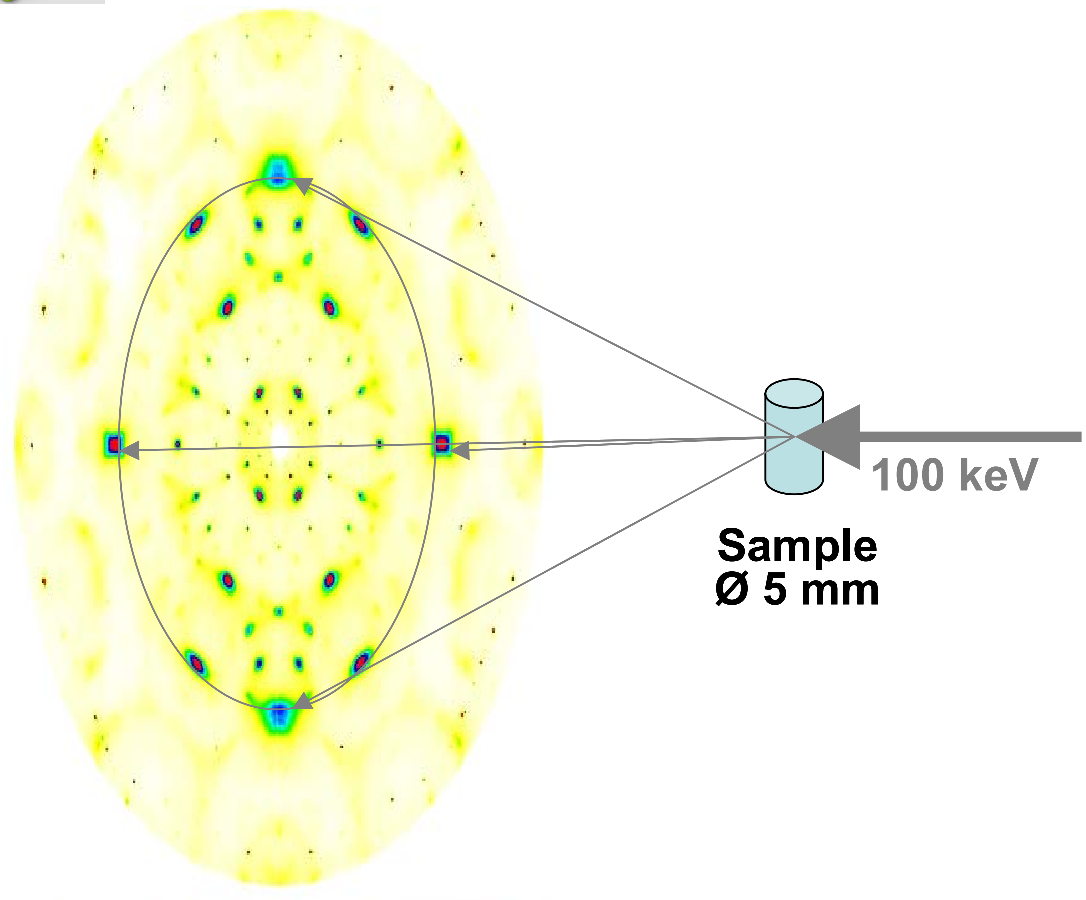

W. Schweika:
ico-AlPdMn: phason modes

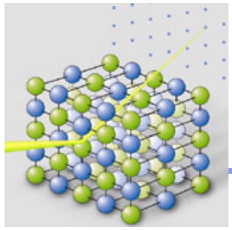

High Energy X-Ray Scattering

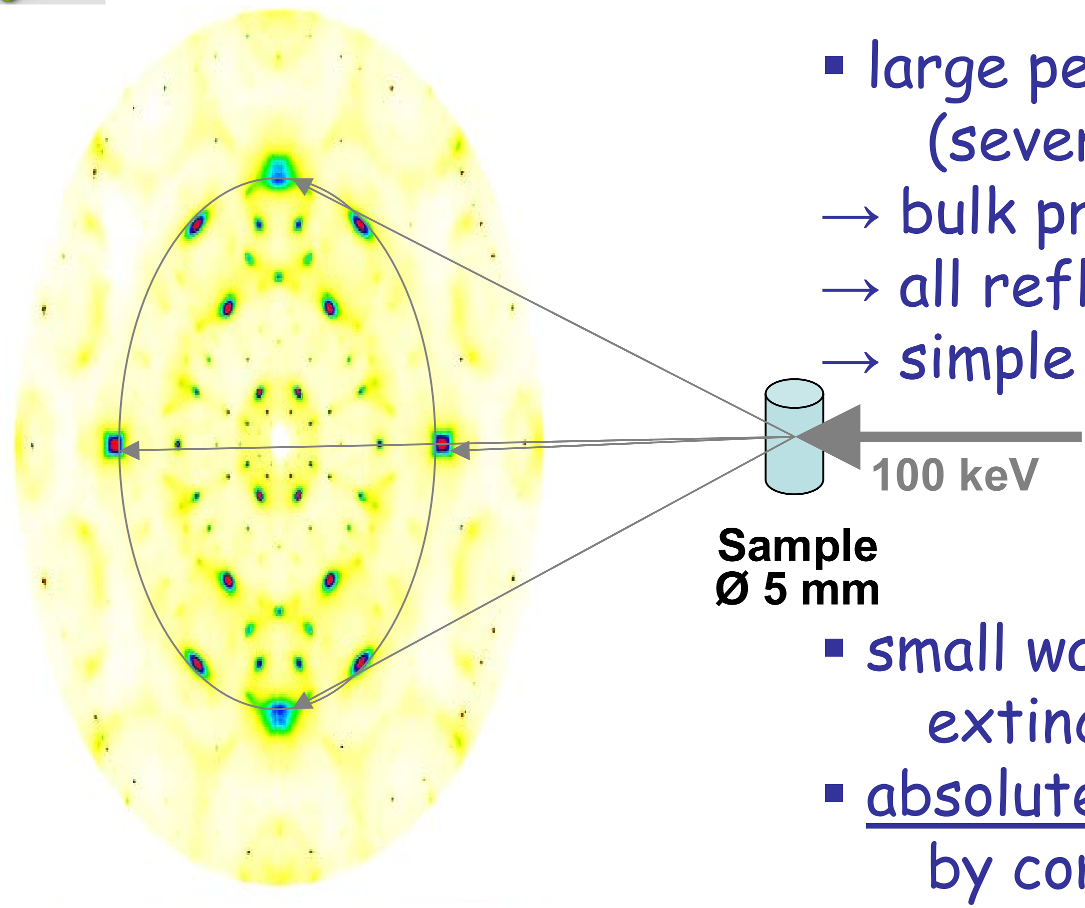

W. Schweika:
ico-AlPdMn: phason modes

- large penetration depth
  (several mm instead of μm)
  → bulk properties
  → all reflections accessible
  → simple sample environment
- small wavelength →
  extinction free
- absolute measurements
  by comparison to charge
  scattering

High Energy X-Ray Scattering

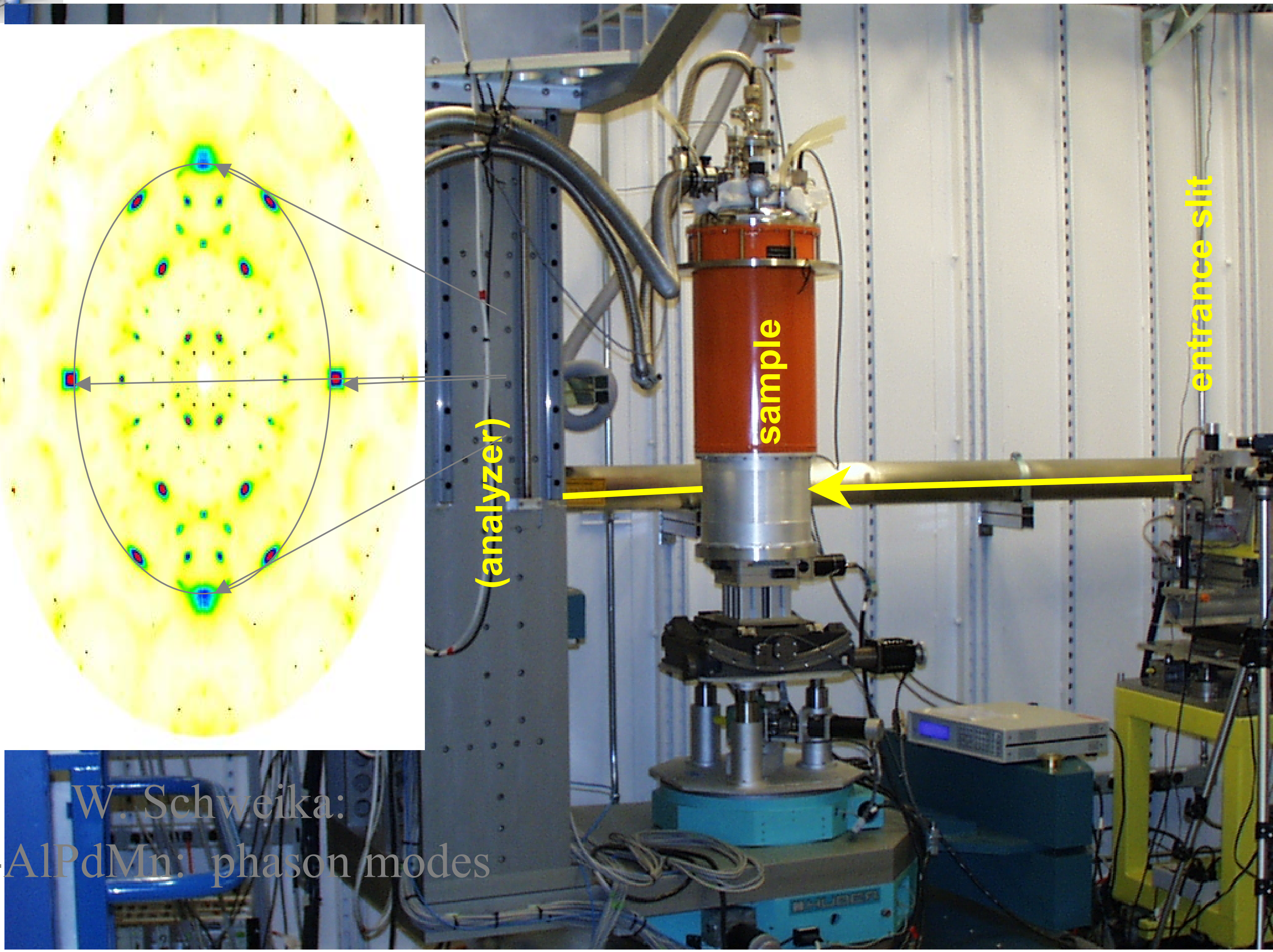

W. Schweika:
ico-AlPdMn: phason modes

High Energy Cross Section

model systems:

MnF_2

FeF_2

CoF_2

(NiF_2)

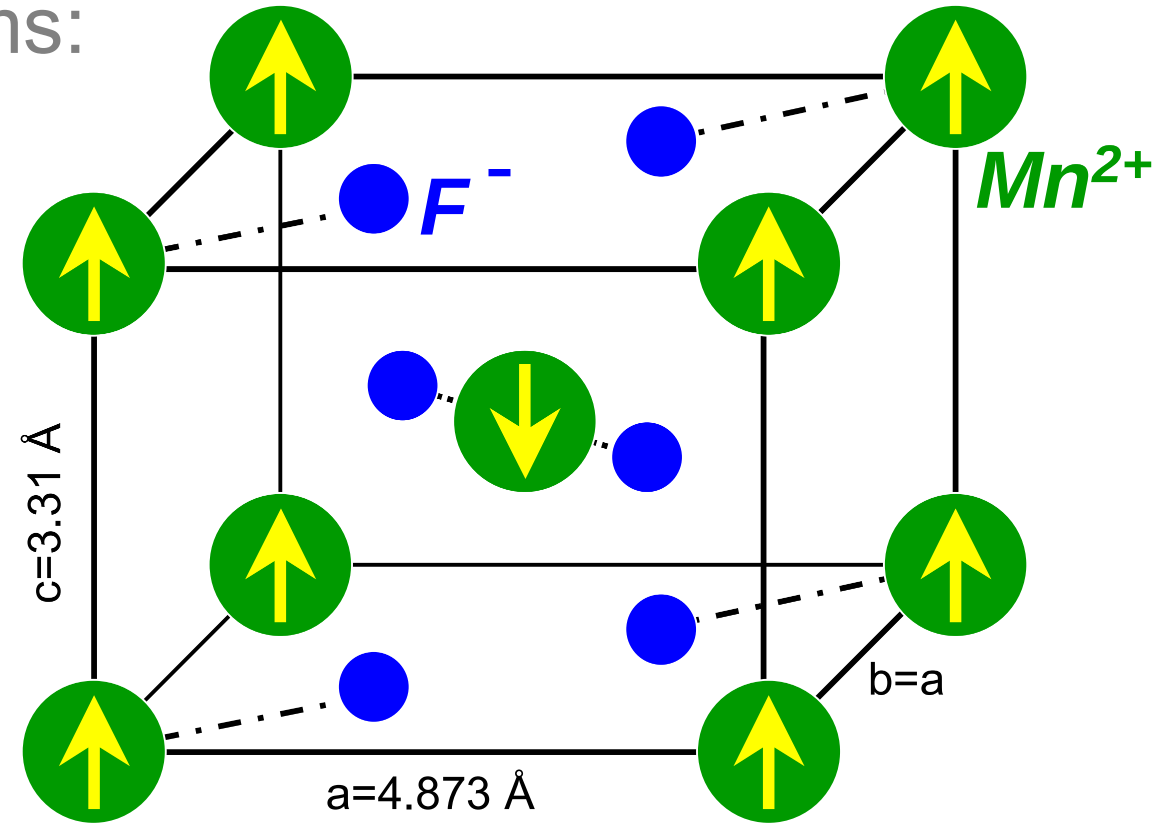

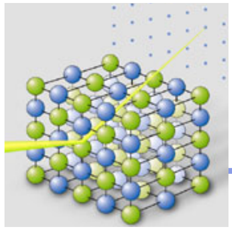

High Energy Cross Section

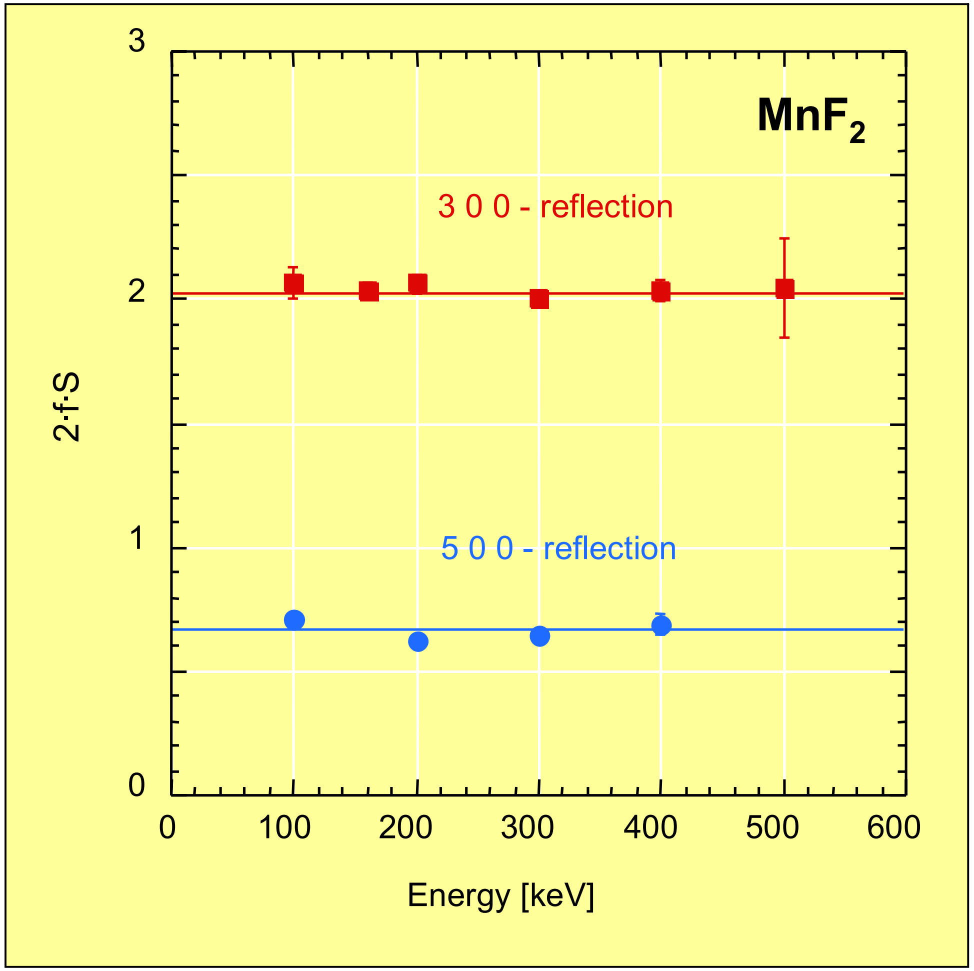

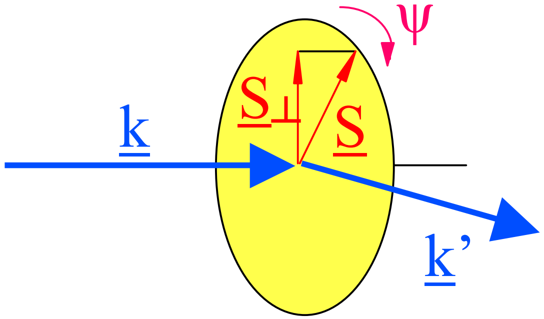

Strempfer, Brückel, Hupfeld, Schneider, Liss, Tschentscher
Europhys. Lett. 40 (1997) 569

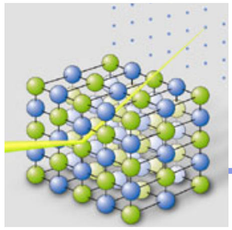

High Energy Cross Section

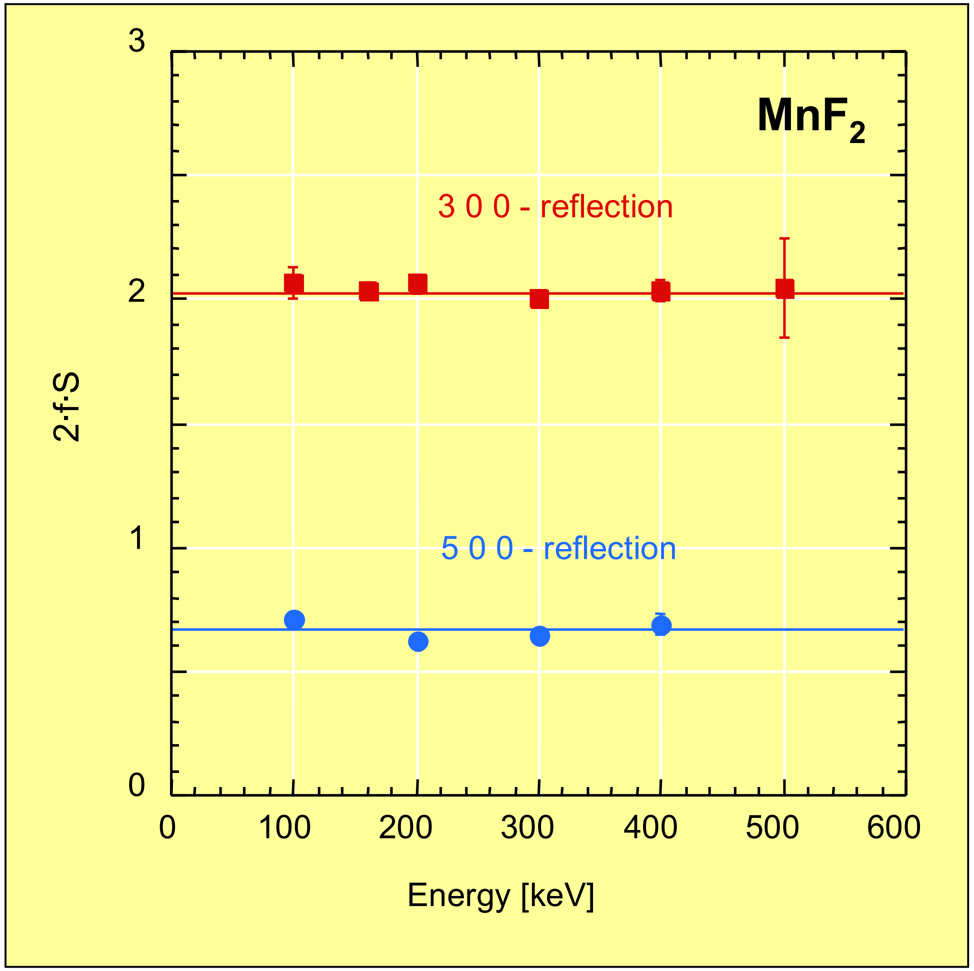

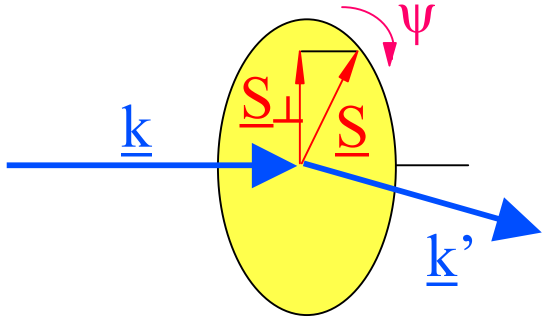

$$\left.\frac{d\sigma}{d\Omega}\right|_{mag} = r_0^2 \left(\frac{\lambda_C}{d}\right)^2 |S_\perp|^2$$

Strempfer, Brückel, Hupfeld, Schneider, Liss, Tschentscher
Europhys. Lett. 40 (1997) 569

High Energy Cross Section

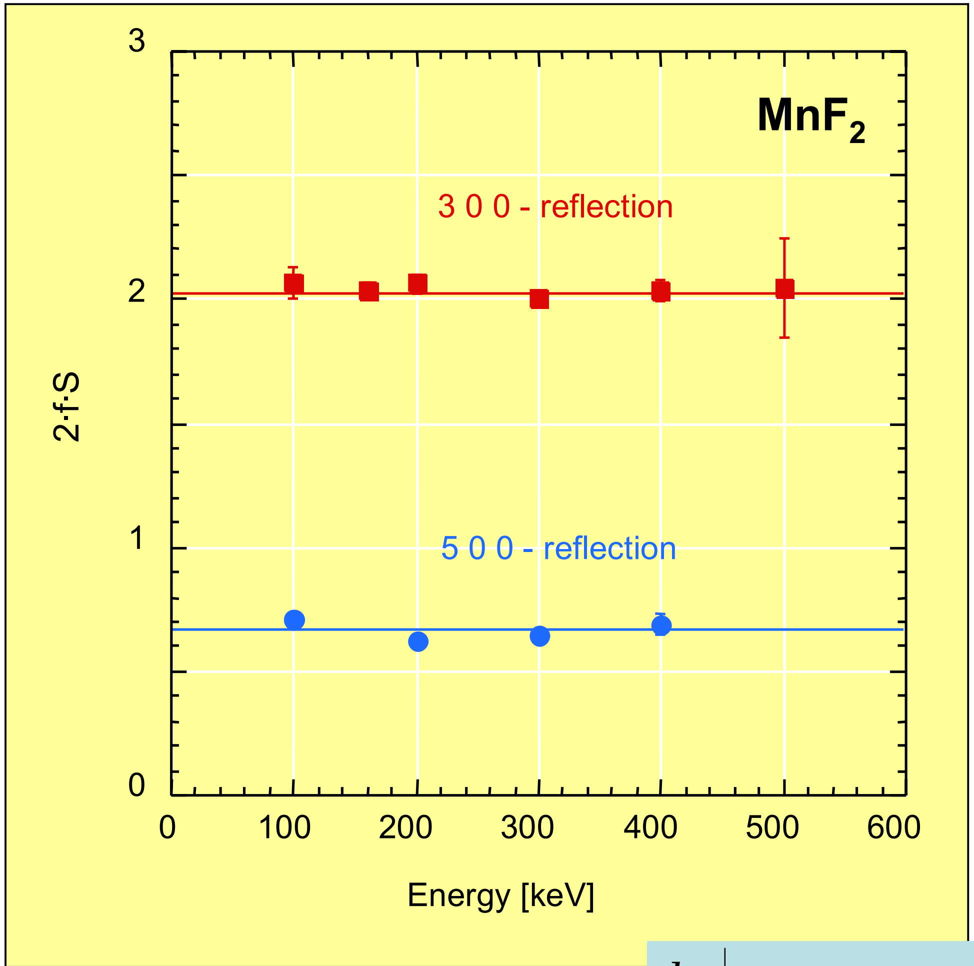

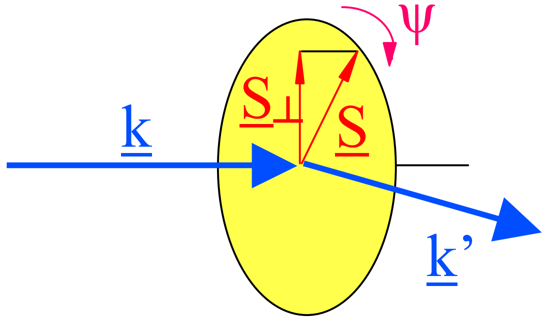

$$\left.\frac{d\sigma}{d\Omega}\right|_{mag} = r_0^2\left(\frac{\lambda_C}{d}\right)^2 \left|\underline{S}_\perp\right|^2$$

Strempfer, Brückel, Hupfeld, Schneider, Liss, Tschentscher
Europhys. Lett. 40 (1997) 569

Compare neutrons:

$$\left.\frac{d\sigma}{d\Omega}\right|_{magnet.,el.} = (\gamma r_0)^2 \left|< \hat{\underline{Q}} \times \left(\underline{L}(\underline{Q}) + 2\underline{S}(\underline{Q})\right) \times \hat{\underline{Q}} >\right|^2$$

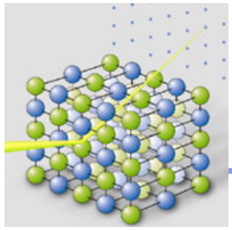

High Energy Cross Section

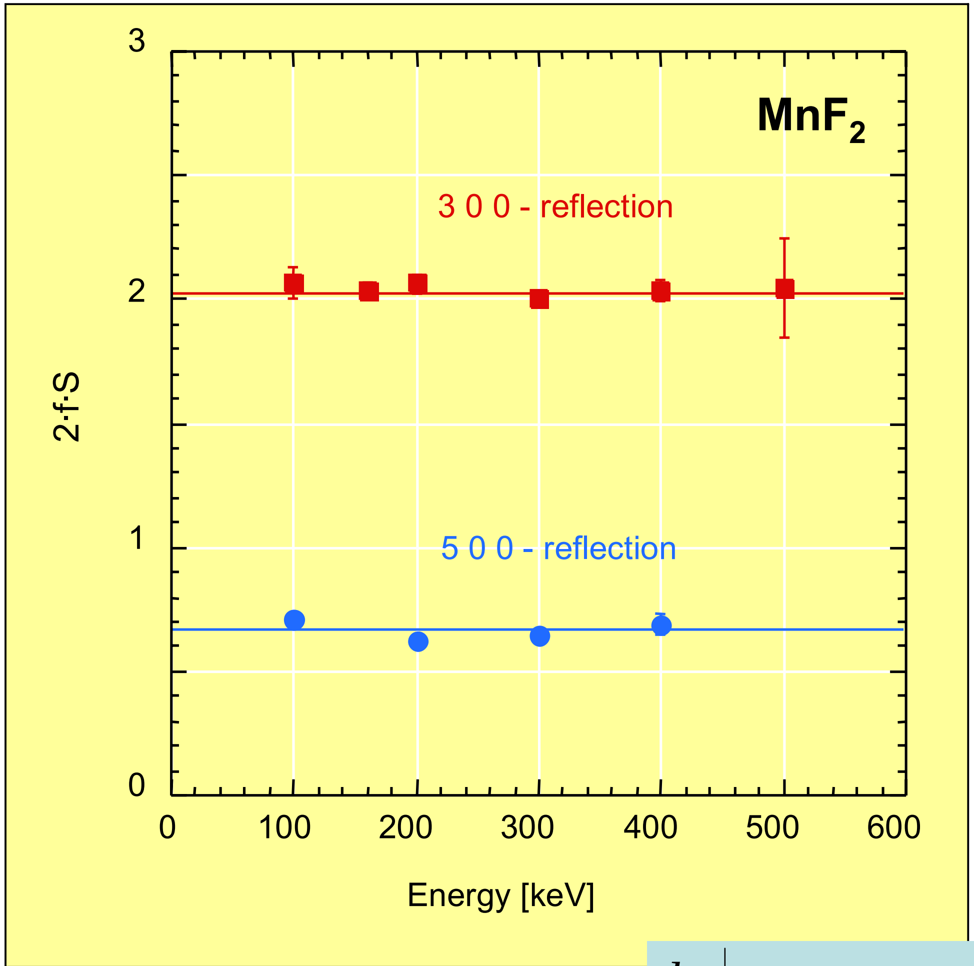

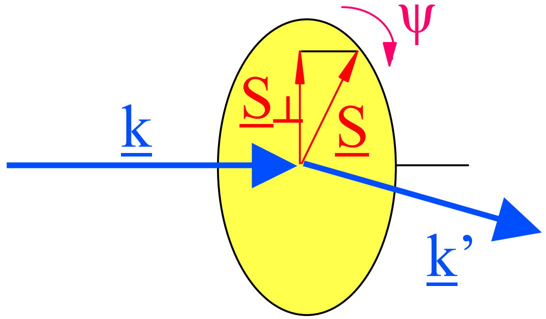

$$\left.\frac{d\sigma}{d\Omega}\right|_{mag} = r_0^2\left(\frac{\lambda_C}{d}\right)^2 \left|\underline{S}_\perp\right|^2$$

Strempfer, Brückel, Hupfeld, Schneider, Liss, Tschentscher
Europhys. Lett. 40 (1997) 569

Compare neutrons:

$$\left.\frac{d\sigma}{d\Omega}\right|_{magnet.,el.} = (\gamma r_0)^2 \left| < \hat{\underline{Q}} \times \left(\underline{L}(\underline{Q}) + 2\underline{S}(\underline{Q})\right) \times \hat{\underline{Q}} > \right|^2$$

High E Magnetic Scattering

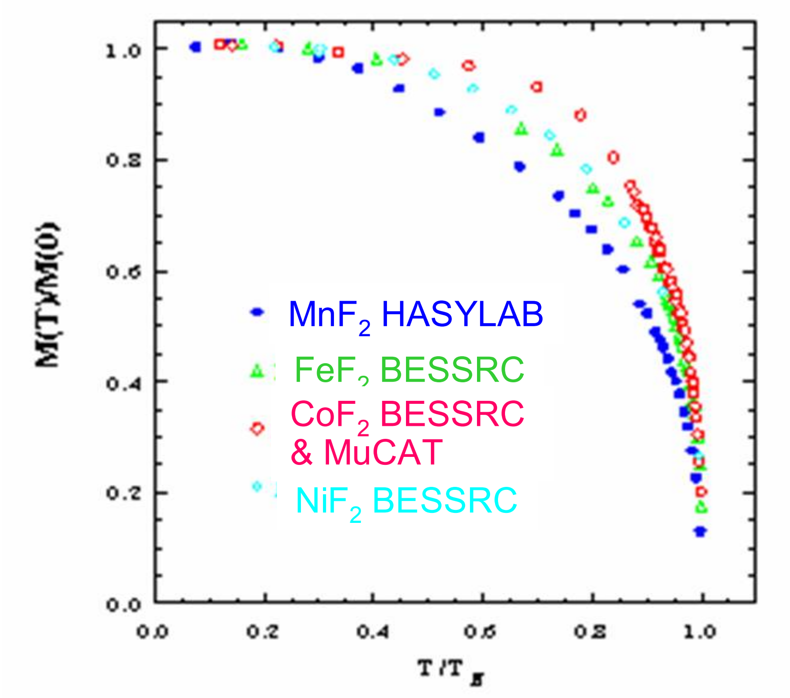

High E Magnetic Scattering

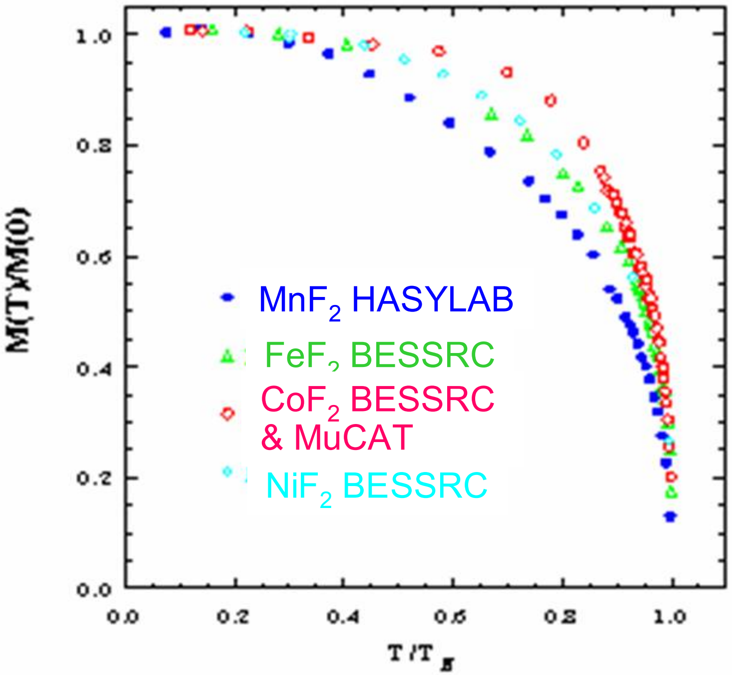

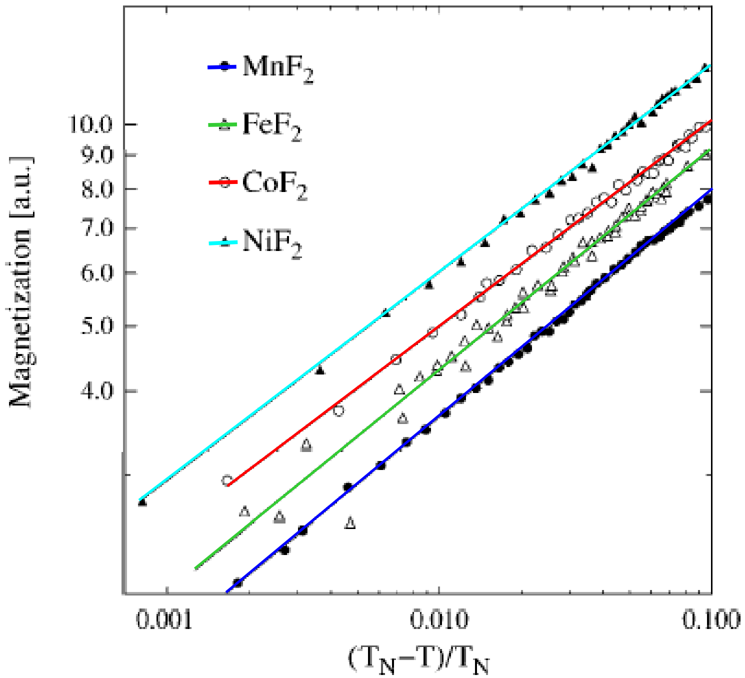

High E Magnetic Scattering

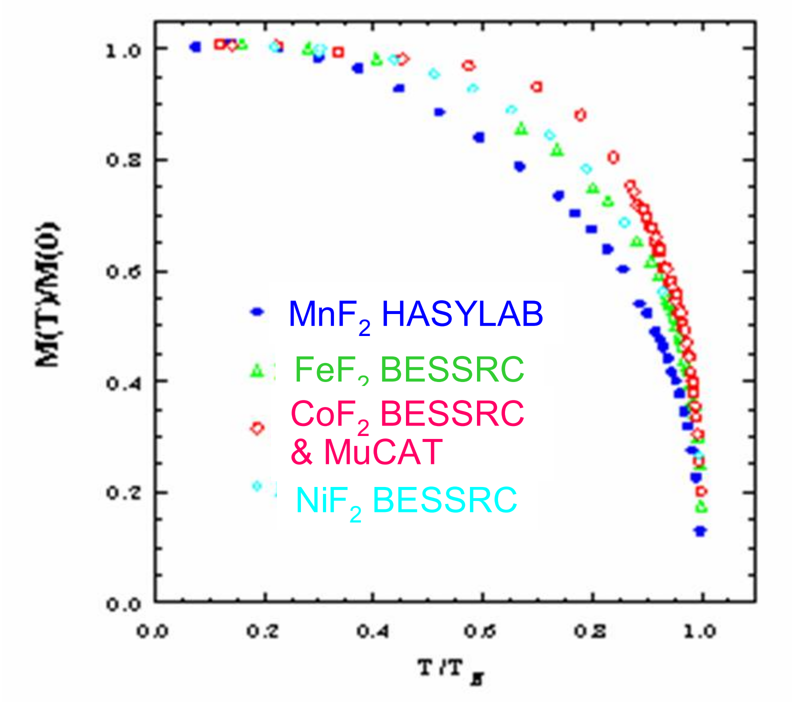

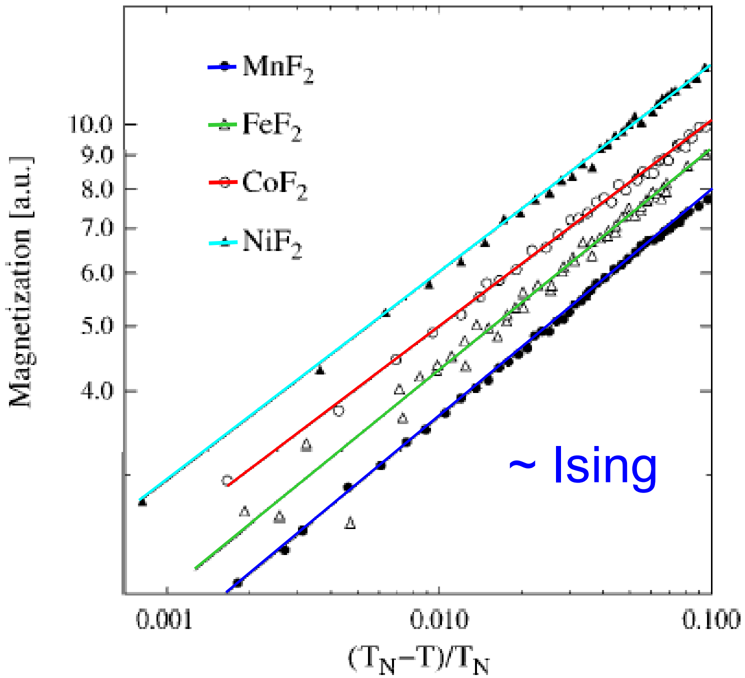

High E Magnetic Scattering

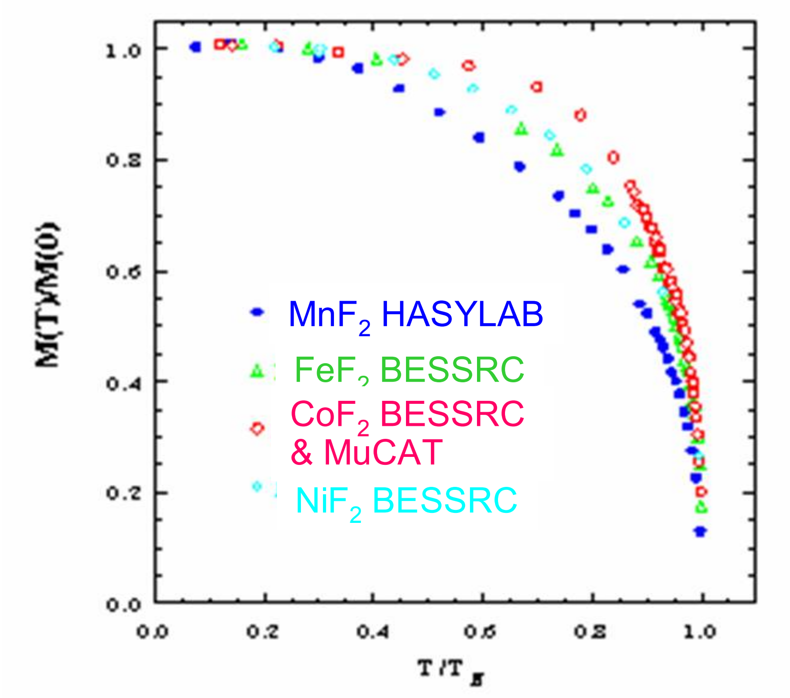

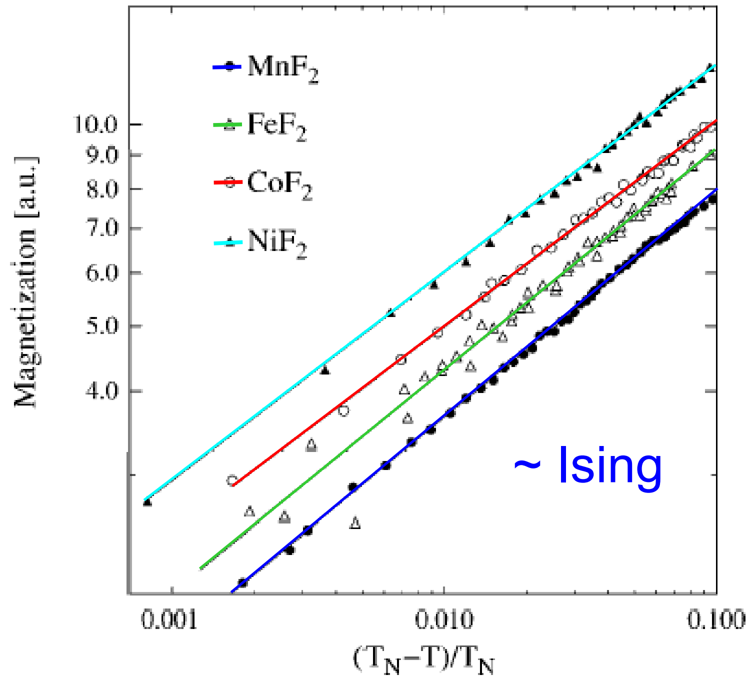

	$S^{f.l.}$	g	$\mu_S^{f.l.}$	μ_S [μ_B]	T_N [K]	β
MnF_2	2.5	2.00	5.0	5.04(6)	67.7	0.333(3)
FeF_2	2	2.25	4.0	3.92(4)	75.8	0.329(18)
CoF_2	1.5	4.25	3.0	2.21(2)	38.1	0.306(6)
NiF_2	1	2.35	2.0	1.96(2)	74.1	0.311(5)

High E Magnetic Scattering

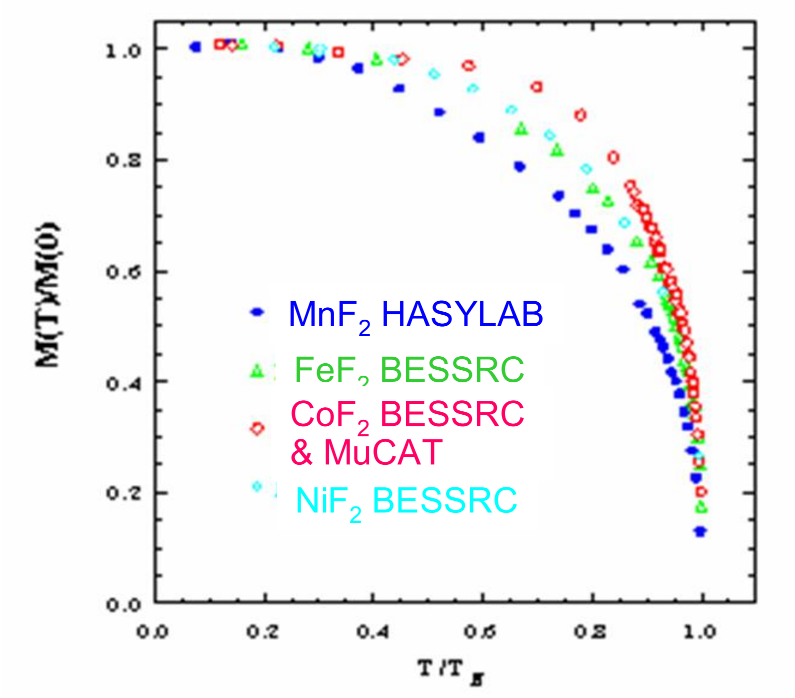

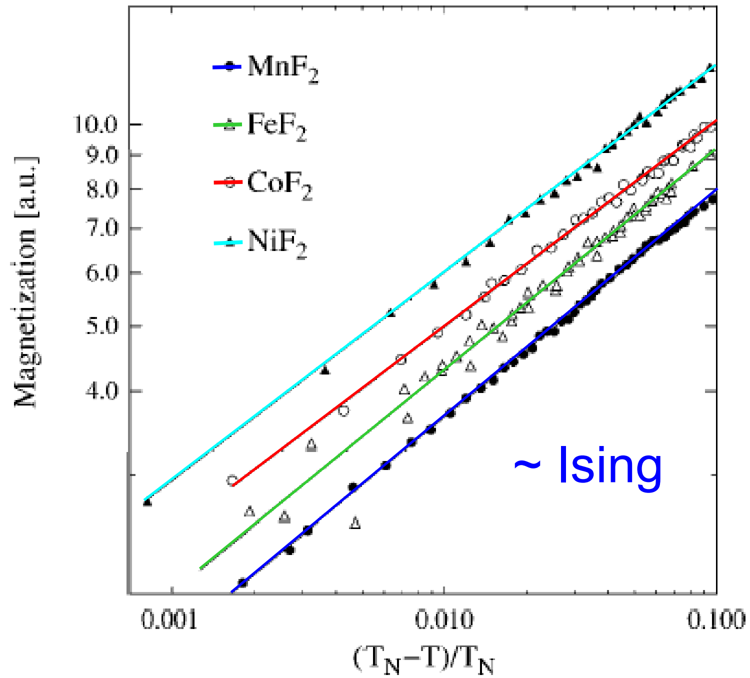

	$S^{f.l.}$	g	$\mu_S^{f.l.}$	μ_S [μ_B]	T_N [K]	β
MnF_2	2.5	2.00	5.0	5.04(6)	67.7	0.333(3)
FeF_2	2	2.25	4.0	3.92(4)	75.8	0.329(18)
CoF_2	1.5	4.25	3.0	2.21(2)	38.1	0.306(6)
NiF_2	1	2.35	2.0	1.96(2)	74.1	0.311(5)

High E Magnetic Scattering

Pure spin form factor

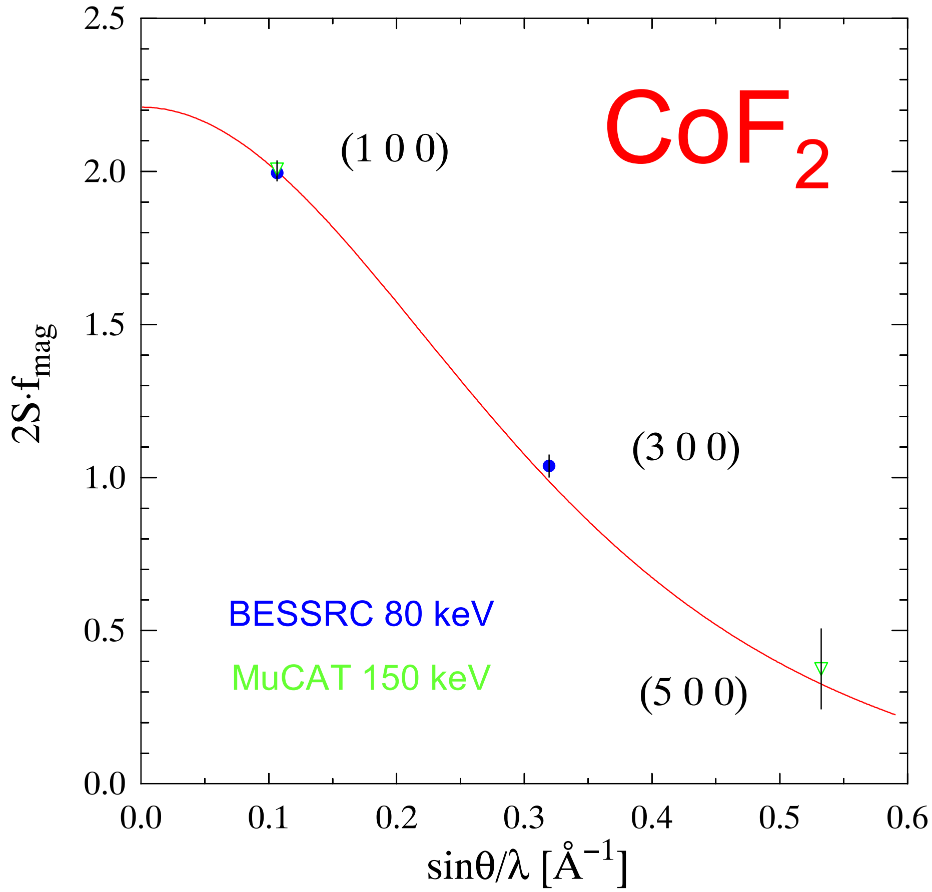

Strempfer, Rütt, Bayrakci, Brückel, Jauch
Physical Review B 69 (2004), 014417

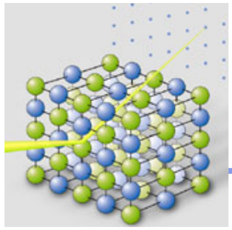

High E Magnetic Scattering

μ_S = 2.21 (2) μ_B

Free ion: 3 μ_B

Γ-Diffr.: full integer 3d occupancy
P(3d) = 6.95

Pure spin form factor

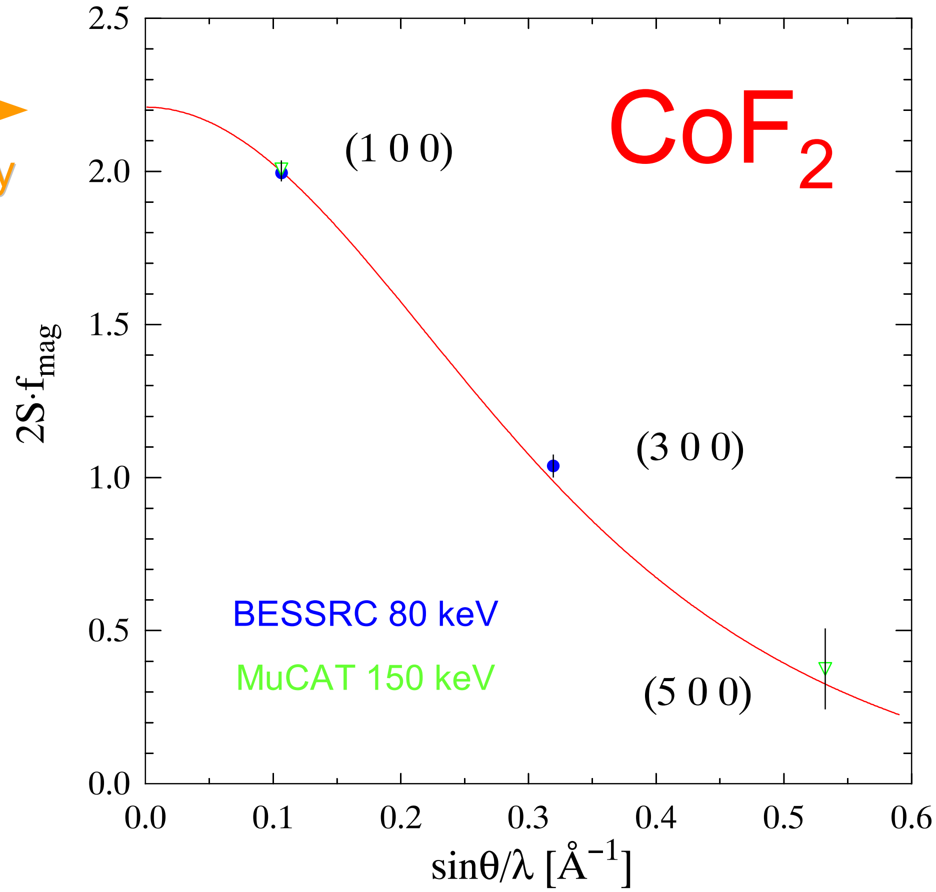

Strempfer, Rütt, Bayrakci, Brückel, Jauch
Physical Review B <u>69</u> (2004), 014417

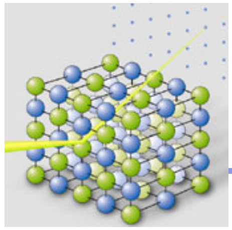

High E Magnetic Scattering

μ_S = 2.21 (2) μ_B

Free ion: 3 μ_B

Γ-Diffr.: full integer 3d occupancy
P(3d) = 6.95

- **absolute determination of spin moment with 1% e.s.d.**

Pure spin form factor

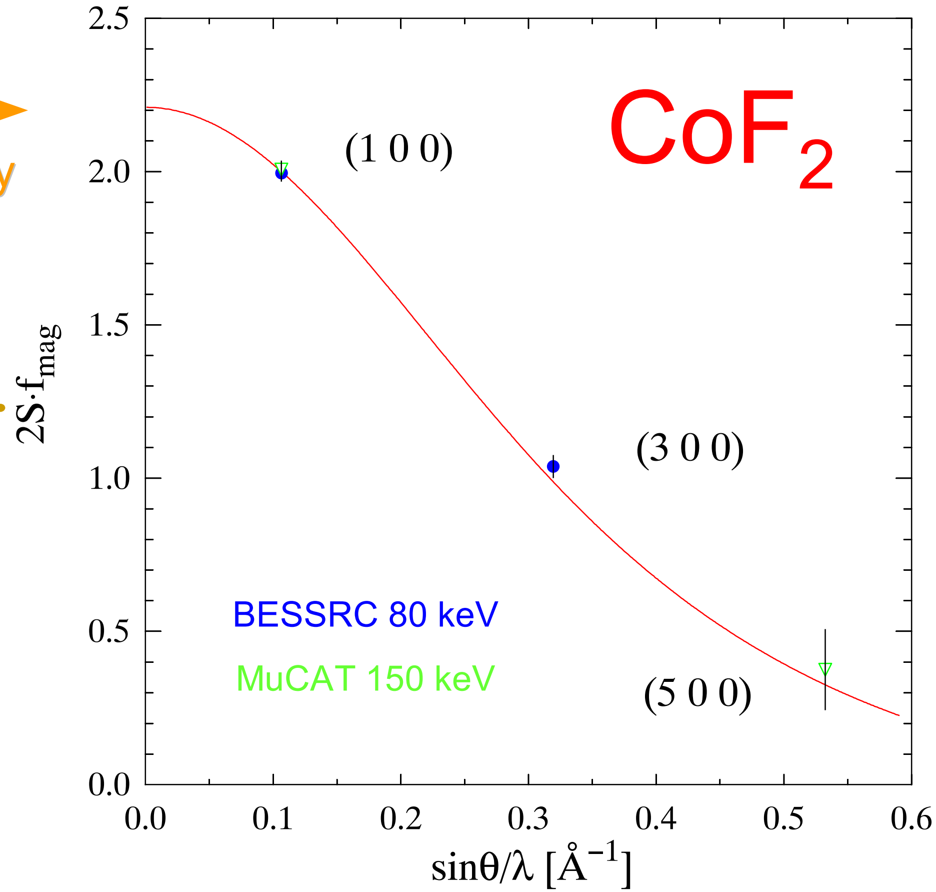

Strempfer, Rütt, Bayrakci, Brückel, Jauch
Physical Review B 69 (2004), 014417

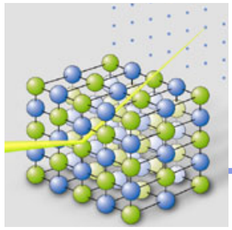

High E Magnetic Scattering

μ_S = 2.21 (2) μ_B

Free ion: 3 μ_B

Γ-Diffr.: full integer 3d occupancy
P(3d) = 6.95

- absolute determination of spin moment with 1% e.s.d.
- pure spin moment reduced by 27% - only for CoF_2

Pure spin form factor

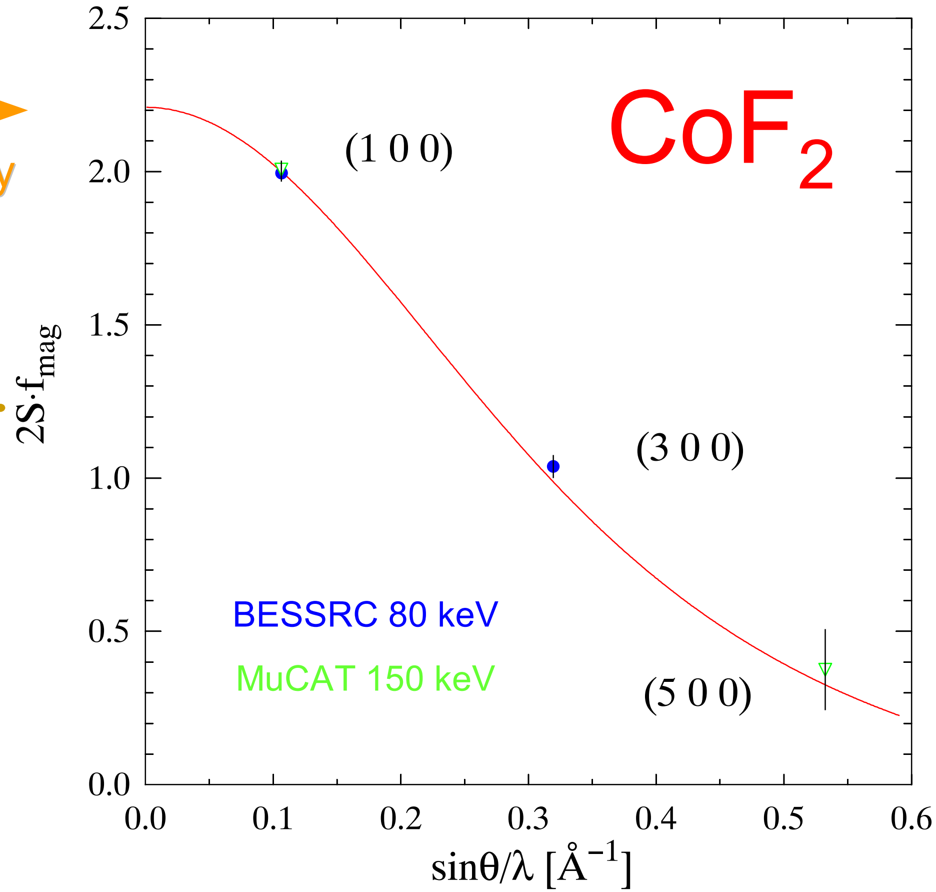

Strempfer, Rütt, Bayrakci, Brückel, Jauch
Physical Review B 69 (2004), 014417

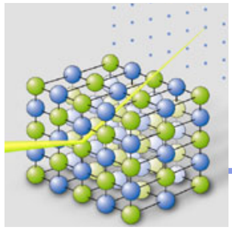

High E Magnetic Scattering

Pure spin form factor

μ_S = 2.21 (2) μ_B

Free ion: 3 μ_B

Γ-Diffr.: full integer 3d occupancy
P(3d) = 6.95

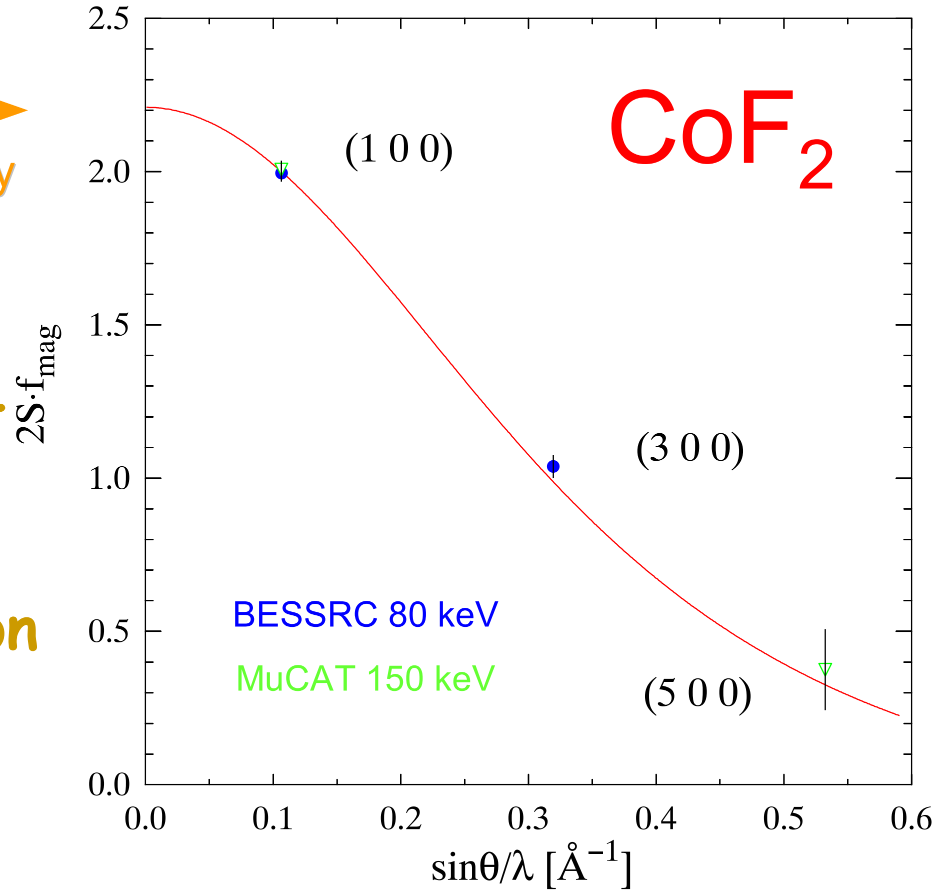

- absolute determination of spin moment with 1% e.s.d.
- pure spin moment reduced by 27% - only for CoF_2
- Contraction of wave function by 4 % along a (b) axis

Strempfer, Rütt, Bayrakci, Brückel, Jauch
Physical Review B 69 (2004), 014417

High E Magnetic Scattering

Pure spin form factor

μ_S = 2.21 (2) μ_B

Free ion: 3 μ_B

Γ-Diffr.: full integer 3d occupancy
P(3d) = 6.95

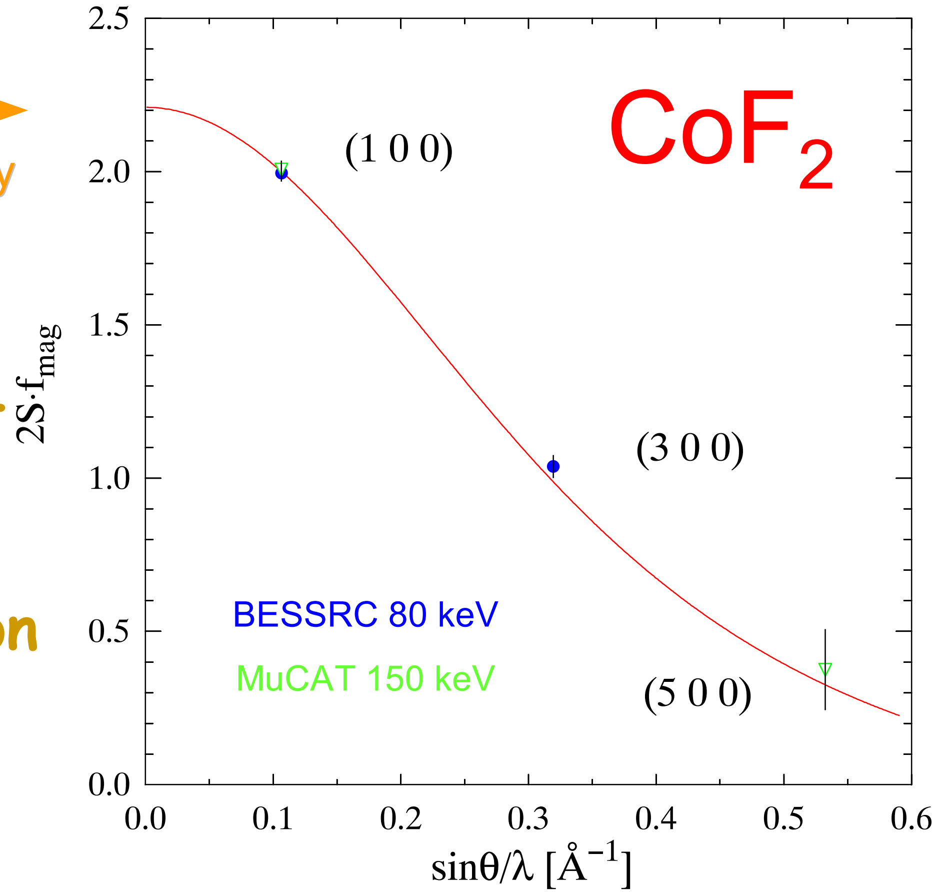

- absolute determination of spin moment with 1% e.s.d.
- pure spin moment reduced by 27% - only for CoF_2
- Contraction of wave function by 4 % along a (b) axis

Solid state effect !

Strempfer, Rütt, Bayrakci, Brückel, Jauch
Physical Review B 69 (2004), 014417

MeF_2 – T Dependence

MnF_2, FeF_2, NiF_2

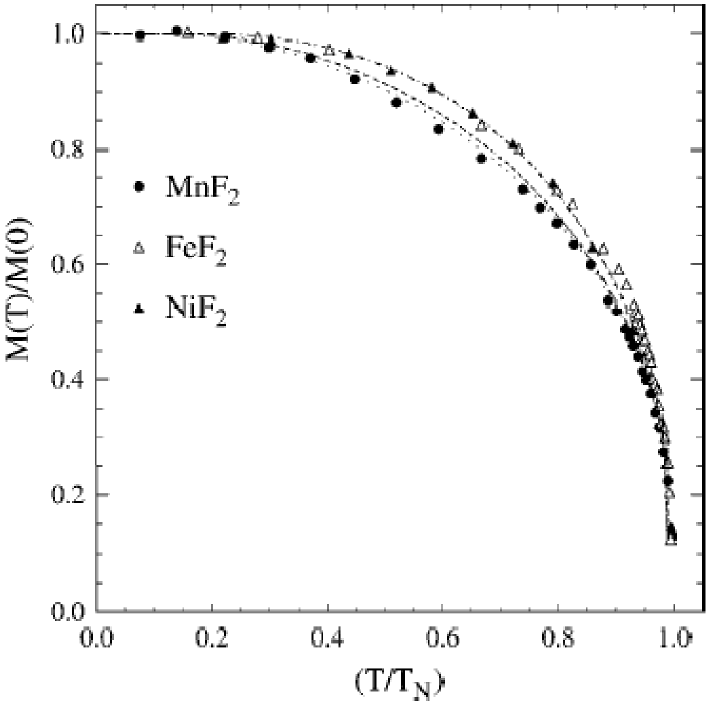

Mean field behavior

CoF_2

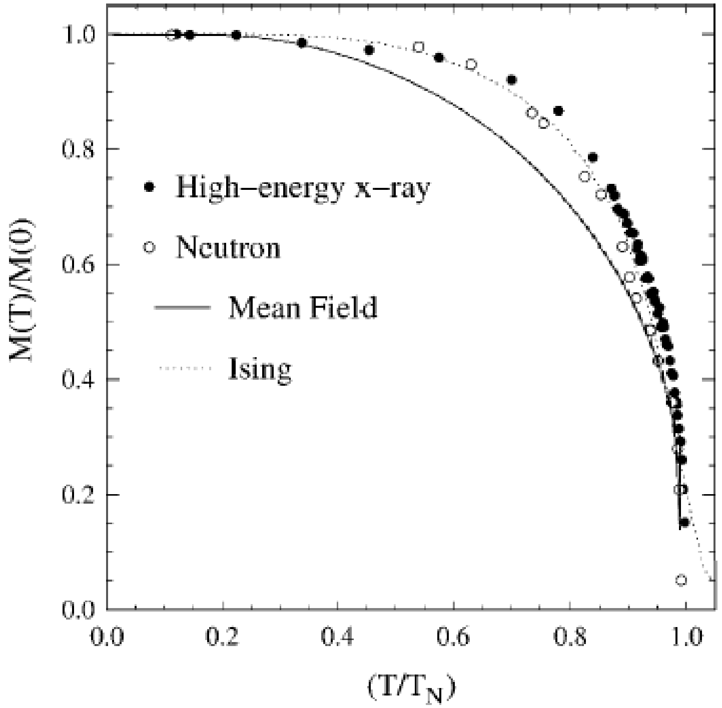

Anisotropic behavior

Spin- and Orbital Moment

Sketch: "Bohr-orbit"

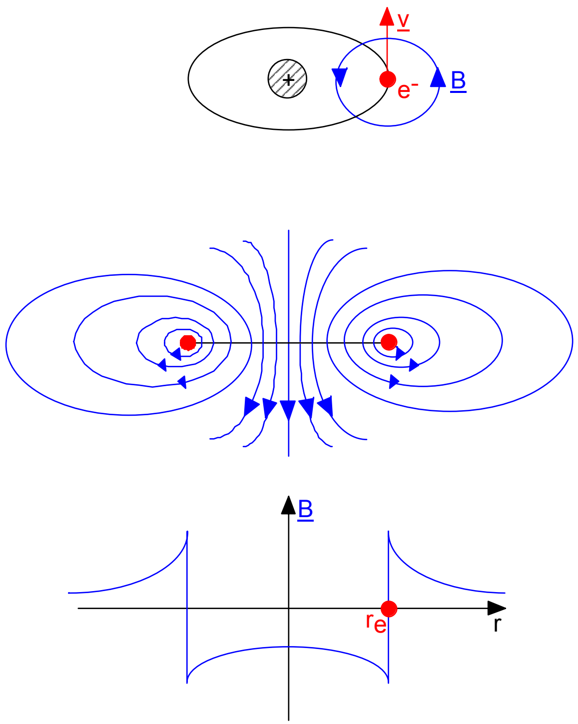

orbital moment

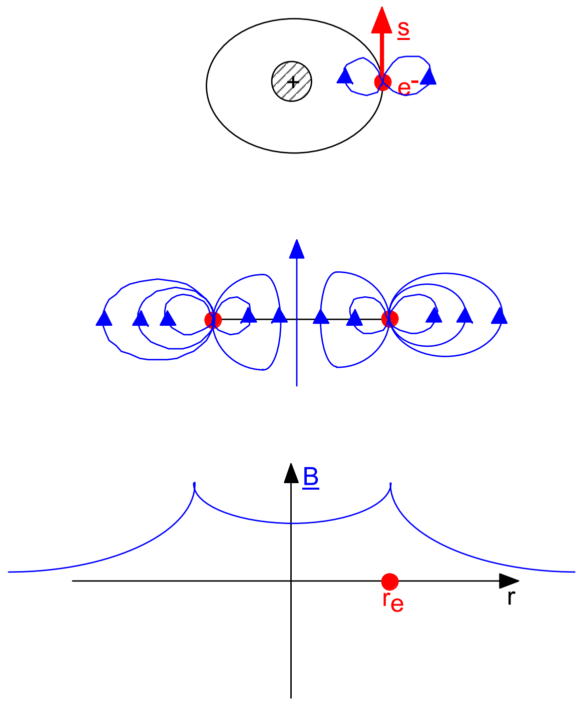

spin moment

magnetic field distribution

L-S-Separation by Polarisation Analysis

Example: NiO

Fernandez, Vettier, de Bergevin, Giles, Neubeck
Phys. Rev. B 57 (1998), 7870

Ratio L / 2 S

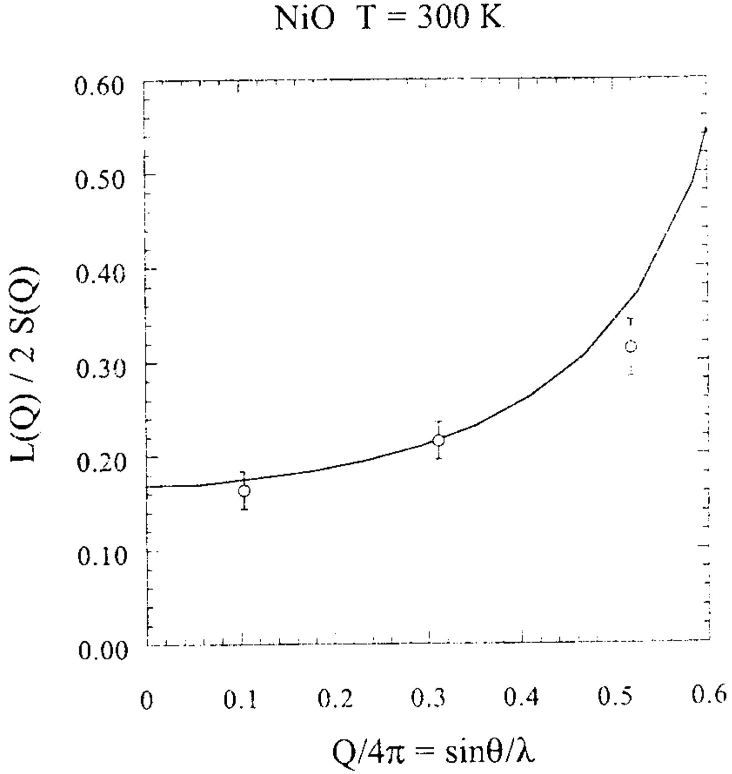

S and L form factors

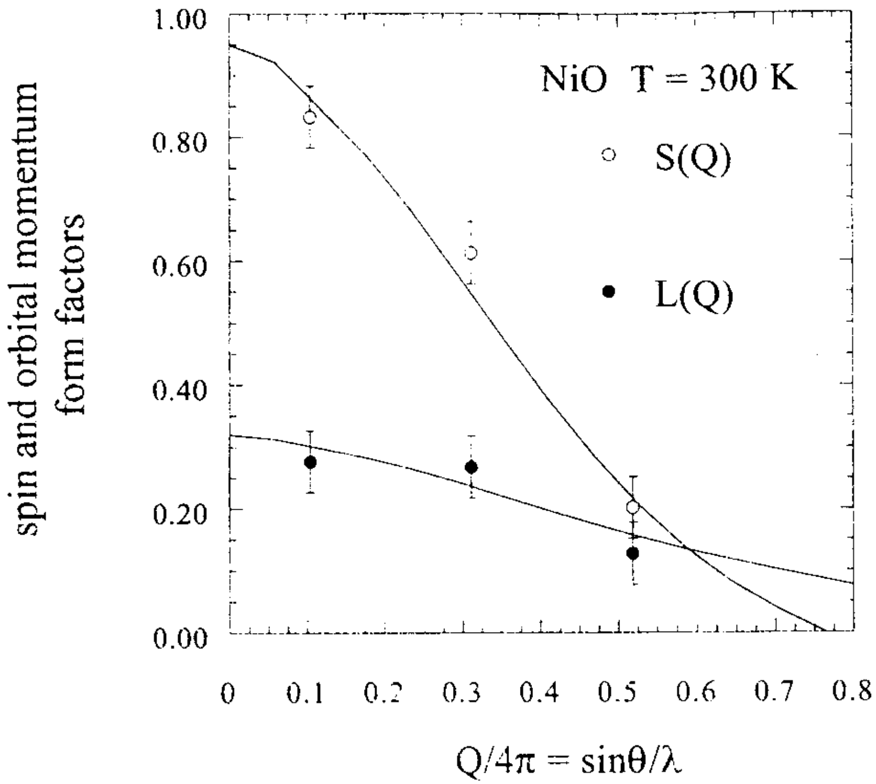

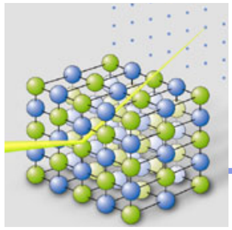

Outline

- What's new in magnetism ?
- Experimental techniques
- Elastic magnetic neutron scattering
- X-ray techniques for magnetism
- Nonresonant magnetic x-ray scattering
- Resonant magnetic x-ray scattering
- Example: Non-resonant scattering from transition metal di-flourides
- Example: Resonance exchange scattering from mixed crystals
- Summary

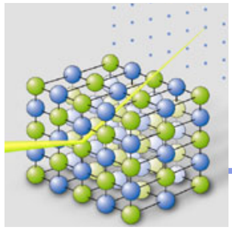

$Gd_xEu_{1-x}S$-Phase-Diagram

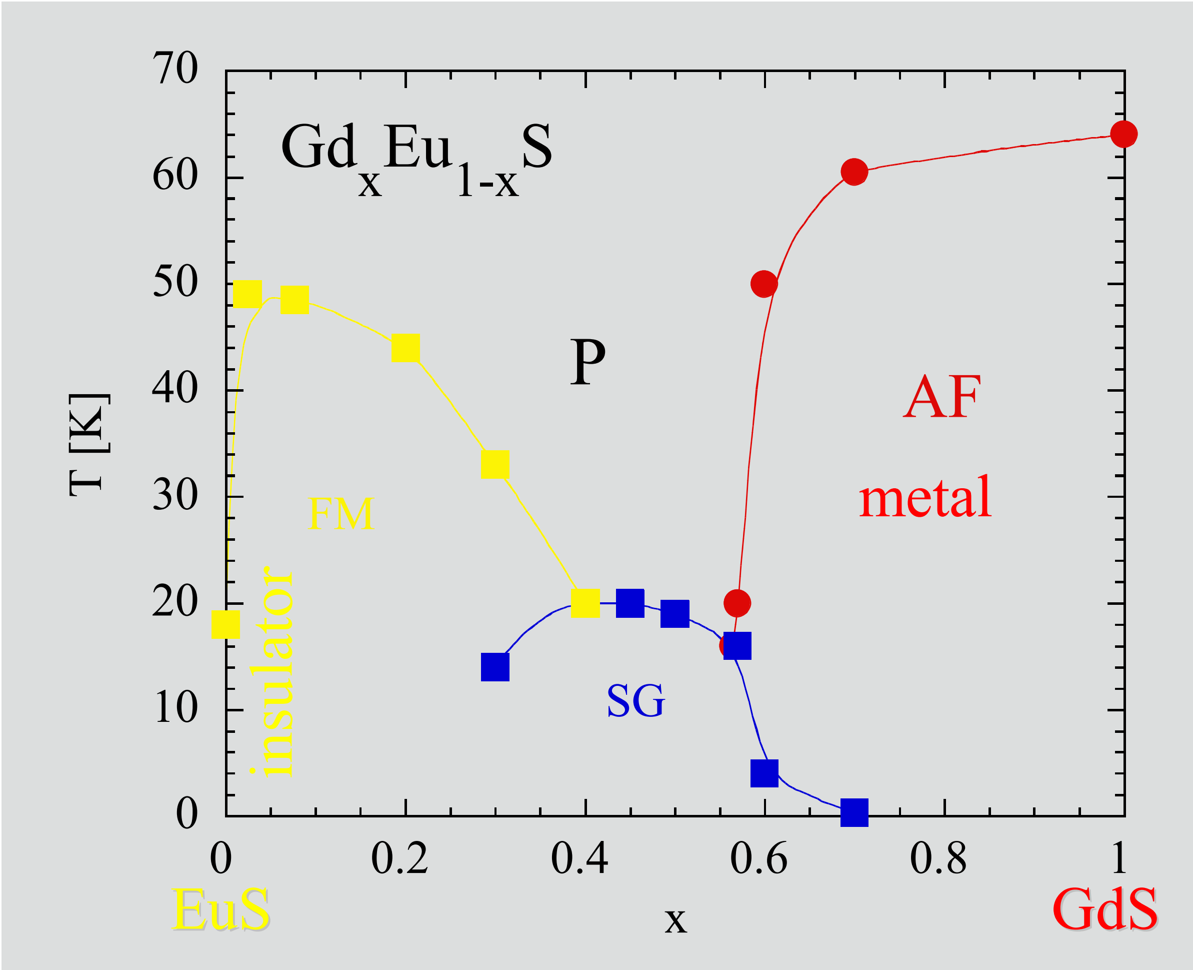

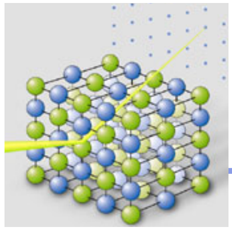

$Gd_xEu_{1-x}S$-Phase-Diagram

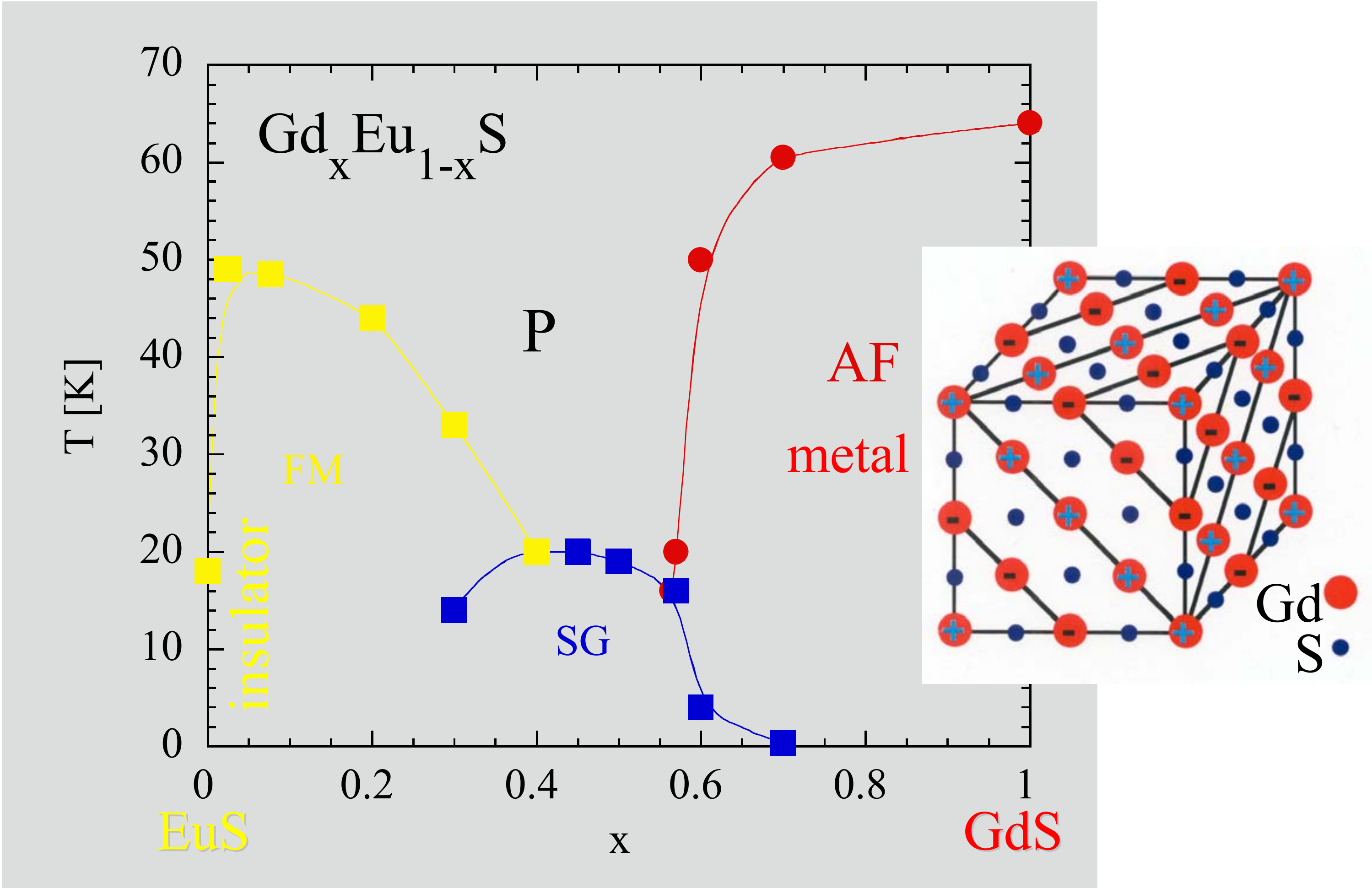

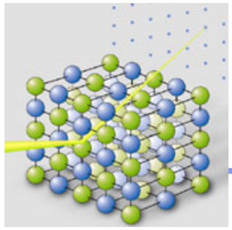

$Gd_xEu_{1-x}S$-Phase-Diagram

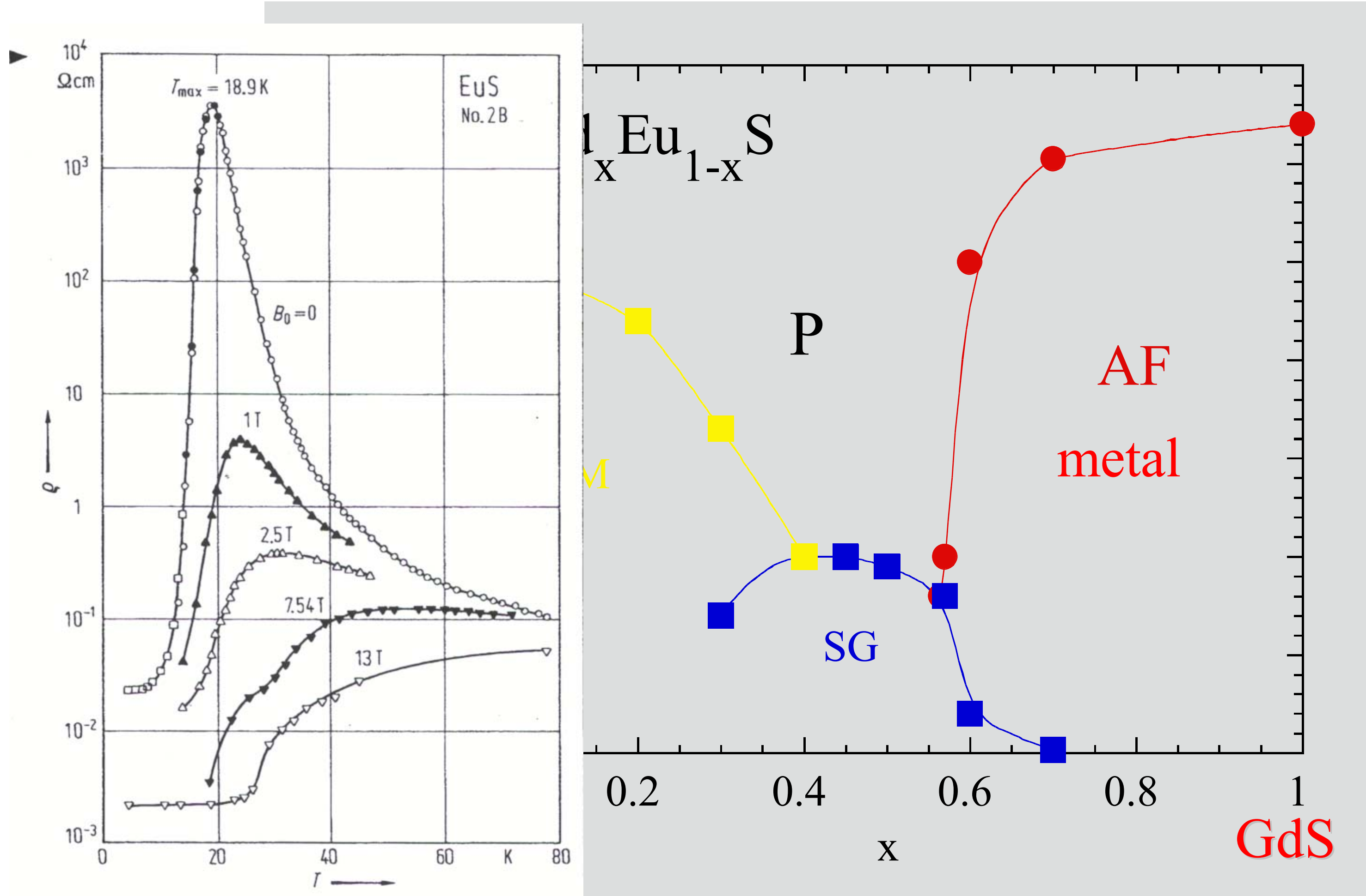

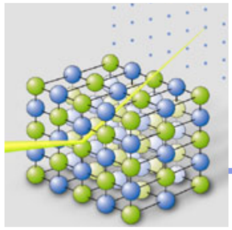

$Gd_{0.73}Eu_{0.27}S$: Resonances

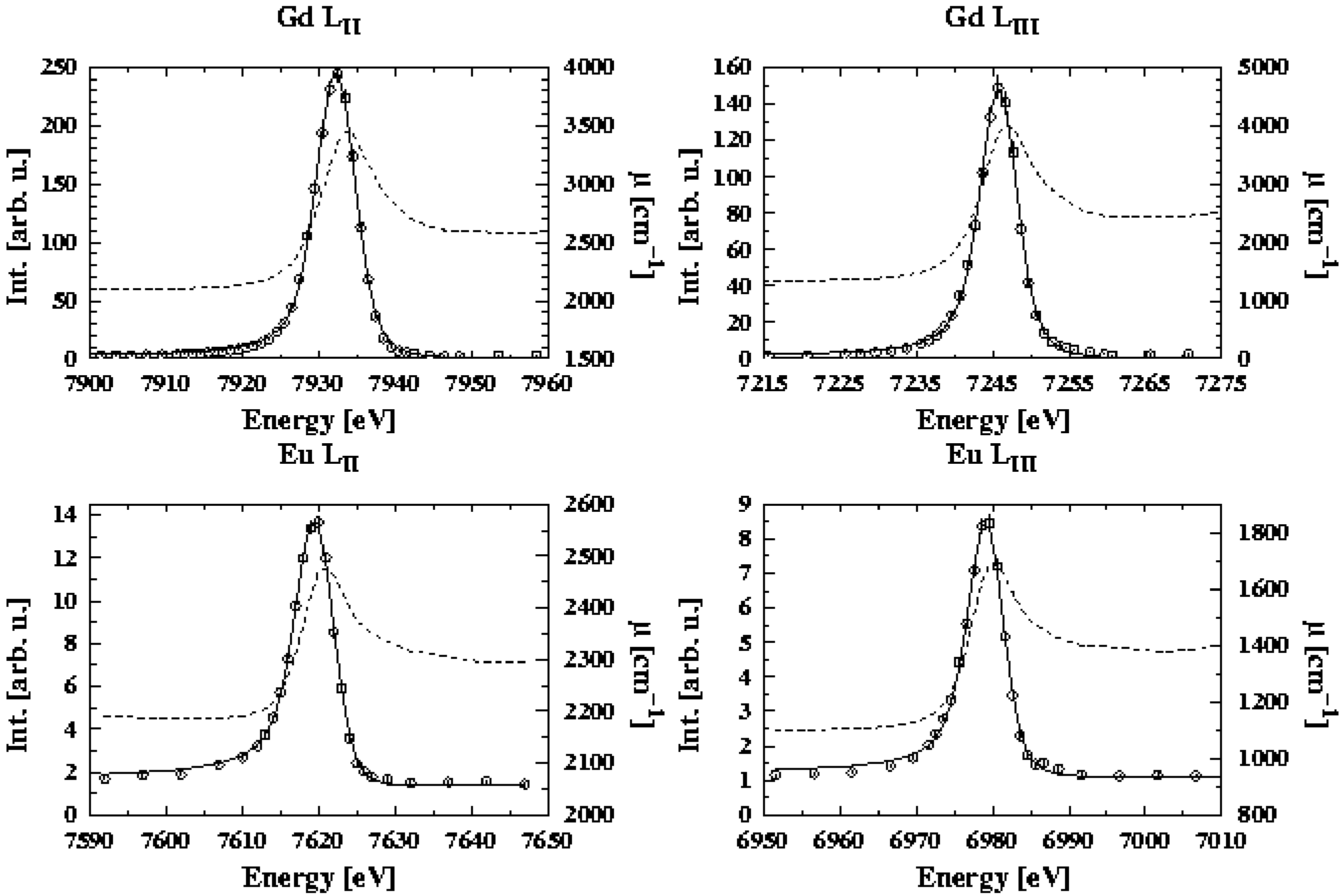

→ dominant dipolar transitions 2p → 5d

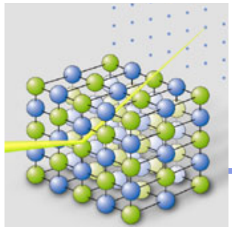

$Gd_{0.8}Eu_{0.2}S$: Temperature Dependence

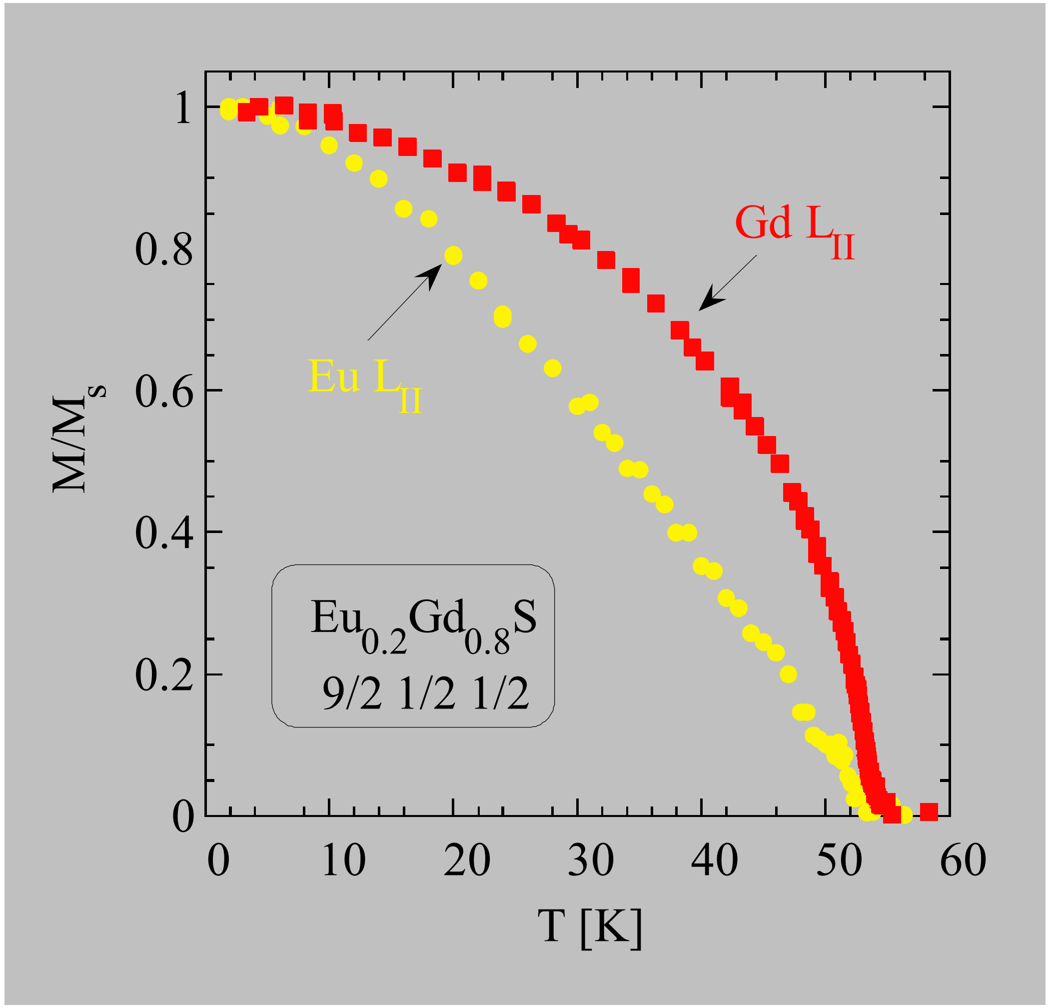

Hupfeld, Schweika, Strempfer, Mattenberger, McIntyre, Brückel
Europhys. Lett. 49 (2000), 92

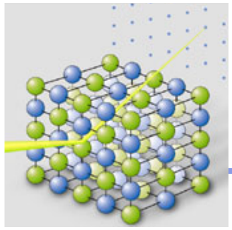

$Gd_{0.8}Eu_{0.2}S$: Temperature Dependence

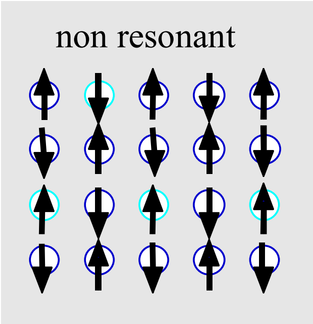

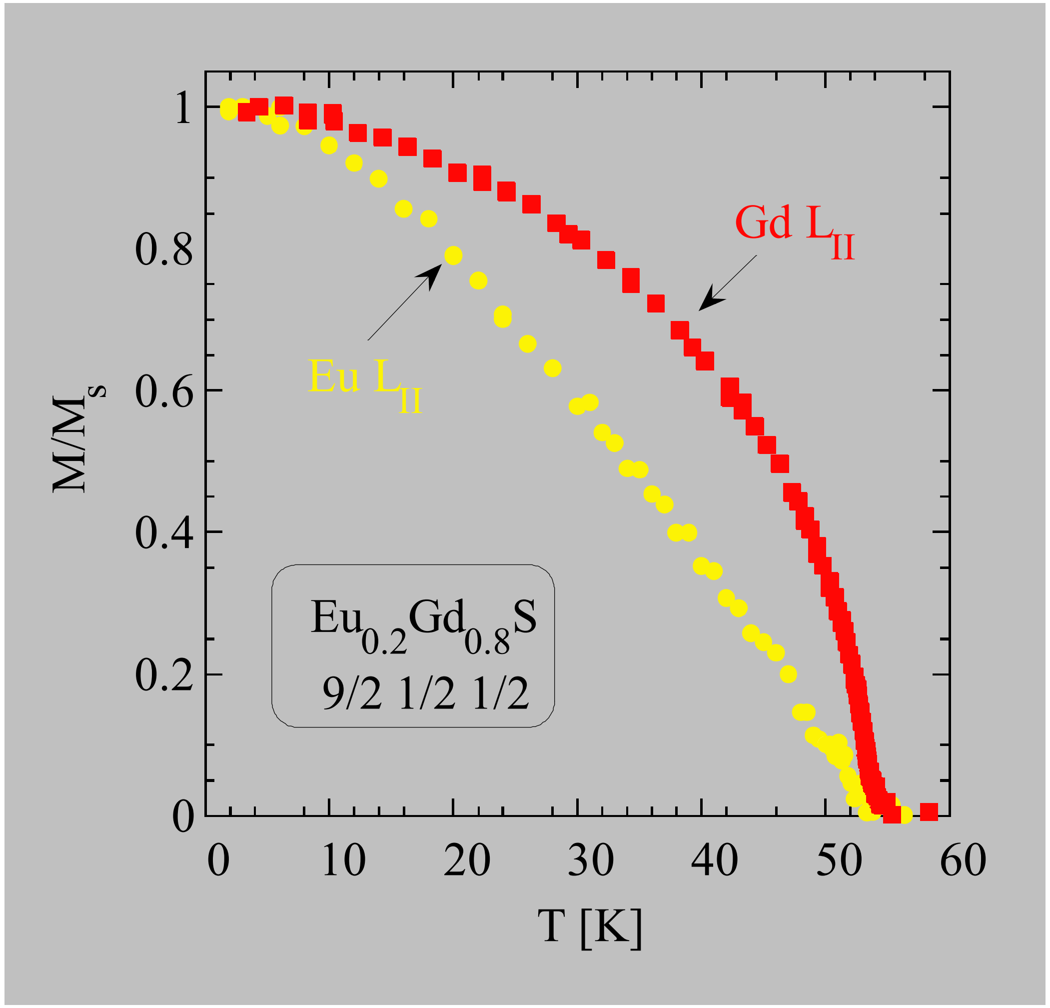

Hupfeld, Schweika, Strempfer, Mattenberger, McIntyre, Brückel
Europhys. Lett. 49 (2000), 92

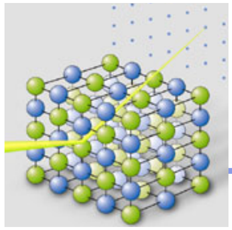

$Gd_{0.8}Eu_{0.2}S$: Temperature Dependence

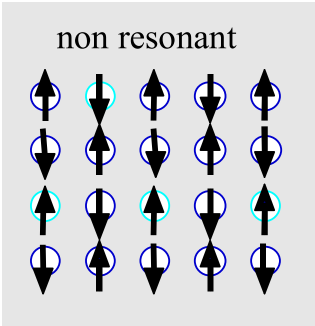

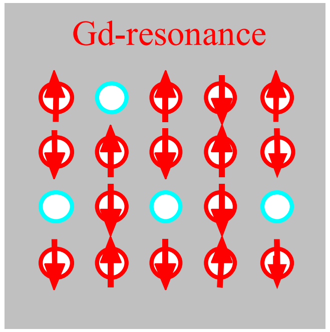

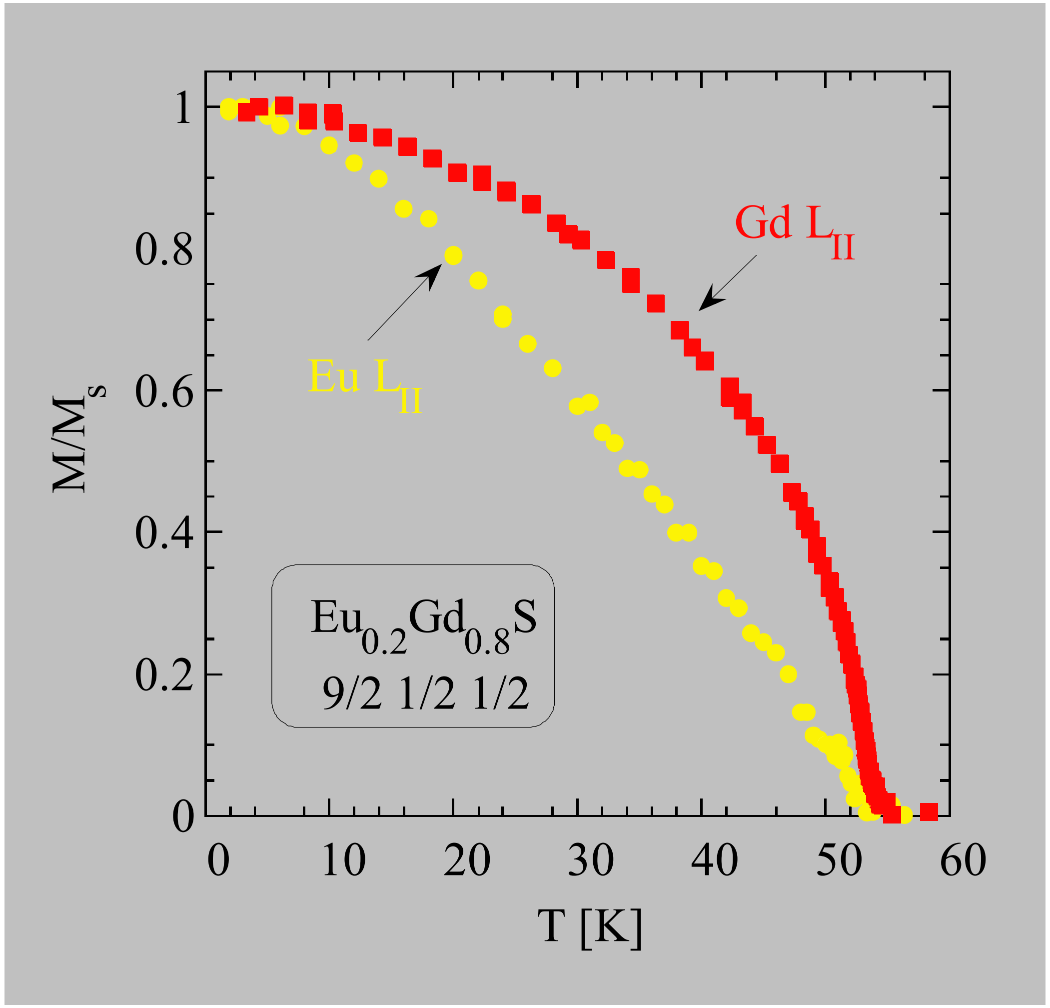

Hupfeld, Schweika, Strempfer, Mattenberger, McIntyre, Brückel
Europhys. Lett. 49 (2000), 92

$Gd_{0.8}Eu_{0.2}S$: Temperature Dependence

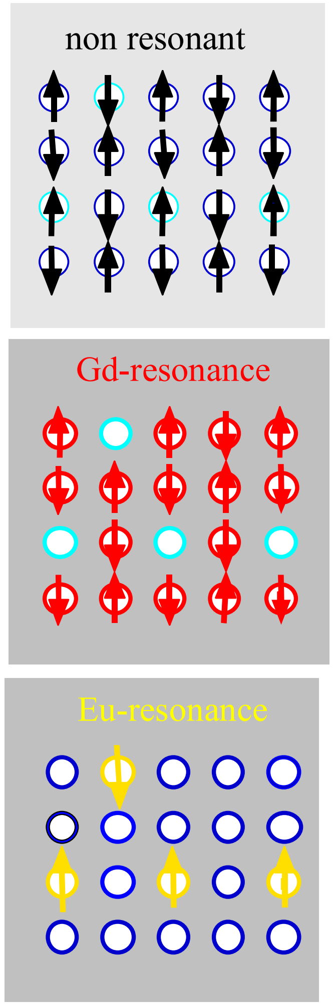

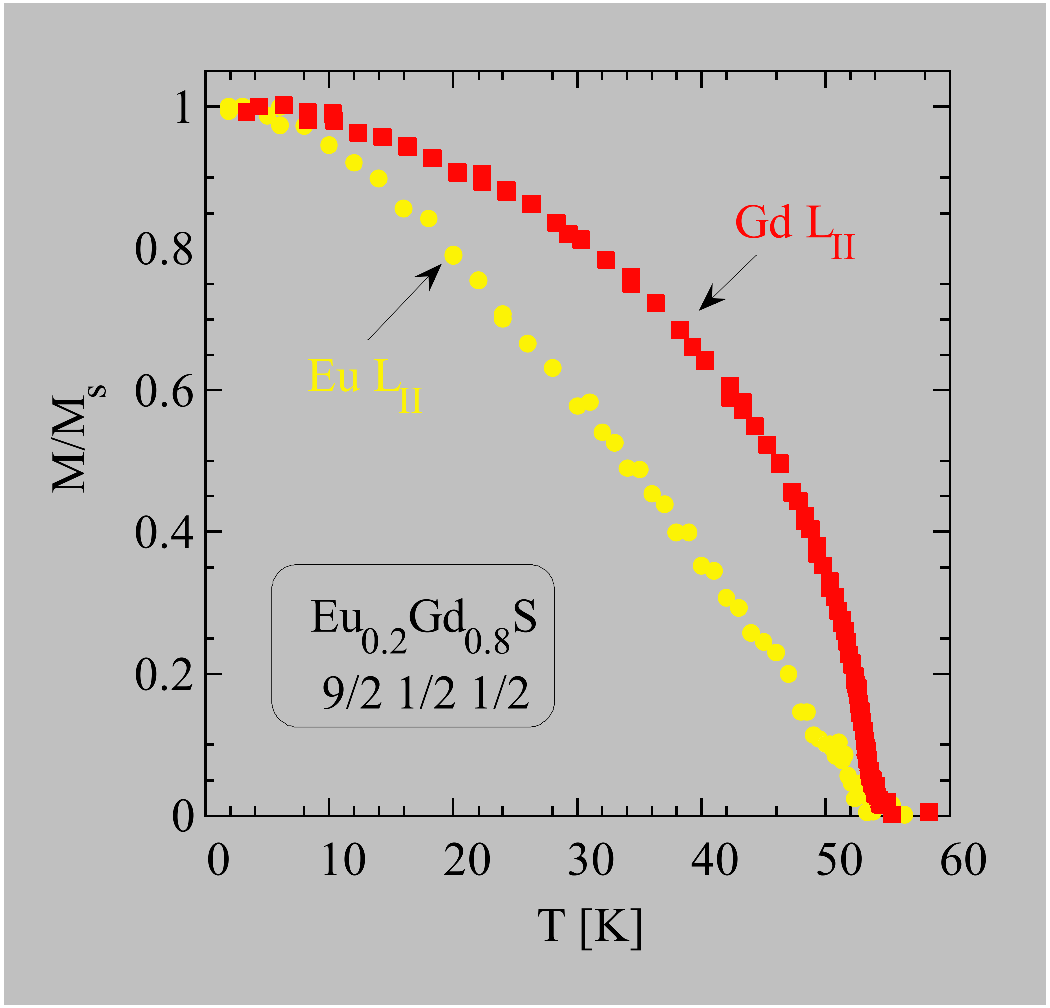

Hupfeld, Schweika, Strempfer, Mattenberger, McIntyre, Brückel
Europhys. Lett. 49 (2000), 92

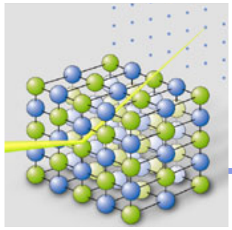

Frustration Model $Gd_{1-x}Eu_xS$

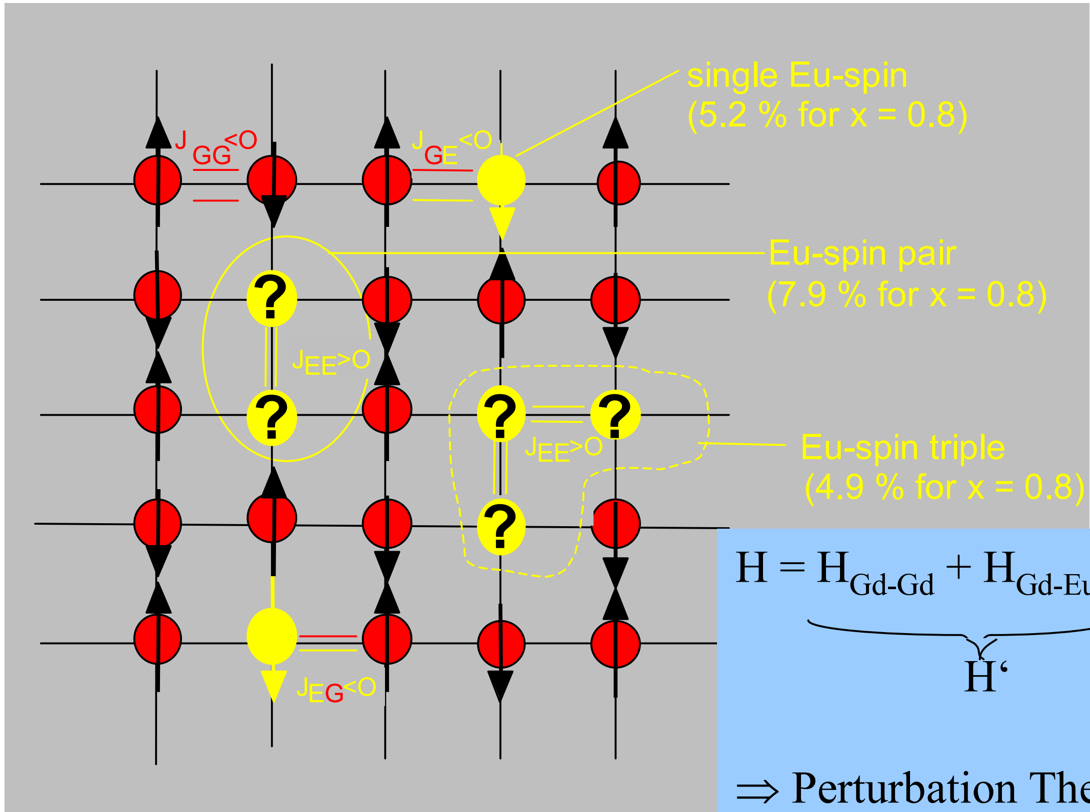

Heisenberg:

$$H = -\sum J_{ij}\ \underline{S}_i \cdot \underline{S}_j$$

$$H = \underbrace{H_{Gd\text{-}Gd} + H_{Gd\text{-}Eu}}_{H'} + \underbrace{H_{Eu\text{-}Eu}}_{\downarrow\ \Delta H}$$

⇒ Perturbation Theory:

H‘: molecular field approximation

$\Delta H = H_{Eu\text{-}Eu}$: exact diagonalization for Eu-pairs, triples,... in the molecular field

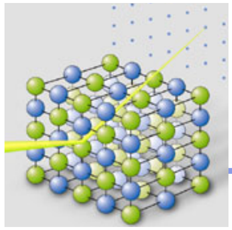

T-Dependence

"Frustration Model"

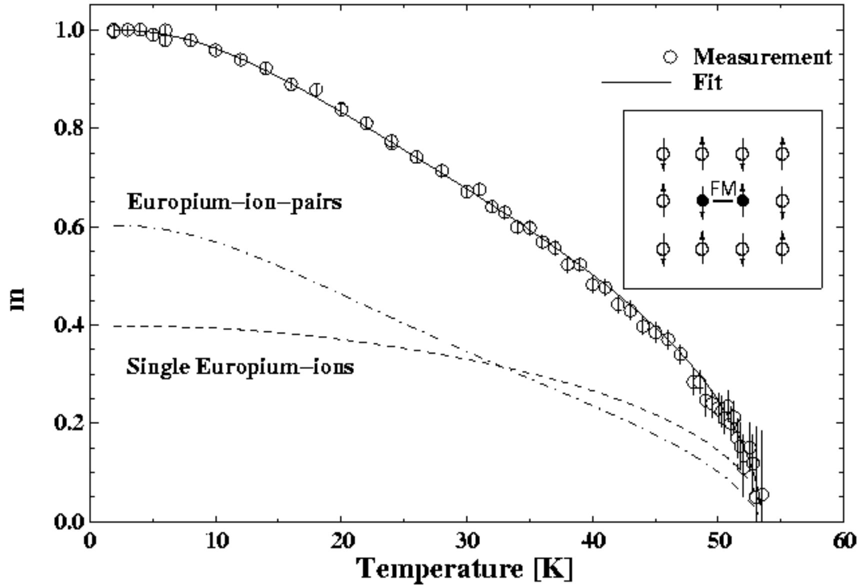

Monte Carlo Simulation

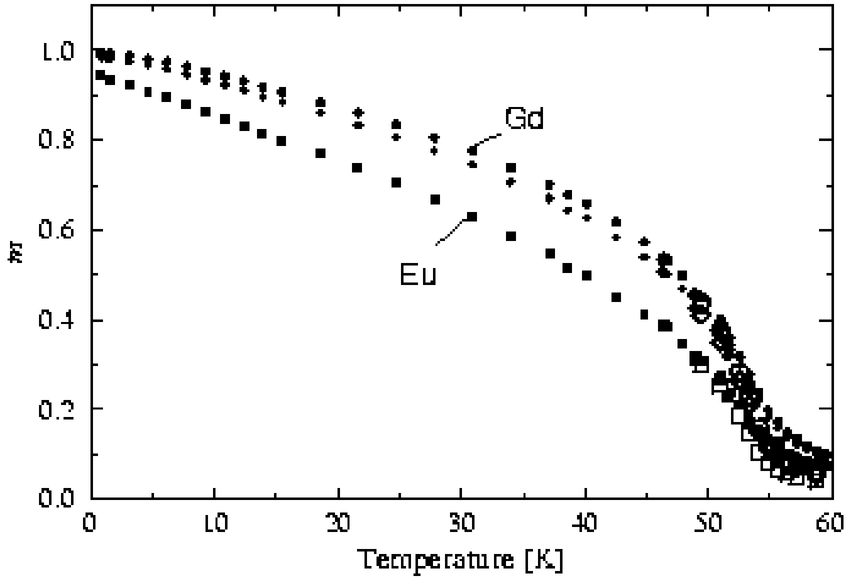

Hupfeld, Schweika, Strempfer, Caliebe, Köbler, Mattenberger, McIntyre, Yakhou, Brückel
Eur. Phys. J. B 26 (2002), 273

	Gd-Gd	Gd-Eu	Eu-Eu
J_1	-1.27 K	-0.85 K	+1.21 K
J_2	-2.82 K	-1.86 K	0

Canted Versus Collinear States

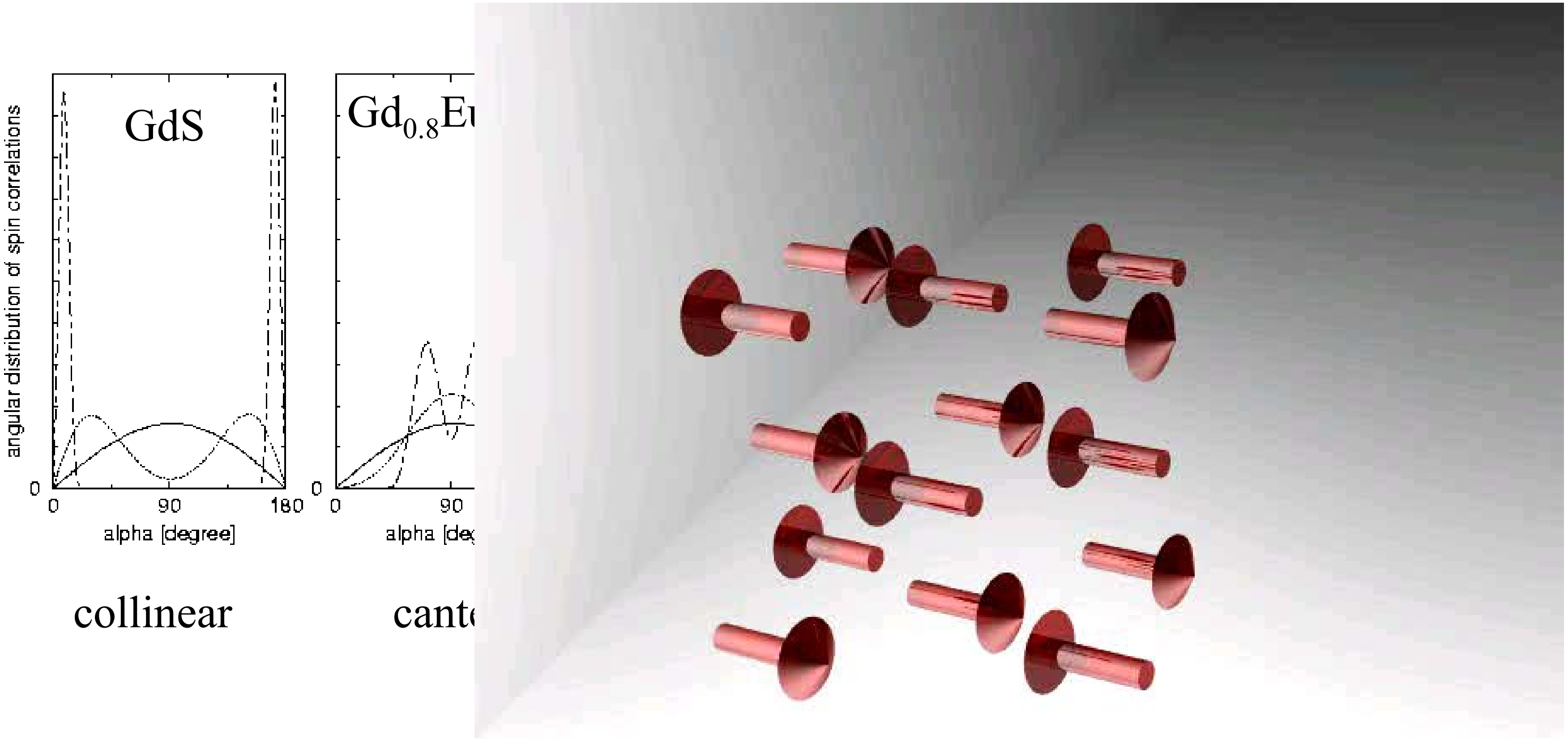

Success!

Wolfgang Caliebe
&
Dirk Hupfeld
@
W1 – DORIS - HASYLAB

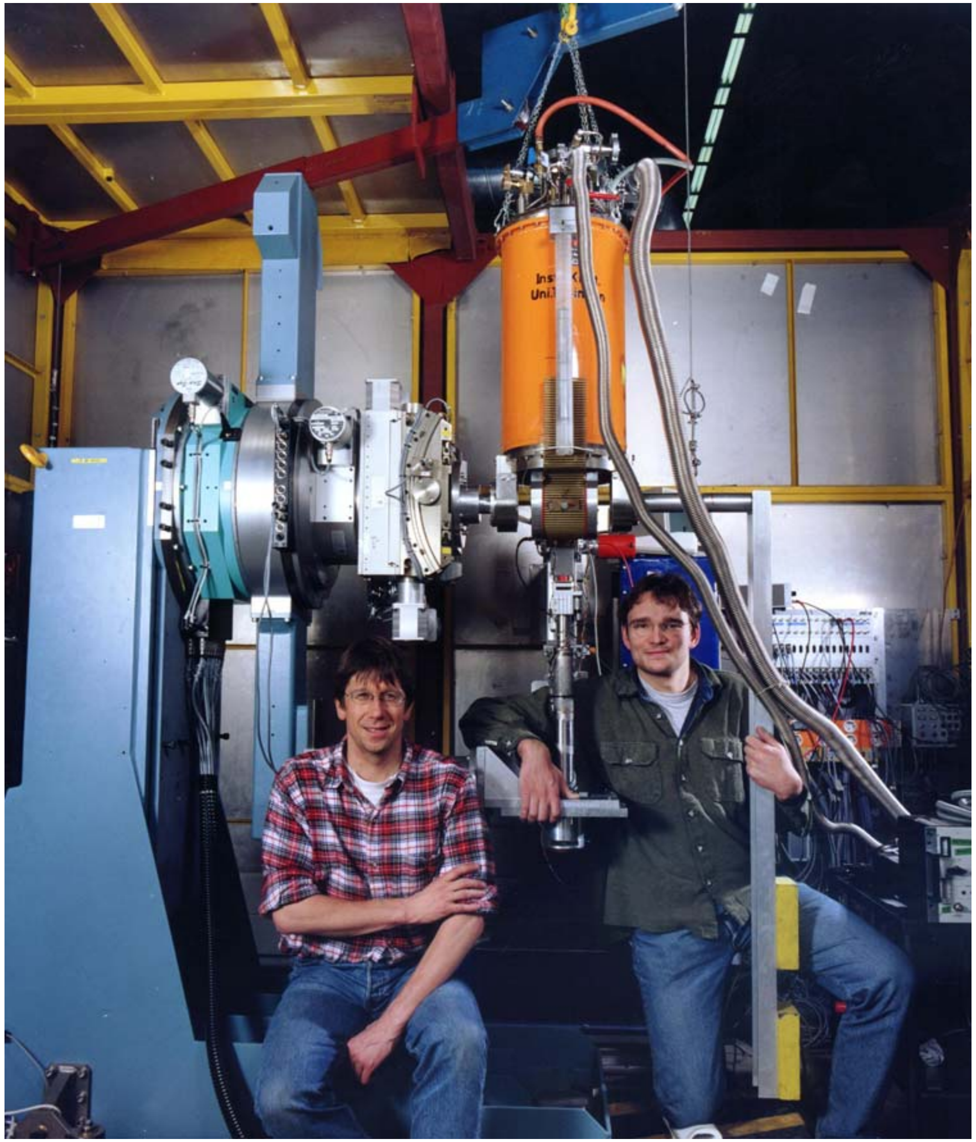

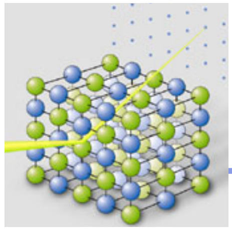

Outline

- What's new in magnetism ?
- Experimental techniques
- Elastic magnetic neutron scattering
- X-ray techniques for magnetism
- Nonresonant magnetic x-ray scattering
- Resonant magnetic x-ray scattering
- Example: Non-resonant scattering from transition metal di-flourides
- Example: Resonance exchange scattering from mixed crystals
- Summary

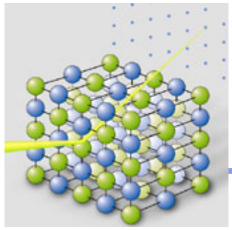

Scattering Methods for Orbital and Spin Physics

Neutrons

☺ powder samples

☺ complex magnetic structures (spherical PA)

☺ excitations

☺ complementarity (probes 4f moments directly, L- determination with "x-n technique", ...)

XRES: element and band sensitive probe!

☺ soft x-rays (≈ 1 keV) for thin film magnetism (3d & 4f): magnetisation density profile, magnetic domain structure

☺ hard x-rays (≈ 10 keV) for thin films and bulk 4f magnets: spin polarisation in conduction band (dipole transitions)

HEX: High energy (≈ 100 keV) non resonant magnetic x-ray scattering

☺ absolute determination of spin form factors (in part. 3d)

Anomalous X-ray scattering:

☺ Local distortions and orbital ordering